NASA CR-165555

National Aeronautics and Space Administration

CF6 JET ENGINE PERFORMANCE IMPROVEMENT - HIGH PRESSURE TURBINE ROUNDNESS

by

W.D. Howard and W.A. Fasching

GENERAL ELECTRIC COMPANY

JANUARY 1982

Prepared For

National Aeronautics and Space Administration

NASA Lewis Research Center

CONTRACT NAS3-20629

1. Report No.	2. Government Accession No.	3. Recipient's Catalog No.
NASA CR-165553		

4. Title and Subtitle	5. Report Date
CF6 Jet Engine Performance Improvement - High Pressure Turbine Roundness	January 1982
	6. Performing Organization Code
7. Author(s)	8. Performing Organization Report No.
W.D. Howard, W.A. Fasching	R82AEB115
	10. Work Unit No.
9. Performing Organization Name and Address	11. Contract or Grant No.
General Electric Company Aircraft Engine Group Cincinnati, OH 45215	NAS3-20629
	13. Type of Report and Period Covered
12. Sponsoring Agency Name and Address	Contractor Report
National Aeronautics and Space Administration Washington, D.C. 20546	14. Sponsoring Agency Code

15. Supplementary Notes

Project Manager - J. McAulay; Project Engineer - R. Antl, NASA Lewis Research Center, Cleveland, Ohio

16. Abstract

As part of the NASA-Sponsored Engine Component Improvement Program, an improved high pressure turbine stator has been developed to reduce fuel consumption in current CF6-50 turbofan engines. The instrumented engine test demonstrated the feasibility of the roundness and clearance response improvements. Application of these improvements will result in a cruise SFC reduction of 0.22 percent for new engines. For high time engines, the improved roundness and response characteristics will result in an 0.5 percent reduction in cruise SFC. The endurance test demonstrated a basic life capability of the improved HP turbine stator in over 800 simulated flight cycles without any sign of significant distress.

17. Key Words (Suggested by Author(s))	18. Distribution Statement
Jet Engine HP Turbine Turbofan Engine Fuel Conservation	Unclassified - Unlimited

19. Security Classif. (of this report)	20. Security Classif. (of this page)	21. No. of Pages	22. Price*
Unclassified	Unclassified	126	

* For sale by the National Technical Information Service, Springfield, Virginia 22161

FOREWORD

The work was performed by the CF6 Engineering Department of General Electric's Aircraft Engine Group, Aircraft Engine Engineering Division, Cincinnati, Ohio. The program was conducted for the National Aeronautics and Space Administration, Lewis Research Center, Cleveland, Ohio, under Subtask 2.5 of the CF6 Jet Engine Performance Improvement Program, Contract Number NAS3-20629. The Performance Improvement Program is part of the Engine Component Improvement (ECI) Project, which is part of the NASA Aircraft Energy Efficiency (ACEE) Program. The NASA Project Engineer for the High Pressure Turbine Roundness Program was R. Antl. The program was initiated October 1978 and completed in June 1981.

The report was prepared by W. A. Fasching, General Electric Program Manager and W. D. Howard, Project Engineer, with the assistance of M.W. Thomas and M.P. Murphy.

TABLE OF CONTENTS

LIST OF ILLUSTRATIONS

LIST OF ILLUSTRATIONS (Continued)

LIST OF ILLUSTRATIONS (Continued)

LIST OF ILLUSTRATIONS (Continued)

LIST OF ILLUSTRATIONS (Continued)

LIST OF ILLUSTRATIONS (Concluded)

1.0 SUMMARY

As part of the NASA sponsored Engine Component Improvement (ECI) Program, an improved high pressure (HP) turbine stator has been developed to reduce the fuel consumption of current CF6-50 engines for today's wide-bodied commercial aircraft. The high pressure turbine roundness program consisted of the design, analysis and manufacture of an improved HP turbine stator and its evaluation in an instrumented engine test and an endurance test.

The instrumented engine test, using a heavily instrumented CF6-50 engine, equipped with the improved hardware, demonstrated the feasibility of the roundness and clearance response improvements. Application of these improvements will result in a net clearance reduction of 0.25 mm (0.010 in) for new engines which results in a 0.58 percent increase in turbine efficiency and a 0.31 percent reduction in specific fuel consumption (SFC) at takeoff power. The equivalent cruise SFC reduction is 0.22 percent.

For a high time engine (3000 hrs) improved roundness and response characteristics will result in a 0.5 percent reduction in cruise sfc.

The CF6-50 engine cyclic endurance test demonstrated a basic life capability of the improved HP turbine stator in over 800 simulated flight cycles without any sign of significant distress.

An economic assessment of the improved turbine applied to engines on the Boeing 747-200 and the Douglas DC-10-30 is included in this report.

2.0 INTRODUCTION

National energy demand has outpaced domestic supply creating an increased U.S. dependence on foreign oil. This increased dependence was dramatized by the OPEC oil embargo in the winter of 1973 to 1974. In addition, the embargo triggered a rapid rise in the cost of fuel which, along with the potential of further increases, brought about a changing economic circumstance with regard to the use of energy. These events, of course, were felt in the air transport industry as well as other forms of transportation. As a result of these experiences, the Government, with the support of the aviation industry, has initiated programs aimed at both the supply and demand aspects of the problem. The supply problem is being investigated by looking at increasing fuel availability from such sources as coal and oil shale. Efforts are currently underway to develop engine combustor and fuel systems that will accept fuels with broader specifications.

Reduced fuel consumption is the other approach to deal with the overall problem. A long-range effort to reduce fuel consumption is to evolve new technology which will permit development of a more energy efficient turbofan or the use of a different propulsive cycle, such as a turboprop. Although studies have indicated large reductions in fuel usage are possible (e.g., 15 percent to 40 percent), any significant impact of this approach is at least 15 years away. In the near term, the only practical propulsion approach is to improve the fuel efficiency of current engines. Examination of this approach has indicated that a 5 percent fuel reduction goal starting in the 1980 to 1982 time period is feasible for current commercial engines. These engines will continue to be significant fuel users for the next 15 to 20 years.

Accordingly, NASA is sponsoring the Aircraft Energy Efficiency (ACEE) Program (based on a congressional request) which is directed at reduced fuel consumption of commercial air transports. The Engine Component Improvement (ECI) Program is the element of the ACEE Program directed at reducing fuel consumption of current commercial aircraft engines. The ECI Program consists of two parts: engine diagnostics and performance improvement. The engine diagnostics effort is to provide information to identify the sources and causes of engine deterioration. The performance improvement effort is directed at developing engine components having performance improvement and retention characteristics which can be incorporated into new production and existing engines.

The performance improvement effort was initiated with a feasibility analysis which identified performance improvement concepts and then assessed the technical and economic merits of these concepts. This assessment included a determination of airline acceptability, the probability of introducing the concepts into production by the 1980 to 1982 time period, and their retrofit potential. The study was conducted in cooperation with the Boeing and Douglas aircraft companies and American and United Airlines, and is reported in Reference 1. In the feasibility analysis task, the CF6 high pressure turbine roundness concept was selected for development and evaluation because of its fuel savings potential and attractive airline payback period. The objective of the

high pressure (HP) turbine roundness program was to develop technology and to verify the predicted fuel savings by engine ground tests. The HP turbine roundness concept consisted of the design, analysis and manufacture of an improved HP turbine stator for the CF6-50 engine and its evaluation in an instrumented engine test and an endurance test. The results of the development and evaluation of the improved HP turbine are presented herein.

3.0 TECHNICAL BACKGROUND AND APPROACH

The objective of this program was to improve the performance of the high pressure turbine of the CF6-50 engine. A cross-sectional view of the CF6-50 engine is shown in Figure 1 and a detailed cross section of the high pressure turbine is shown in Figure 2.

The main thrust of this effort was to reduce the blade-to-shroud clearance. Clearances were established such that blade-on-shroud rubs would be eliminated or minimized. In order to reduce this clearance, turbine out-of-roundness and clearance transient response must be controlled. Turbine out-of-roundness in conjunction with the basic turbine response characteristics results in local rubs while adverse clearance transient response can result in rubs even for a totally round turbine. That both roundness and clearance improvements are necessary was obvious because rubs up to 1 mm (0.040 in) occurred in normal factory testing and revenue flight service, while calculations indicated that for a fully round engine clearances of 0.38 mm (0.015 in) are feasible. The results of the Engine Diagnostic Test showed that both out-of-roundness and clearance response must be improved (Ref. 2).

3.1 ROUNDNESS CONTROL

The control of the roundness of a gas turbine engine structure requires a balanced and thorough evaluation of all of the primary engine structural members. Figure 3 highlights and defines the critical structural members of the engine. Included are the fan casing, compressor casing, compressor rear frame (CRF), the high pressure turbine (HPT) Stage 1 and 2 nozzle supports, the turbine midframe (TMF), the low pressure turbine (LPT) casing and the turbine rear frame (TRF).

Each of these components is subjected to varying levels of nonaxisymmetric loading and thermal gradients which tend to induce out-of-roundness distortions in these components. These distortions tend to propagate through the entire length of the engine.

This program implemented an analytical computer model, the General Electric CLASS MASS Program, to evaluate the magnitudes of out-of-roundess of each component and the effect of each component out-of-roundness. Typical models of the CF6-50 structural system are shown in Figures 4 and 5.

CLASS MASS, while being an axisymmetric structural analysis program, can calculate deflections and stresses due to nonaxisymmetric loading and thermal gradients through Fourier Series approximations. However, nonaxisymmetric frame structures must first be modeled on a three-dimensional structural analysis program, and the deformations thus calculated applied to the CLASS MASS program as a boundary condition. The program used to supply the boundary conditions was the General Electric MASS structural analysis program. This program employs three-dimensional analysis and has the capability of handling nonaxisymmetric structures consisting of plate, brick, shell, and beam elements.

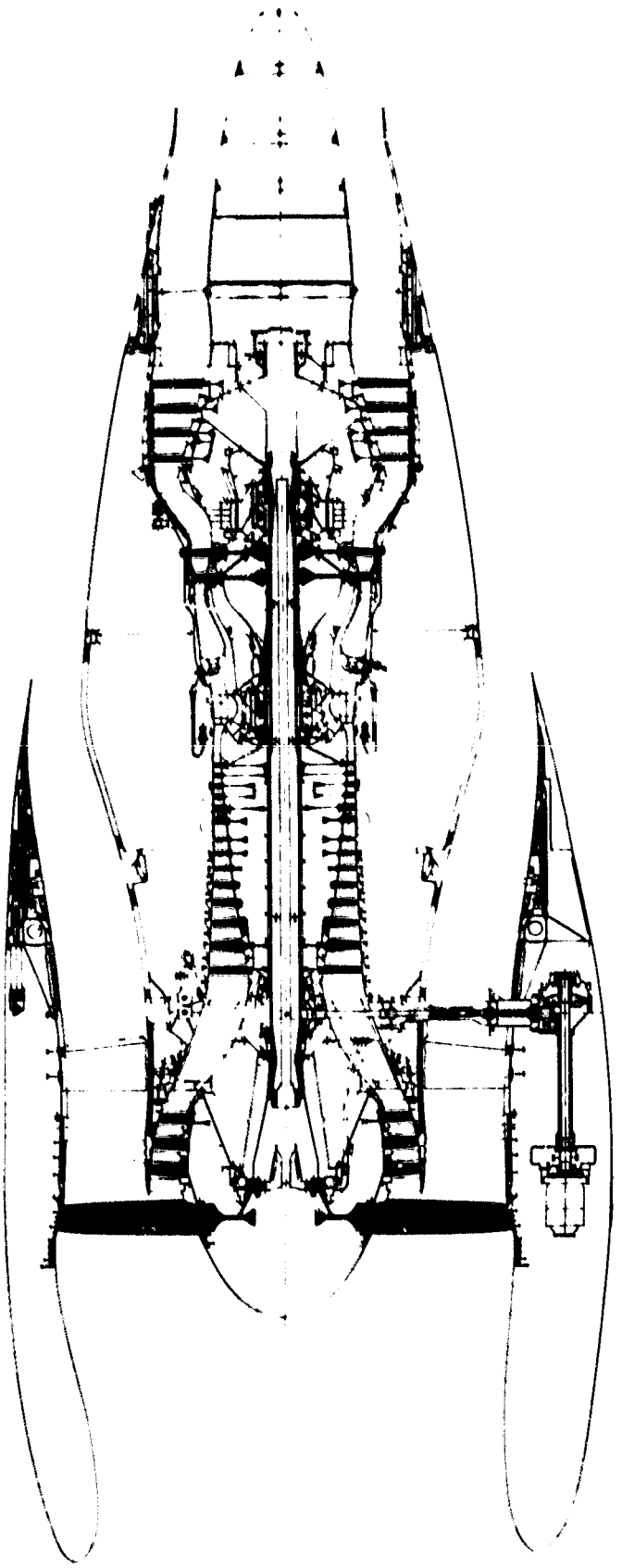

Figure 1. CF6-50 Engine Cross Section.

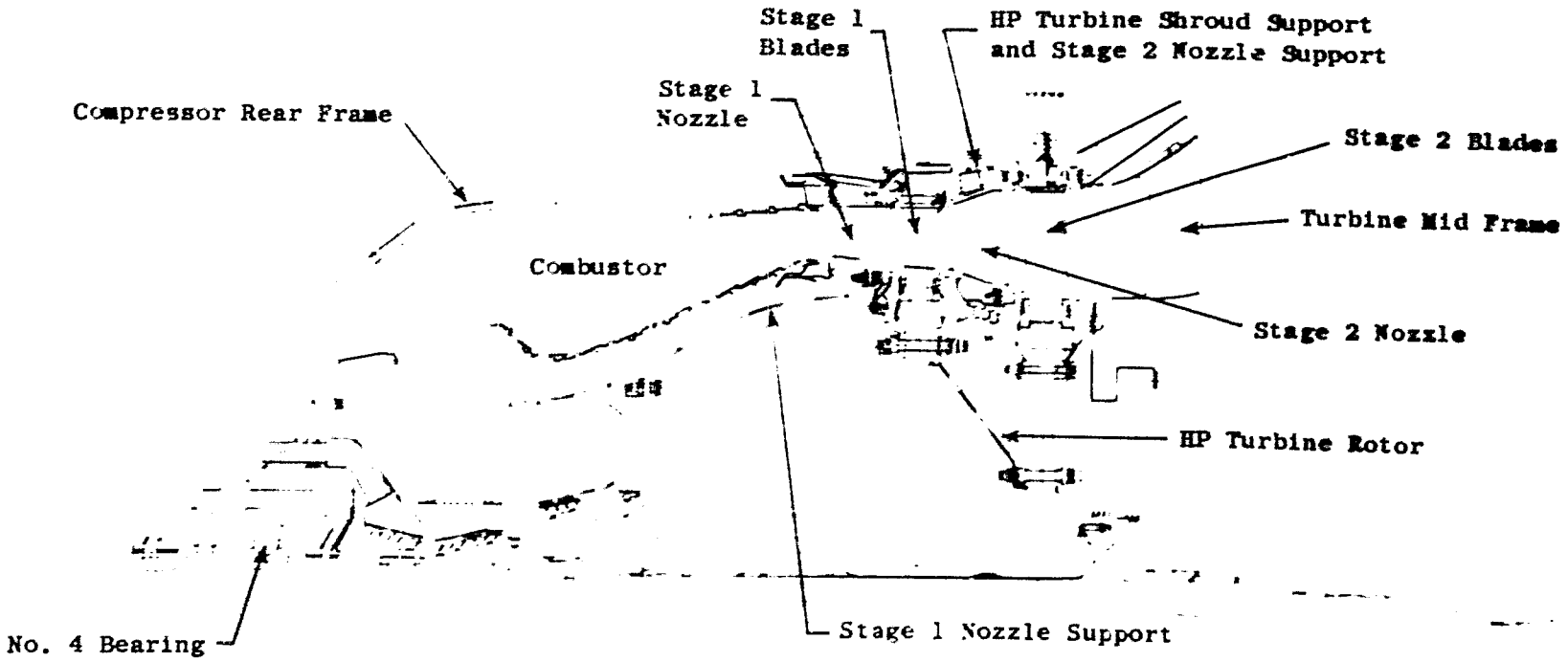

Figure 2. CF6-50 HPT Cross Section.

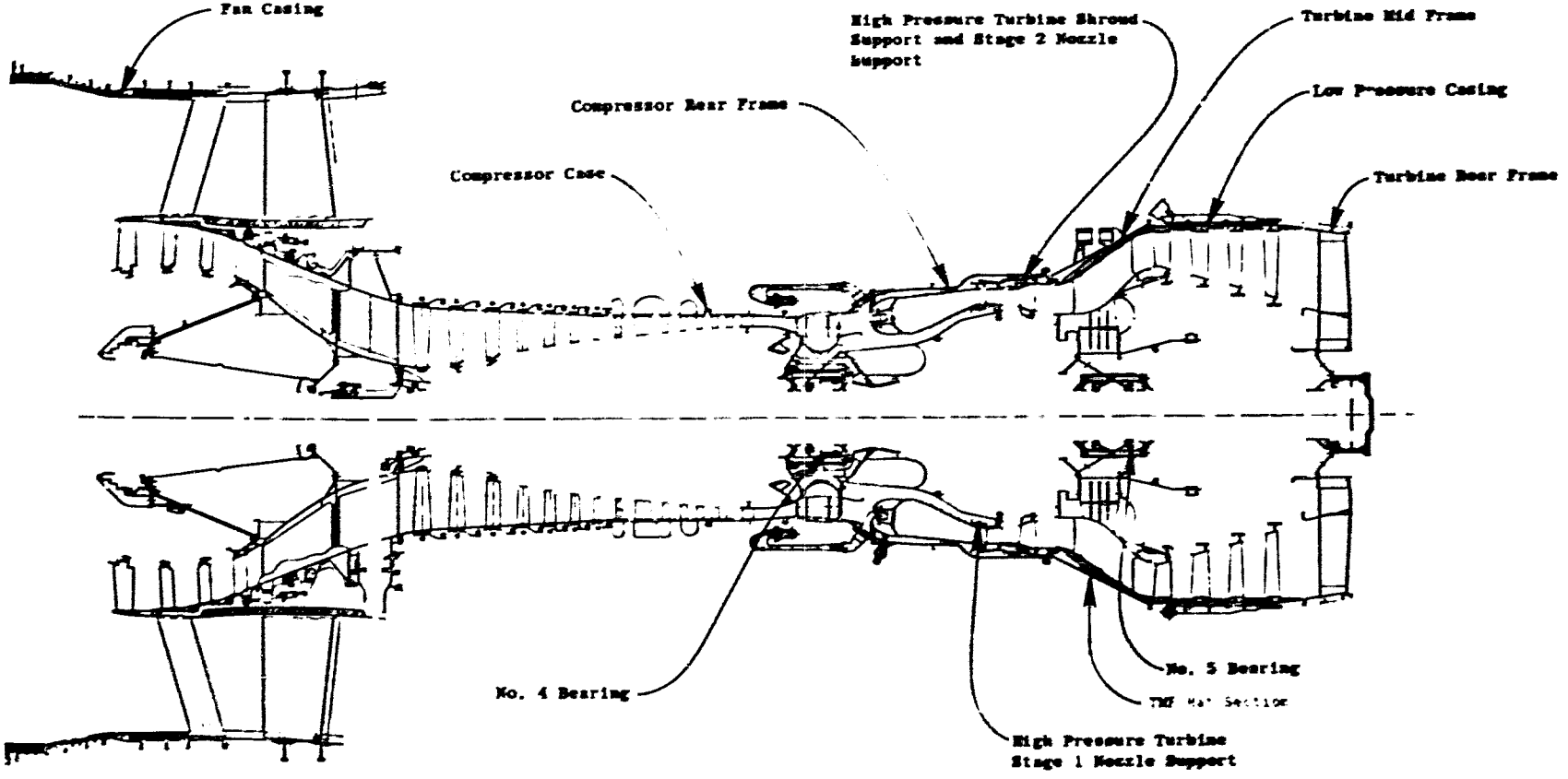

Figure 3. CF6-50 Major Cases and Frames.

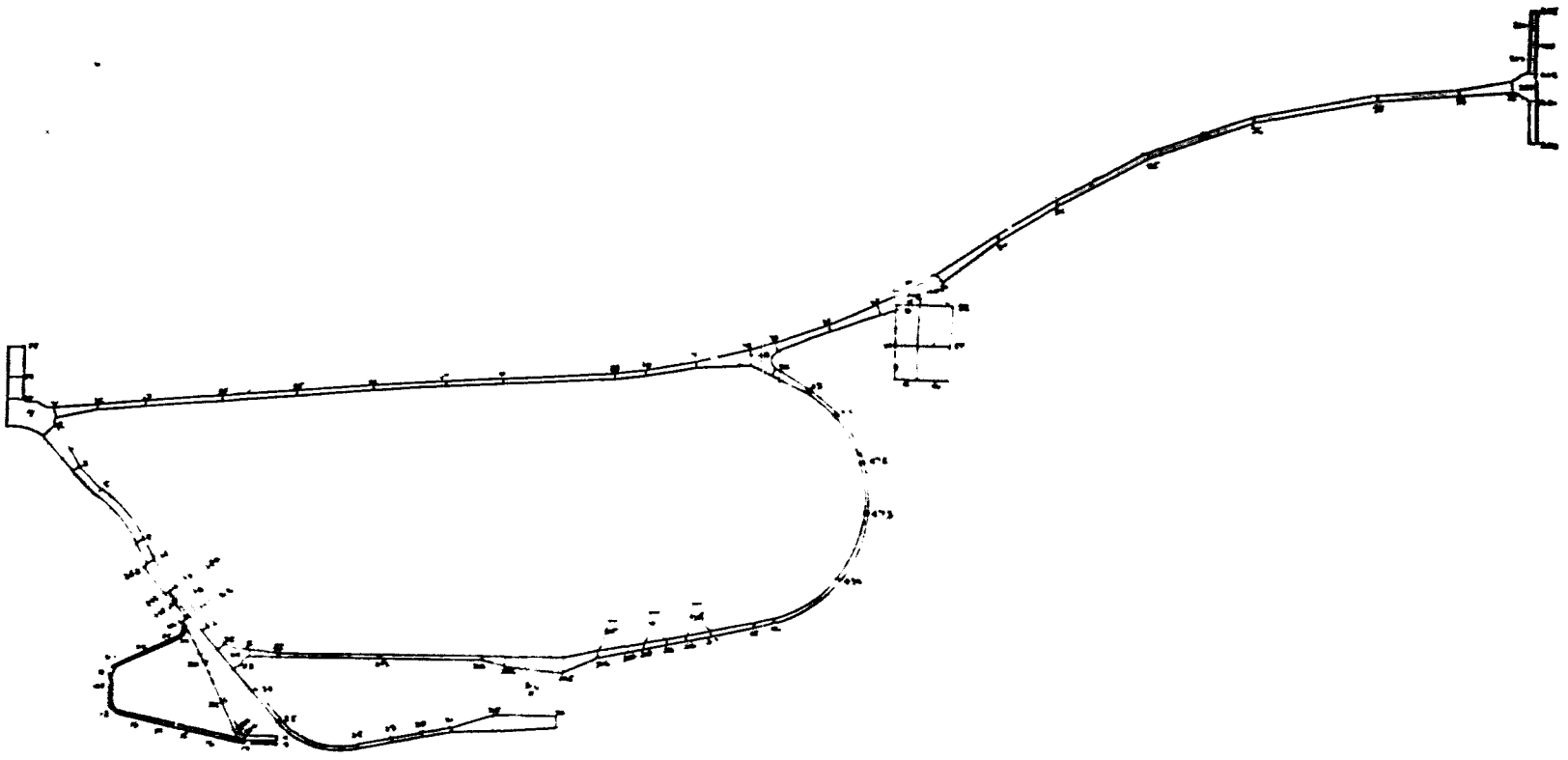

Figure 4. Typical CLASS MASS Model of HPT Stage 1 Nozzle Support.

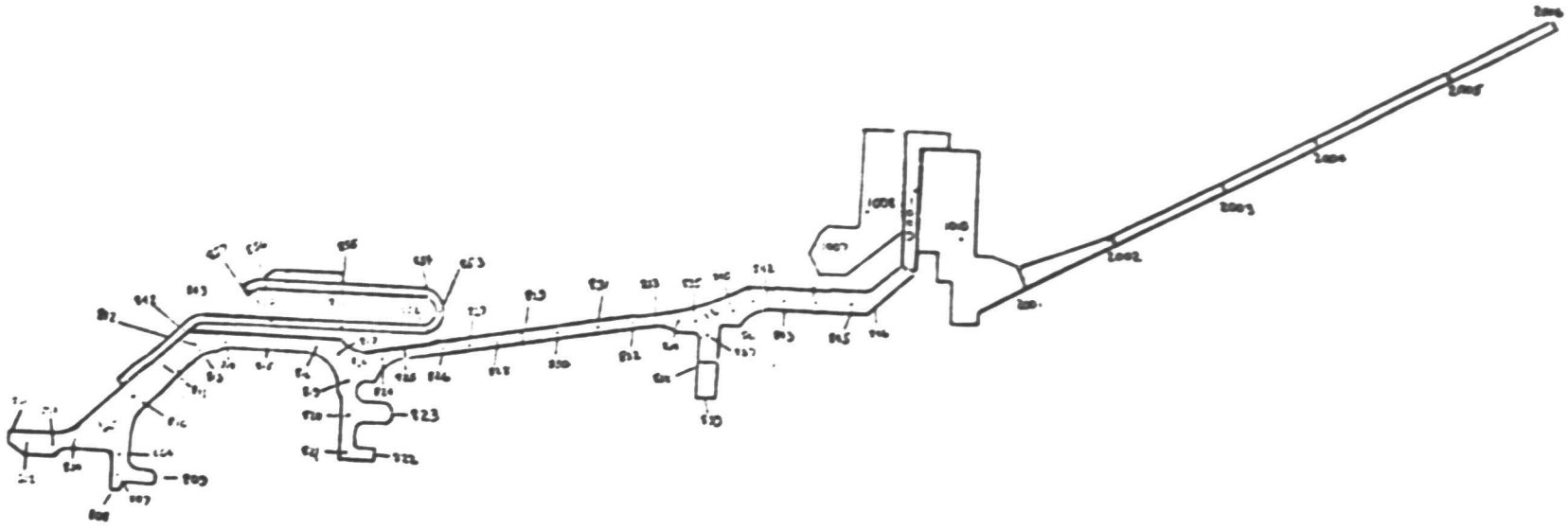

Figure 5. Typical CLASS MASS Model of HPT Shroud Support, Stage 2 Nozzle Support and Turbine Midframe.

Transient engine conditions were included in these analyses since the most severe thermal effects do not coincide, timewise, with the most severe loading effects. In addition, some of these effects are off-setting. When the minimum clearance point of the turbine blade and tip shroud was established, this determined, when combined with clearance control work to be discussed later, the level of tip clearance reduction which can be achieved by eliminating harmful component distortions.

Turbine Midframe Effects

One of the principal causes of HPT stator out-of-roundness is distortion of the adjacent structure. Previous analytical studies indicated that radial distortions in the production TMF structural hat sections are the major contributor to HPT stator distortion. The HPT stator shrouds in the CF6-50 are supported from the TMF forward flange joint which is connected to the TMF structural hat sections by a sheet metal cone. Distortions in the TMF structural hat sections are transmitted to the HPT shrouds through this supporting structure and were calculated to cause a 0.4 mm (0.016 in) inward distortion of the HPT shrouds at steady-state takeoff. Distortions in the production TMF structural hat sections occur due to:

(a) Mechanical loading resulting from engine mount reactions (the engine aft mount is an integral part of the structural hat section) and internal component loads being transmitted through the struts to the outer casing structure.

(b) Temperature differentials within the TMF structure due to different thermal response rates throughout the structure, strut internal air temperature variations, and variations in the air temperature and heat transfer rates throughout the TMF.

(c) Non-uniformity of the structural hat section stiffness around the TMF circumference.

Analysis of HPT stator distortion resulting from TMF distortion was done using the General Electric structural analysis computer programs. The analysis method had been correlated by means of GE funded static testing of the full engine structure during which both the production TMF hat section and HPT stator out-of-roundness was measured. Three tests were run for the following loadings:

(a) Vertical load reaction at engine aft mount points.

(b) Torque load reaction at engine aft mount point.

(c) Thermal loading where three of eight TMF struts were heated 90°C above the rest of the structure.

The correlation between measured and calculated out-of-roundness for the production HP turbine is shown in Figures 6 through 8.

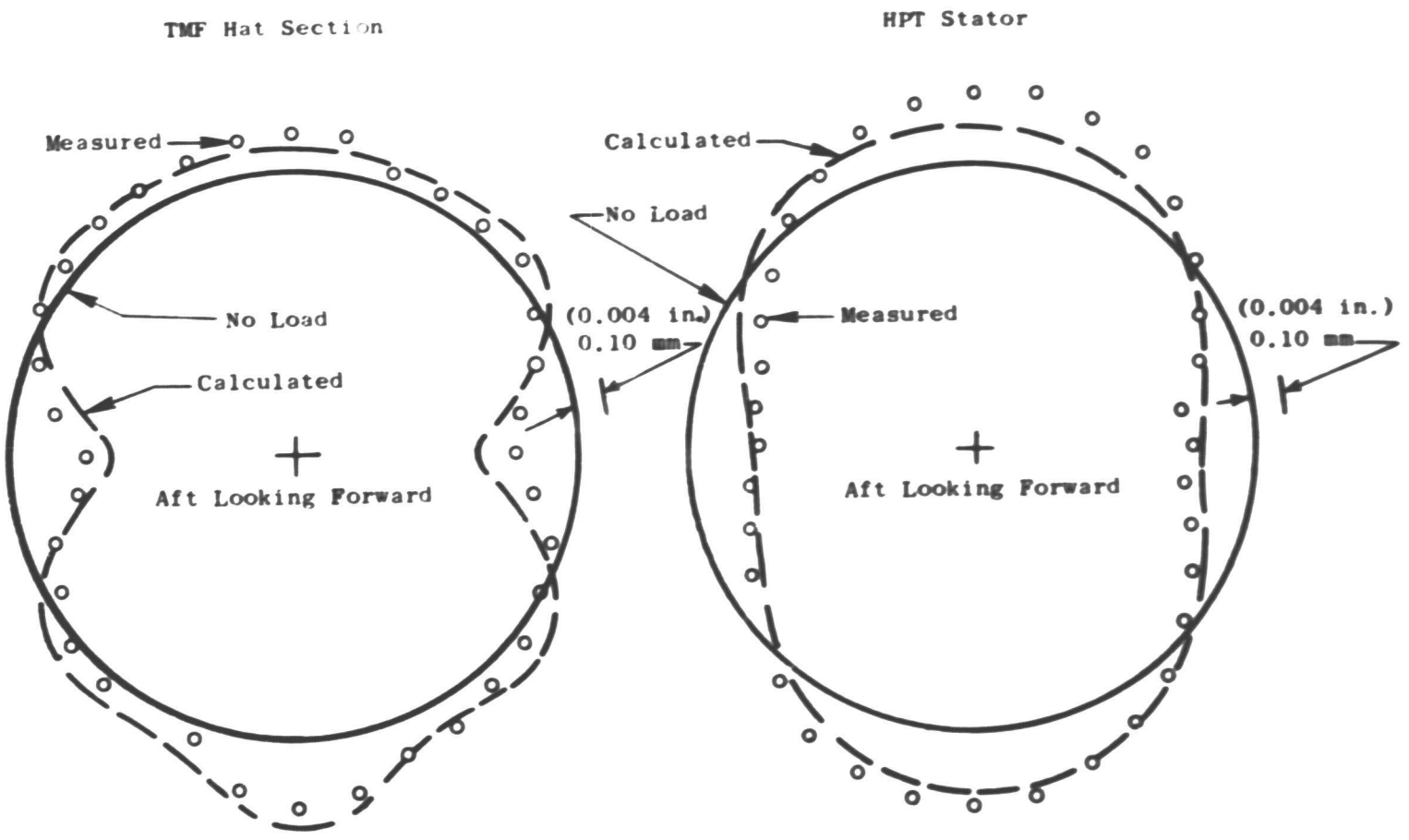

Figure 6. Comparison of Calculated Versus Measured Distortion for the Production HP Turbine in Static Test, Vertical Mount Reaction Loading.

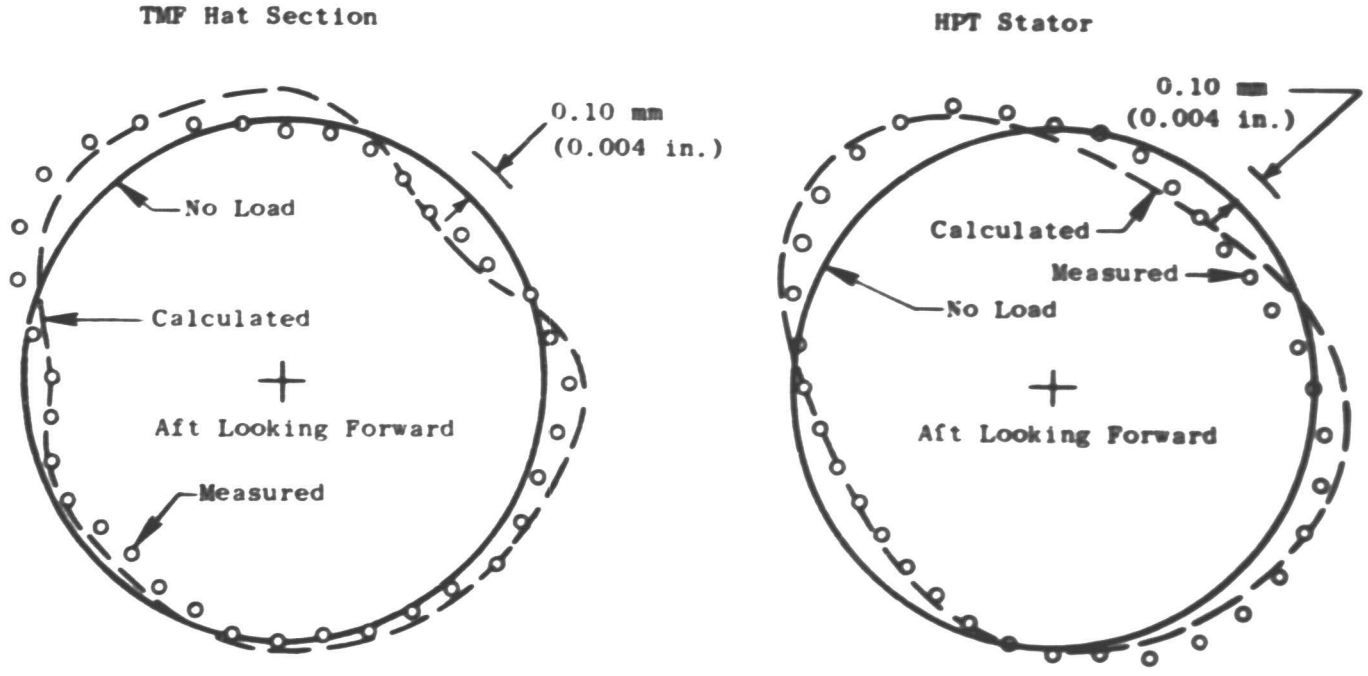

Figure 7. Comparison of Calculated Versus Measured Distortion for the Production HP Turbine in Static Test, Torque Reaction Mount Loading.

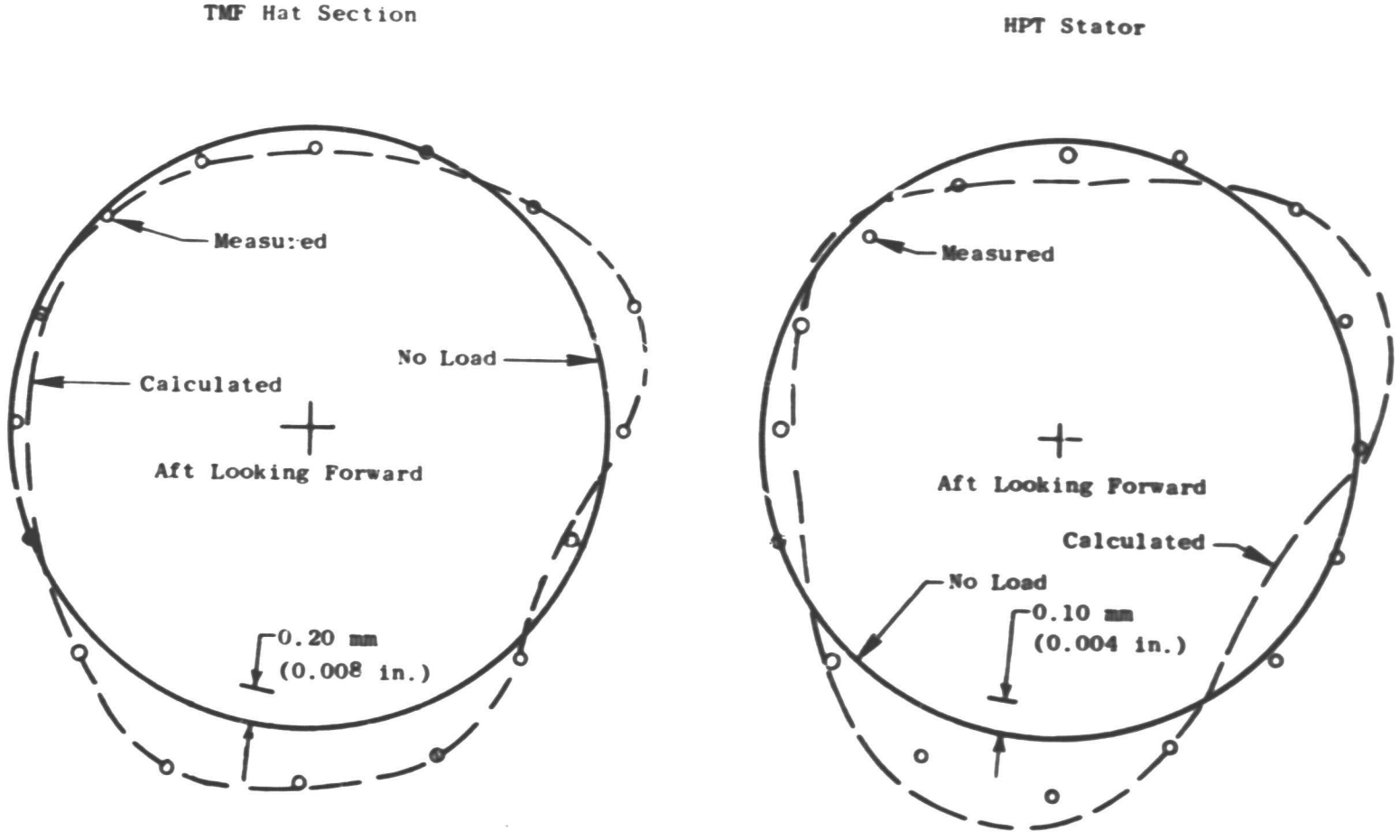

Figure 8. Comparison of Calculated Versus Measured Distortion for the Production HP Turbine in Static Test, TMF Struts Number 2,4,5, Heated Above Rest of of Structure.

The production TMF was redesigned to reduce the structural non-uniformity and thermal differentials throughout the structure in order to reduce the distortion of the TMF and, therefore, the out-of-roundness in the HPT stator.

The major elements in the TMF redesign were as follows:

(a) Relocation of the engine mount points on the outer casing allowing the structural hat sections to become the same configuration around the frame circumference. This results in uniform stiffness and temperature of the hat sections around the circumference. A comparison between the production TMF outer casing and the redesign configuration can be seen in Figures 9, 10, and 11.

(b) Thermal insulating liners were added to the inner diameter of several of the struts. In the present design the struts heat up to different temperatures of the cooling and pressurization air routed into and out of the frame through the struts. The added liners were designed to isolate the struts from the cooling effects of this air. The liner lengths and the number of struts to which liners were added were chosen to control the strut temperature differential. The strut temperature differential was set to take advantage of the resultant distortion of the structural hat sections and to have the strut temperature variation distortion cancel out the distortion caused by the mechanical and mount loads.

(c) A shield was added around the outside of the TMF/CRF flange joint to isolate the flange from the non-uniform cooling effects of the secondary air flowing through the aft core compartment. This secondary air cools these flanges non-uniformly around the circumference resulting in a non-uniform flange temperature. The non-uniform flange temperature results in a distortion of the flange, which in turn, distorts the HPT stator (See Figure 13).

Analytical studies of the redesigned TMF were done prior to testing to predict the TMF caused HPT stator out-of-roundness and indicated an approximately 0.1 mm (0.004 in) inward distortion of the HPT shrouds at steady-state takeoff.

Two turbine midframes were manufactured incorporating the above roundness control features for use in engine testing to demonstrate their effect on changing HPT stator out-of-roundness.

HPT Shroud Temperature Effects

Since, as previously stated, roundness must be assured before any significant work can be directed toward blade tip clearance reduction, the turbine shroud structure itself must stay round. In addition to being influenced by other engine structures, turbine structures may lose their roundness due to circumferentially non-uniform heating or cooling such as recirculation of hot flowpath gases into the cavities between the turbine flowpath hardware. This recirculation of hot gases can induce local overheating of the turbine structural members, causing them to deform.

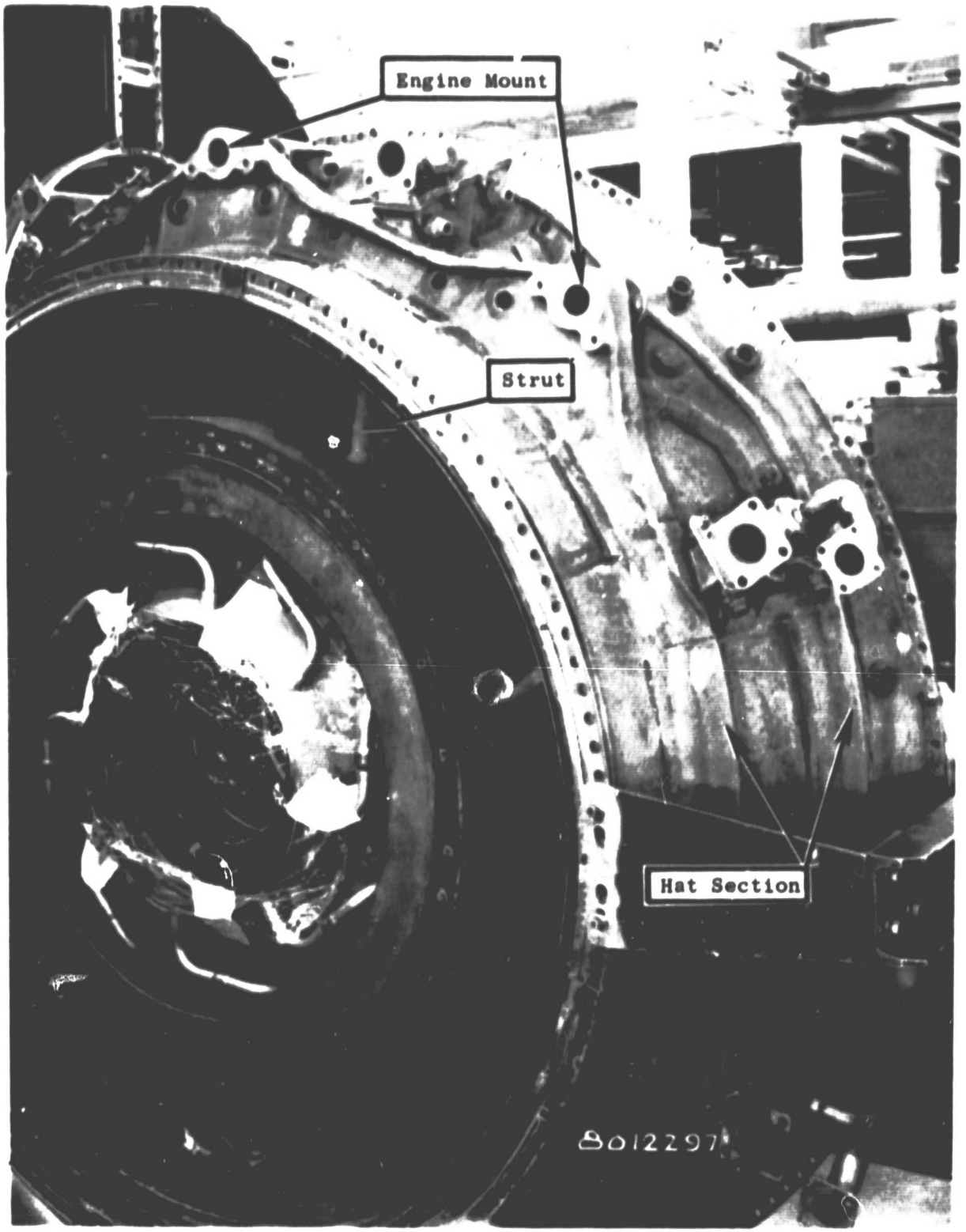

Figure 9. Current Production Turbine Midframe (Right Side) Forward Looking Aft.

ORIGINAL PAGE
BLACK AND WHITE PHOTOGRAPH

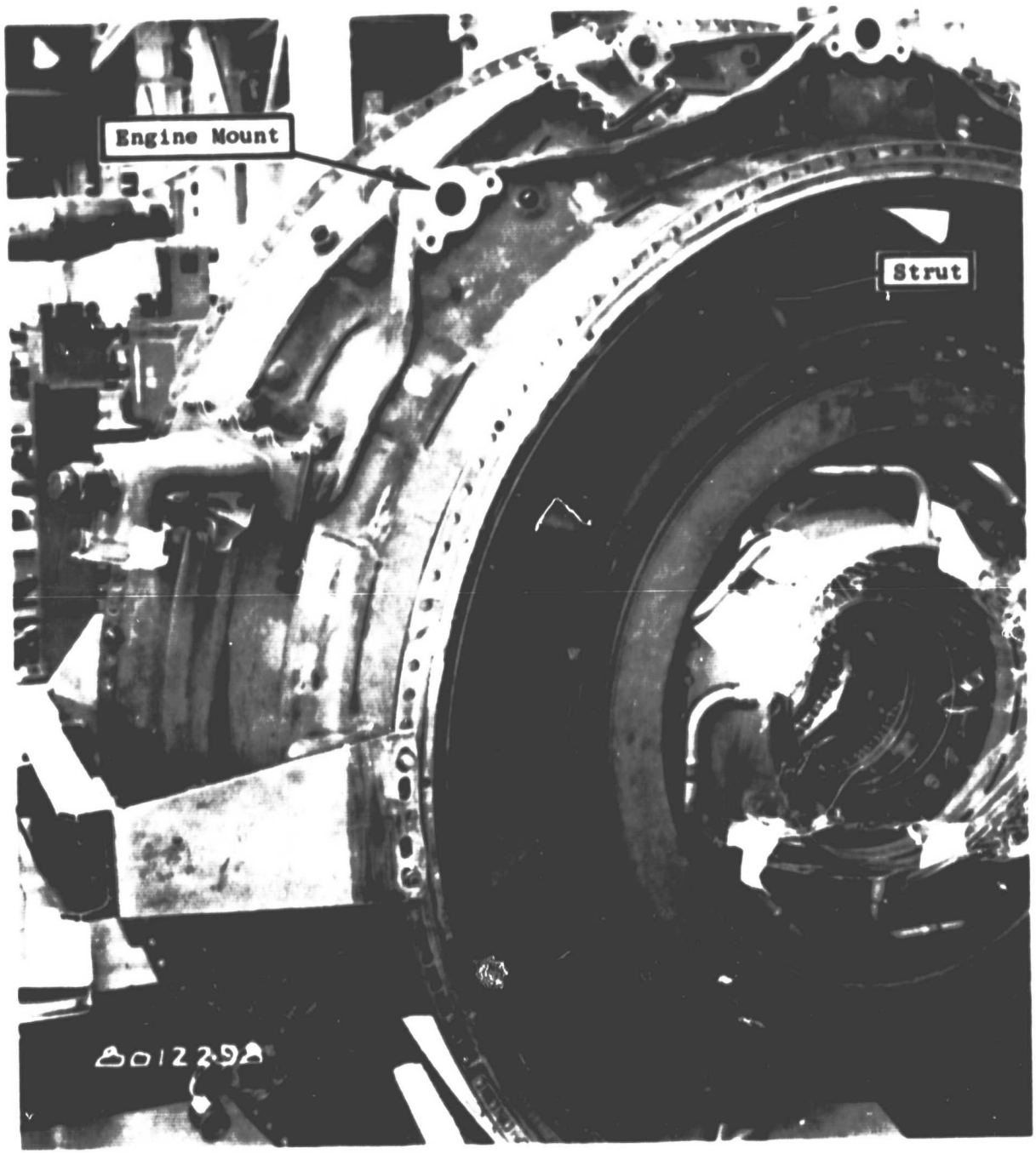

Figure 10. Current Production Turbine Midframe (Left Side).

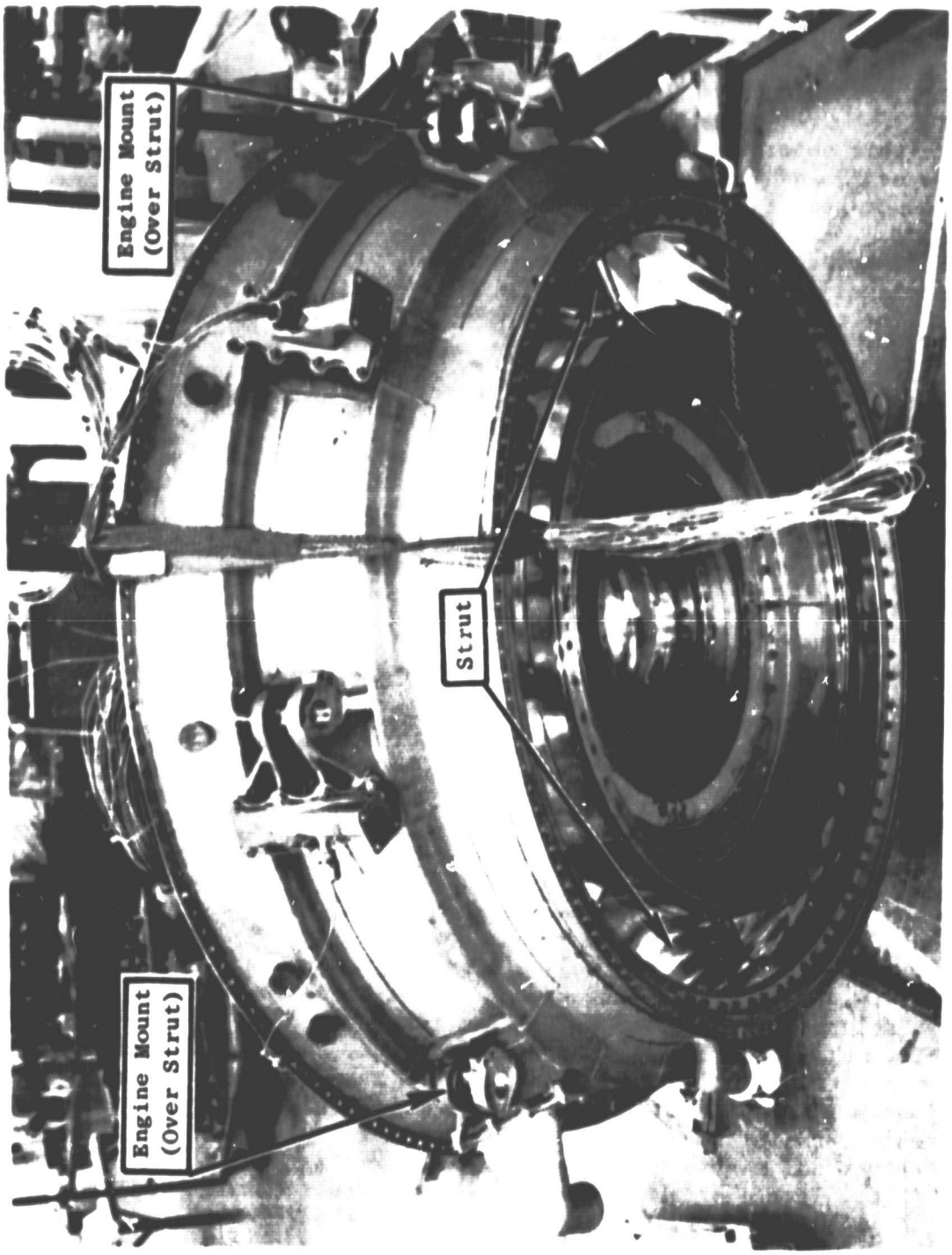

Figure 11. Redesigned Turbine Midframe with Engine Mount Points in Line with Struts.

Prevention of this occurrence can be accomplished by properly shielding the structural members from the flowpath. Reduction in cavity size, creation of narrow, tortuous paths which hot gas must follow to be exposed to the supporting members, and adequate cavity purge air are required to accomplish this.

To achieve this objective, a modified CF6-50 turbine support system was designed. Figures 12 and 13 show the types of improvements the final design contained to reduce recirculation.

It should be noted that there is no calculated out-of-roundness associated with hot gas recirculation effects. The emphasis of this facet of the program is to eliminate the possibility of this unpredictable problem.

Other Sources of Out-of-Roundness

Out-of-roundness caused by other sources, as investigated by the methods of this program, were deemed to be neglible. When the magnitudes of the deflections caused by the turbine midframe are considered, this is certainly a justifiable assumption because the TMF effects must be controlled before any secondary effects would be evident.

3.2 CLEARANCE CONTROL

In conjunction with the improvements in engine roundness, a parallel effort focused on improvements in the turbine supporting structure which allow the establishment of reduced turbine operating clearances.

Clearance Transient Response

Once turbine structural influences have been minimized, clearance control improvements can be defined. Experience has shown that steady-state engine operating clearances are set at some engine transient operating condition. Usually, the "worst case," or minimum clearance condition occurs during a hot reburst. This is defined as an engine decel from takeoff to idle, holding at idle for a period of time, generally less than five minutes, and then accelerating the engine back to full takeoff power. The turbine shroud support member, being considerably less massive than the turbine disk, cools quickly in comparison to the disk. A reacceleration of the engine, which occurs in approximately ten seconds, adds rotational stress growth and blade thermal growth to the disk thermal growth, very little of which was lost due to the slow disk cooling rate. The net result is a hot blade tip radius greater than that of the supporting structure, in which case a rub occurs. This is shown graphically in Figures 14 and 15.

Elimination or minimization of the level of this rub does, therefore, establish both the installed cold clearance and the steady-state hot running clearance of the turbine system, since the depth of rub is directly a function of the starting radii of the shroud and the blade tips.

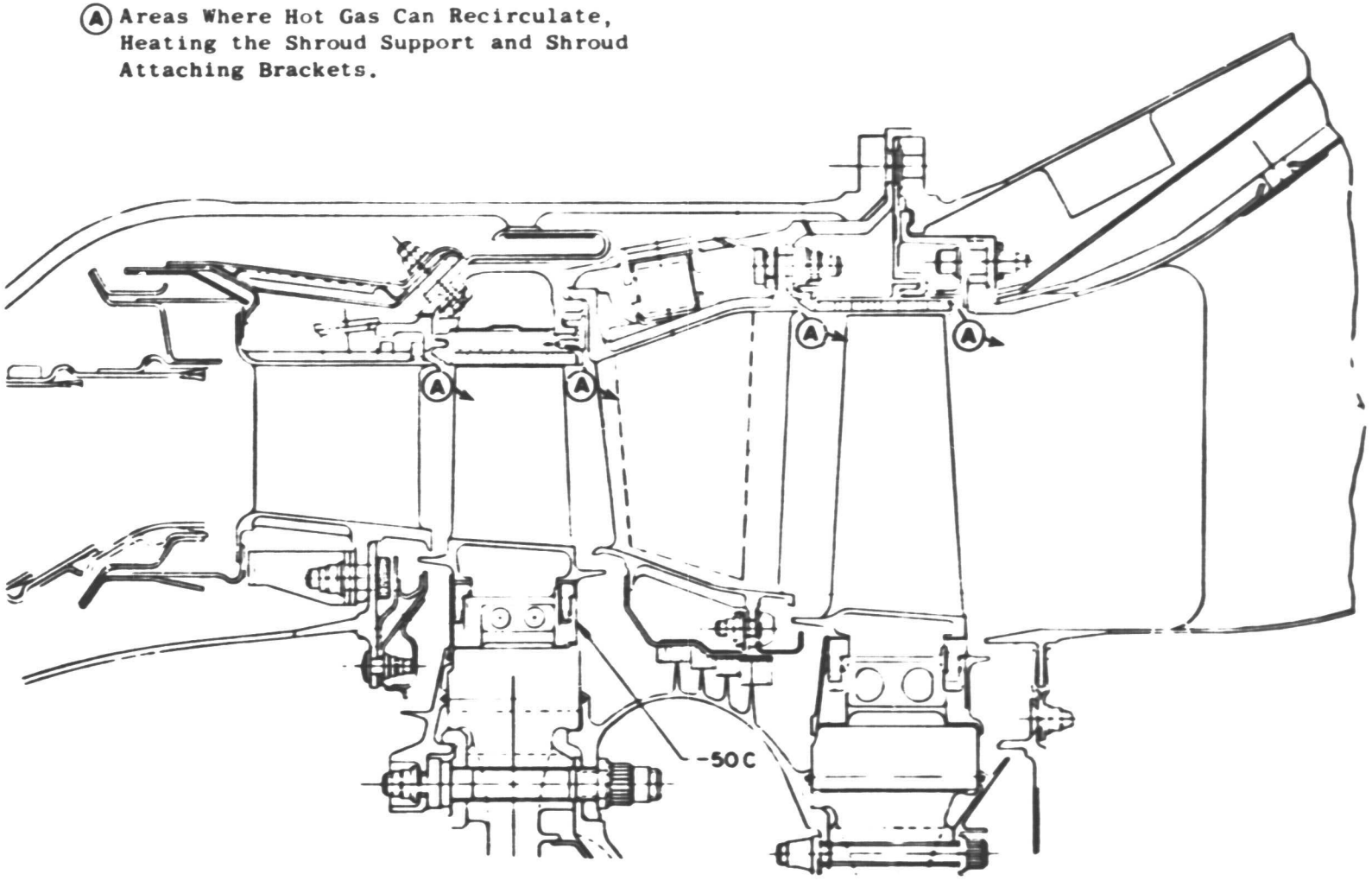

Figure 12. Current CF6-50 Turbine Support System Design.

(A) Areas Closed or Reduced to Lessen Hot Gas Recirculation
(B) Components Revised and Segmented to Shield and Insulate the Shrouds Support from Hot Gases

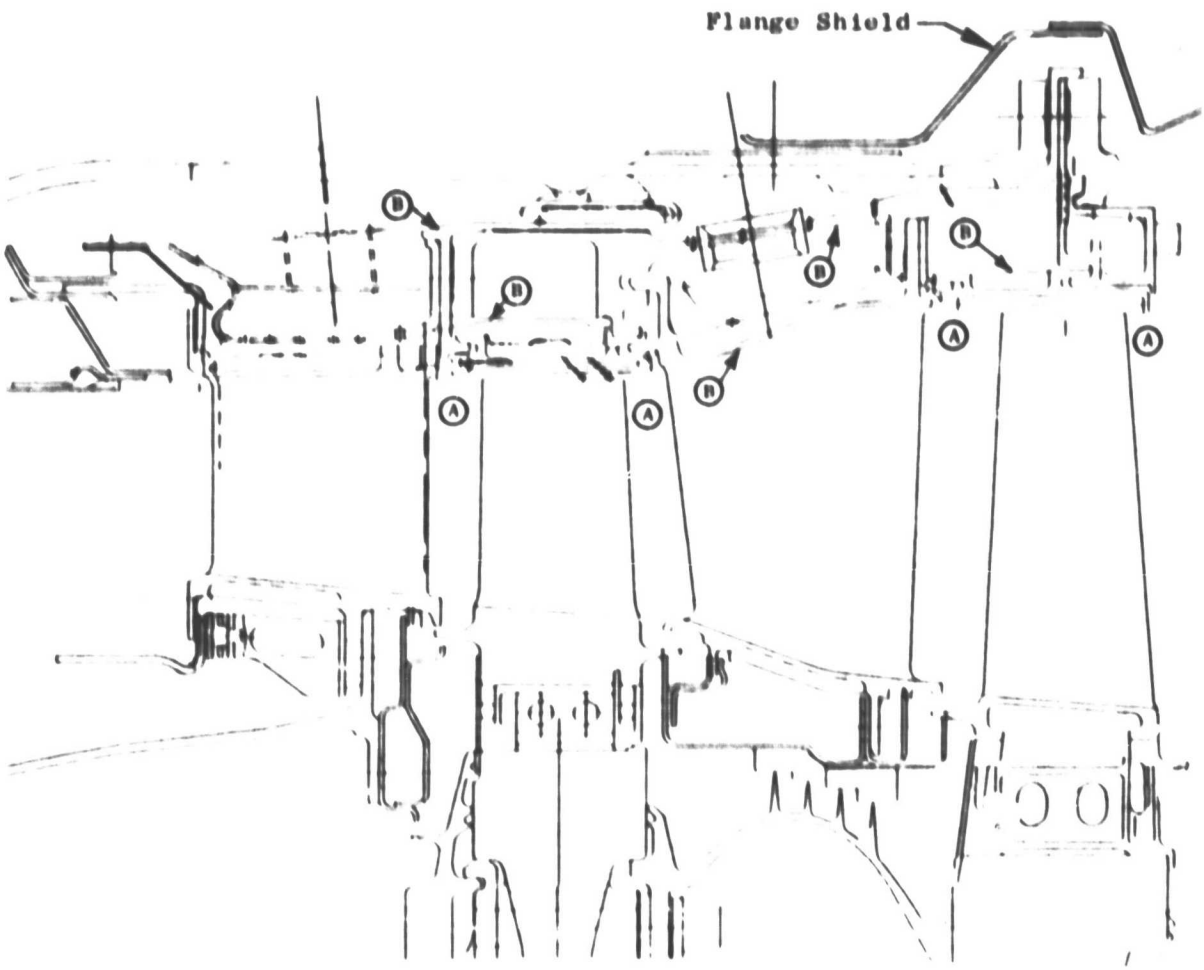

Figure 13. Revised Configuration - CF6-50 Turbine Support System.

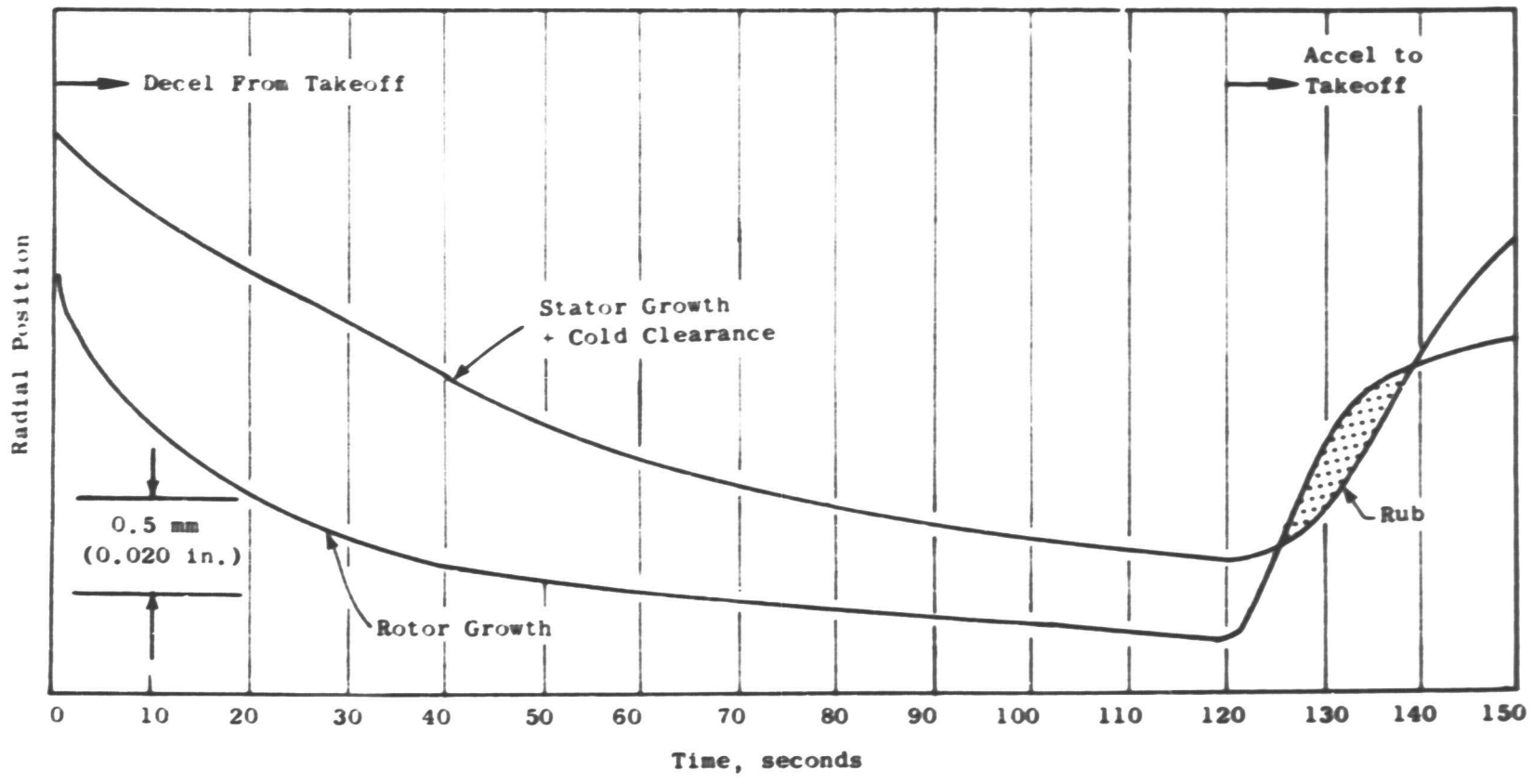

Figure 14. Typical Hot Rotor Reburst.

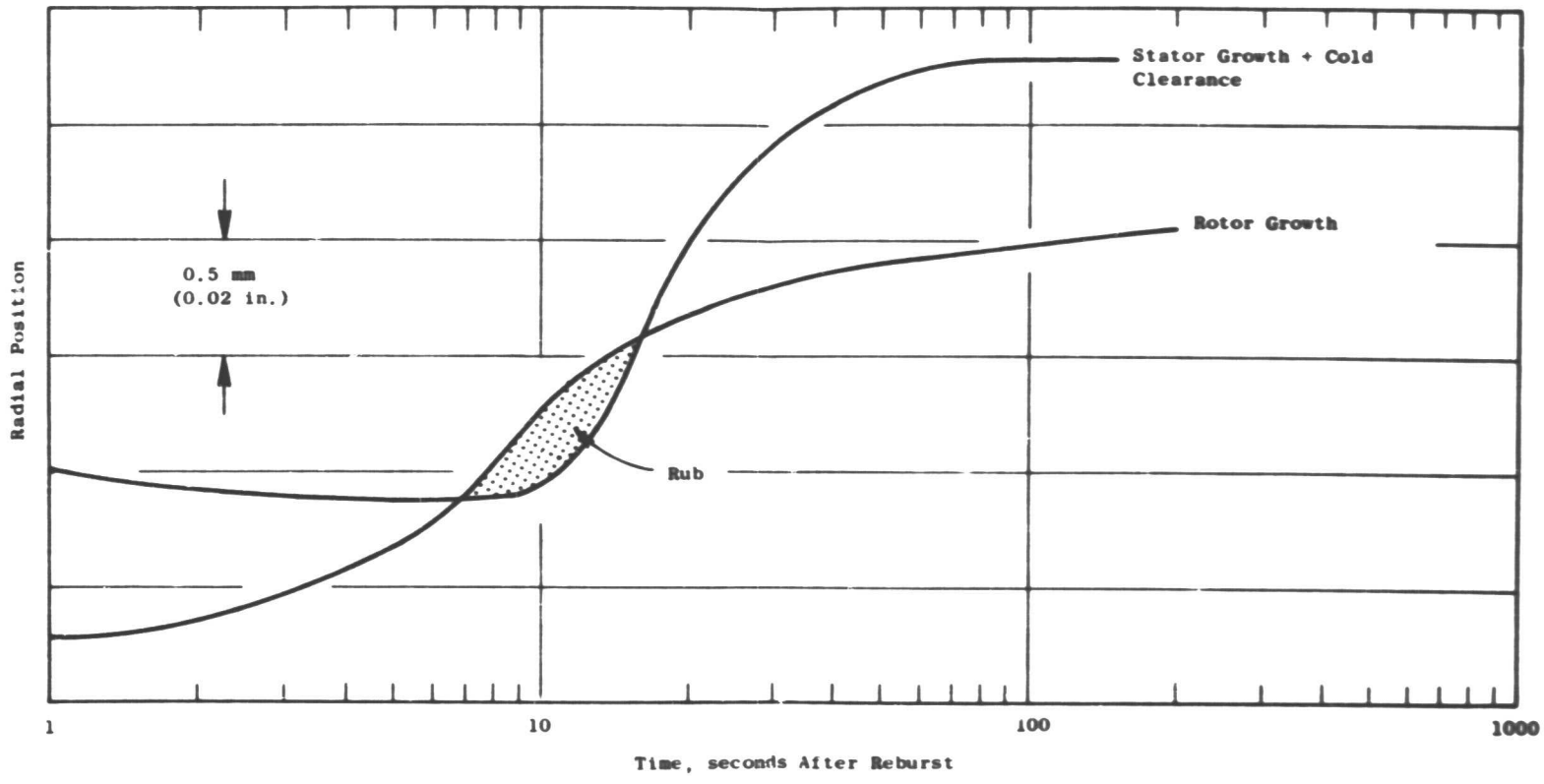

Figure 15. Typical Hot Rotor Reburst - 2 min After Decel from T/O to Idle.

Therefore, a modification of the shroud decel transient response rate, so as to slow down the radial inward growth rate of the shroud, increases the clearance margin on a reburst. Rub severity is, consequently, reduced so steady-state running clearances can be reduced. Accel and cruise clearances were evaluated as well to assure that no significant losses occur during these phases of operation.

Reduction in support structure radial excursion rate may be accomplished by increasing support mass, i.e., thermal inertia, by reduction in cooling cavity heat transfer to the supporting structure through the use of shielding or baffling or by substitution of support materials to achieve a more favorable thermal growth relationship. Figures 16 and 17 show analytically how the addition of mass and the inclusion of thermal baffling alter the support structure transient response. These figures also show how alteration of the support environment to reduced temperature levels affect clearances. The figures are graphs of rotor and stator response as a function of time for an accel from stabilized ground idle and a decel from steady-state take-off. The cold clearance between the Stage 1 blade and shroud is 2 mm (0.080 in).

HPT Shroud Materials

Alternate materials investigated included a class of alloys with "controlled" thermal expansion coefficients such as IN903, CTX1 and CTX2. These alloys possess a characteristic unique to ferromagnetic alloys; that is, an inflection point or "knee" in the thermal expansion coefficient curve. This "knee" occurs at approximately 427° C (800° F) as shown in Figures 18 and 19 which compare the thermal expansion characteristics of a typical turbine support alloy (IN718) with those of an alternate material (IN903).

This peculiarity of the thermal-expansion coefficient can be used to advantage since tighter clearances can be set at high power settings while maintaining more open clearances for reburst margin. These materials match closely the growths of the rotating structural components above 427° C, while below they lag the rotor growth. Therefore, an increase in the critical reburst clearance, as well as an increase in the minimum accel clearance can be achieved from their use. These transient clearance increases can be used to reduce rub levels or to reduce steady-state clearances. Figures 20, 21, and 22 show the effect of IN903 on turbine clearances for an accel, a decel and a two-minute reburst, and can be compared with Figures 23, 24, and 25 which are the clearance responses during an accel, a decel, and a two-minute reburst for the current IN718 stator.

The cold clearance between the Stage 1 blade and shroud necessitated by the controlled thermal expansion coefficient alloy is 2.82 mm (0.111 in) while that of the current stator is 2.03 mm (0.080 in).

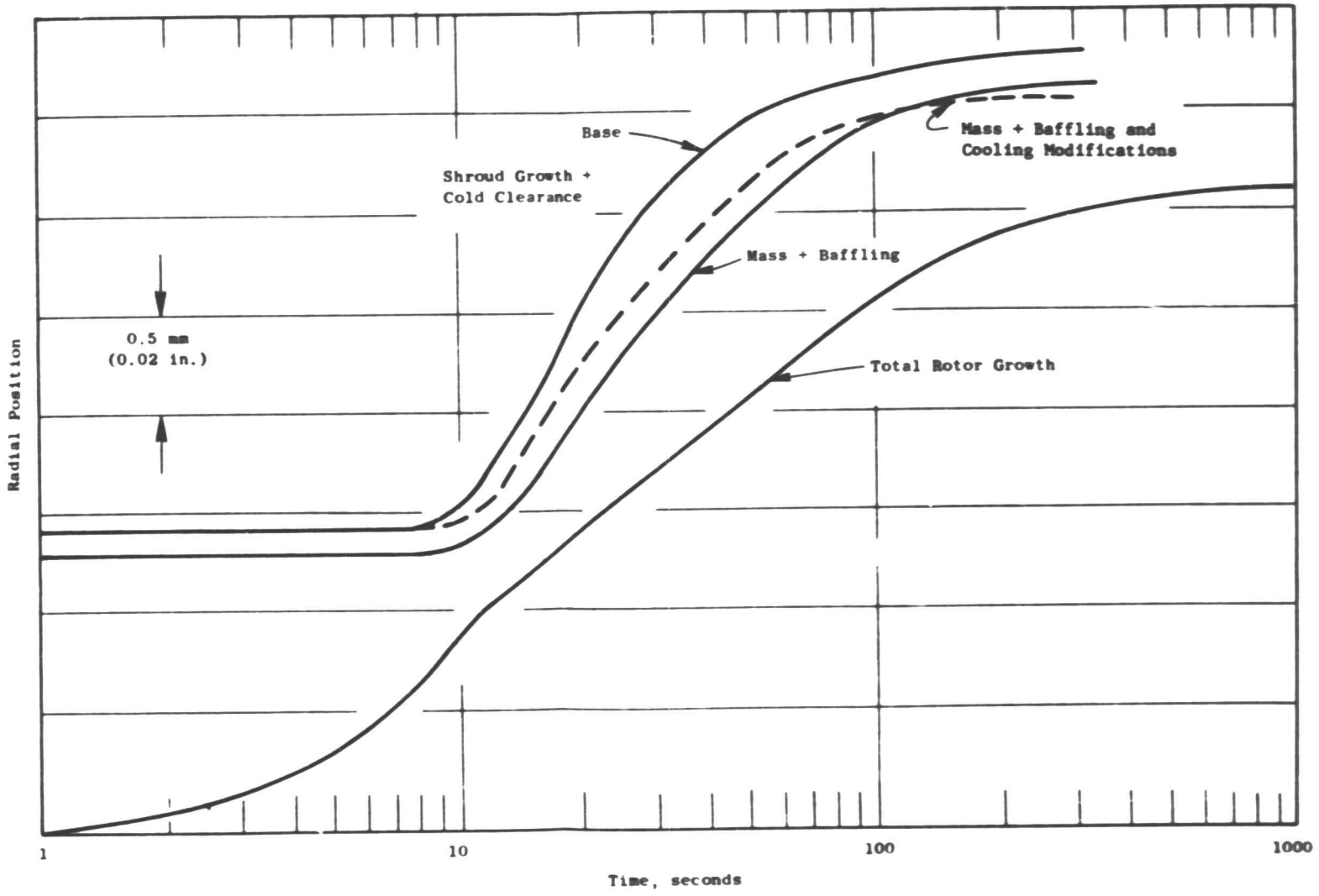

Figure 16. Typical Accel Transient - Stage 1 HPT Support Structure.

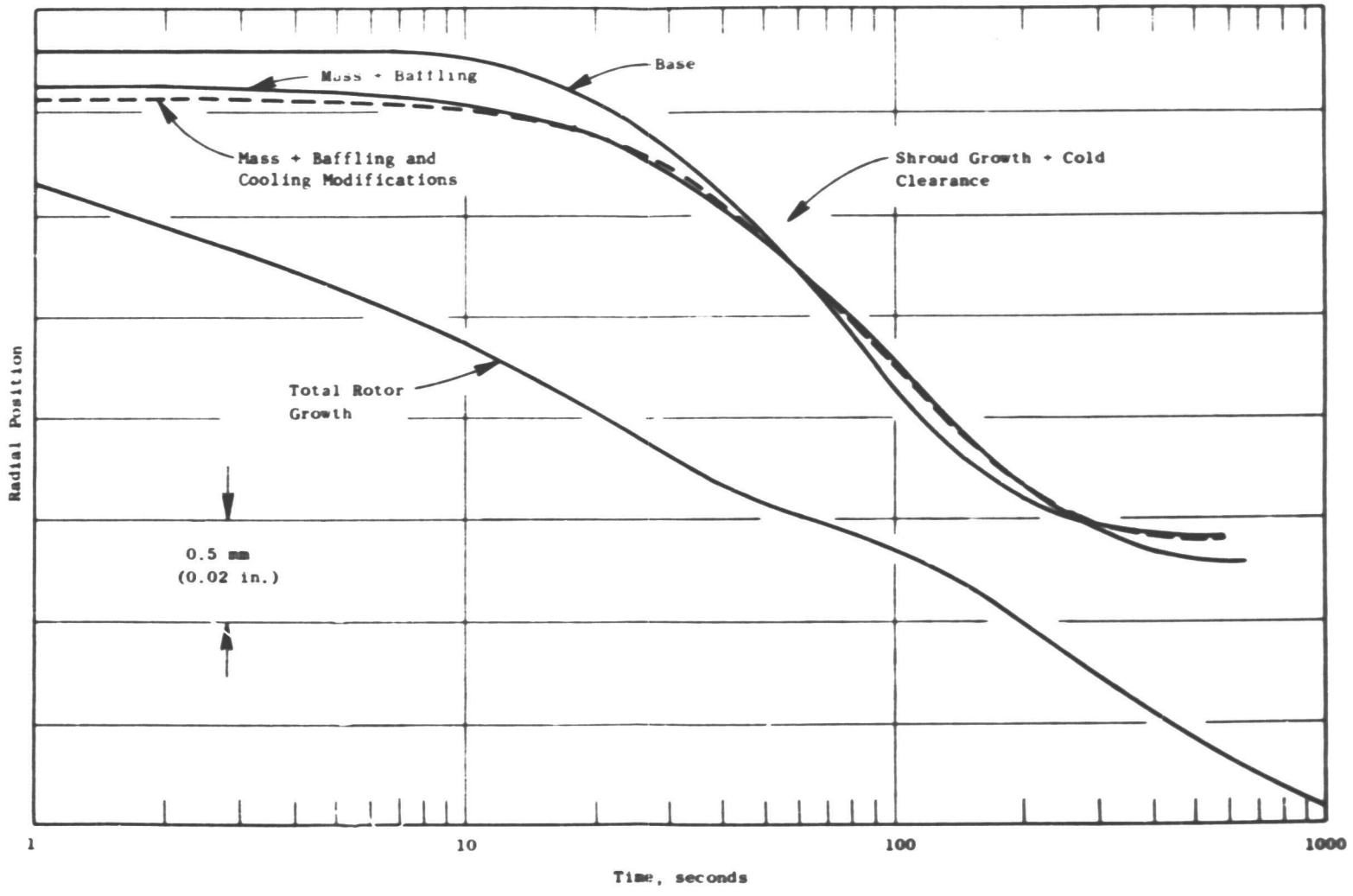

Figure 17. Typical Decel Transient - Stage 1 HPT Support Structure.

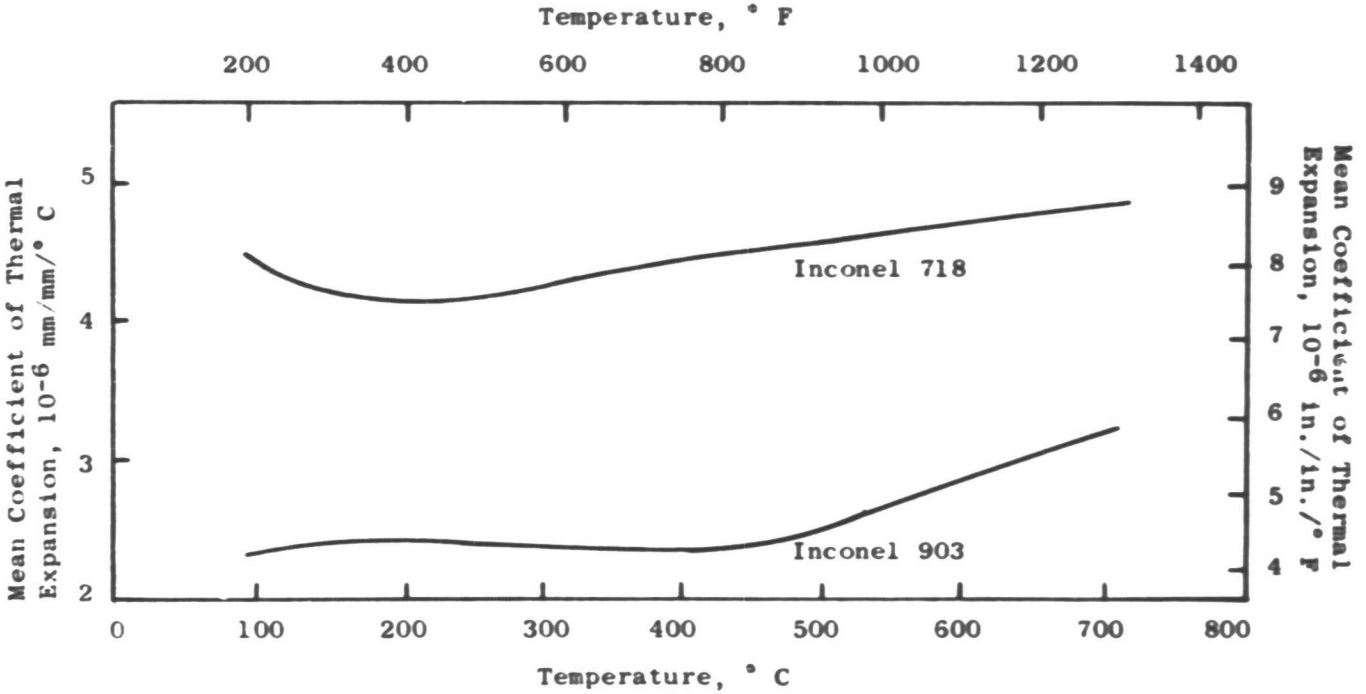

Figure 18. Thermal Expansion Characteristics - Coefficient of Expansion.

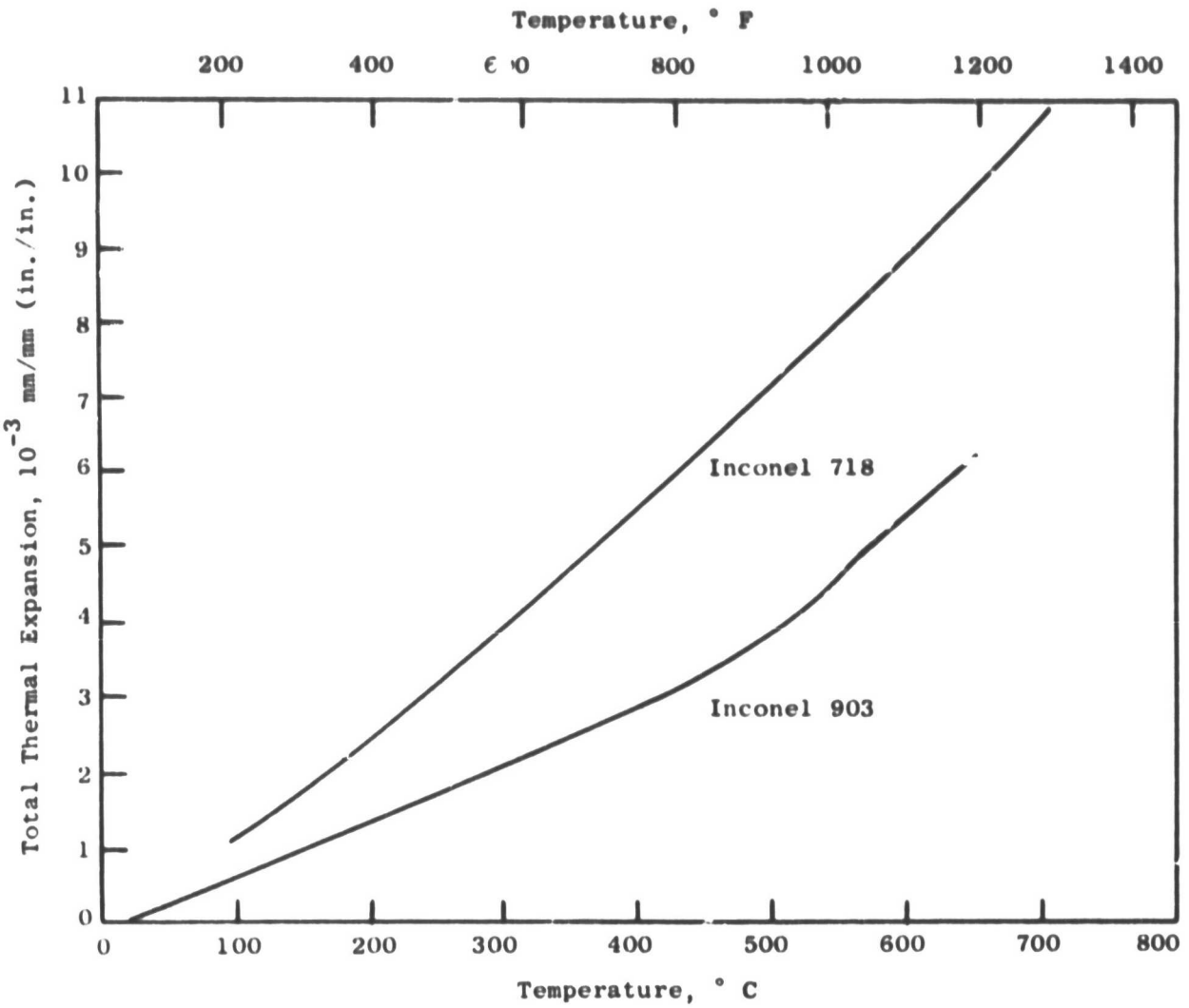

Figure 19. Thermal Expansion Characteristics - Total Thermal Expansion.

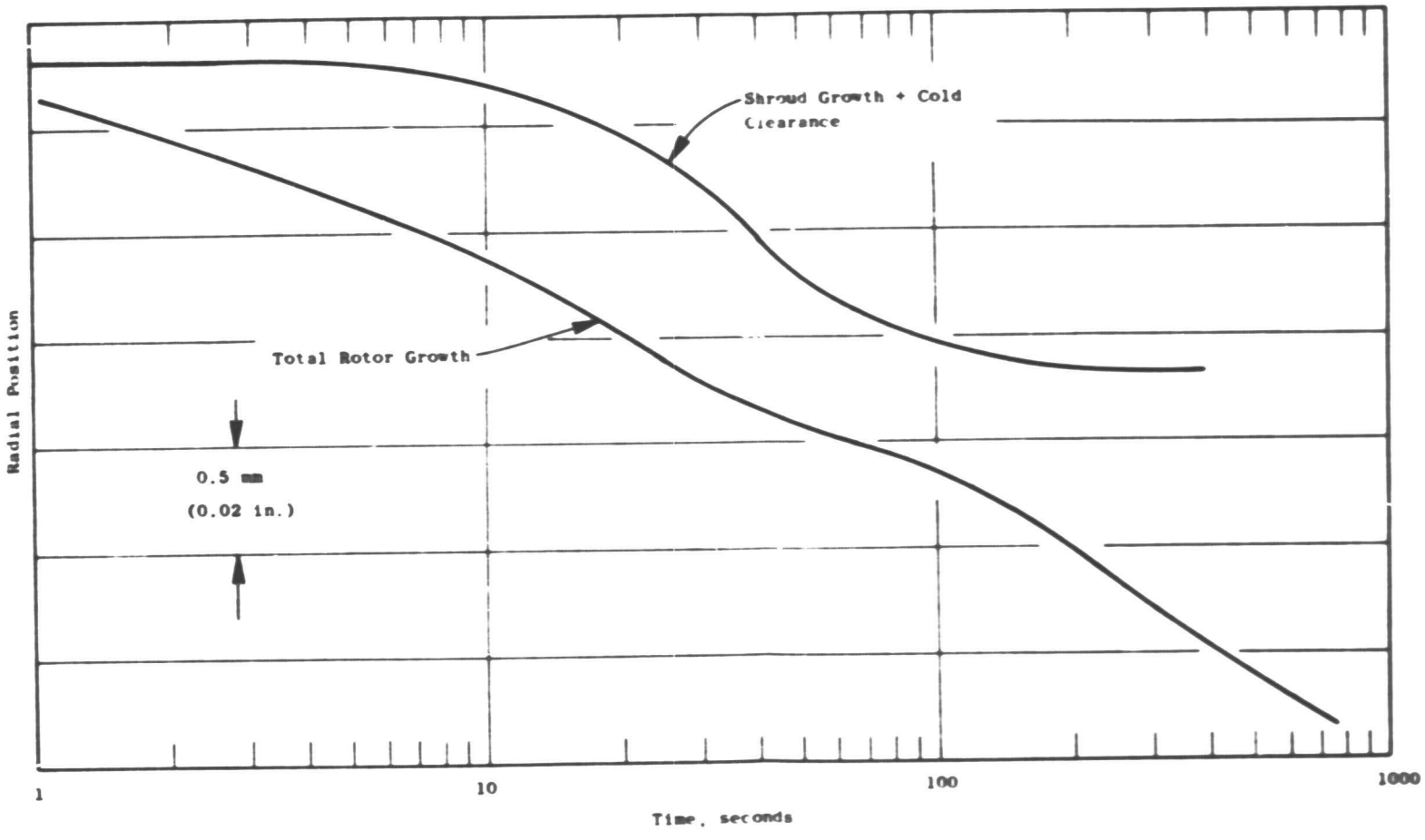

Figure 20. Typical Decel Transient - Stage 1 HPT I-903 Support Structure.

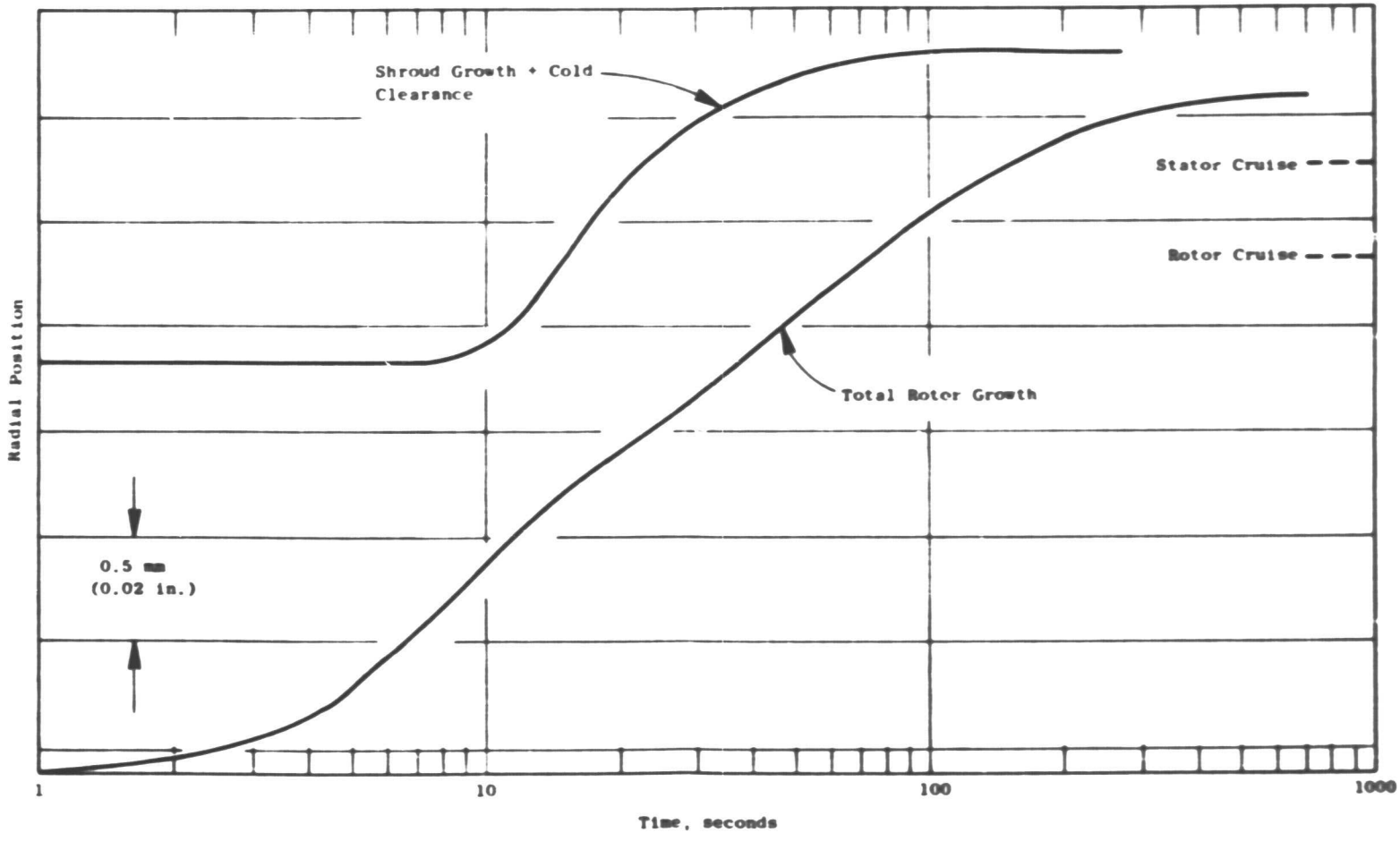

Figure 21. Typical Accel Transient - Stage 1 HPT I-903 Support Structure.

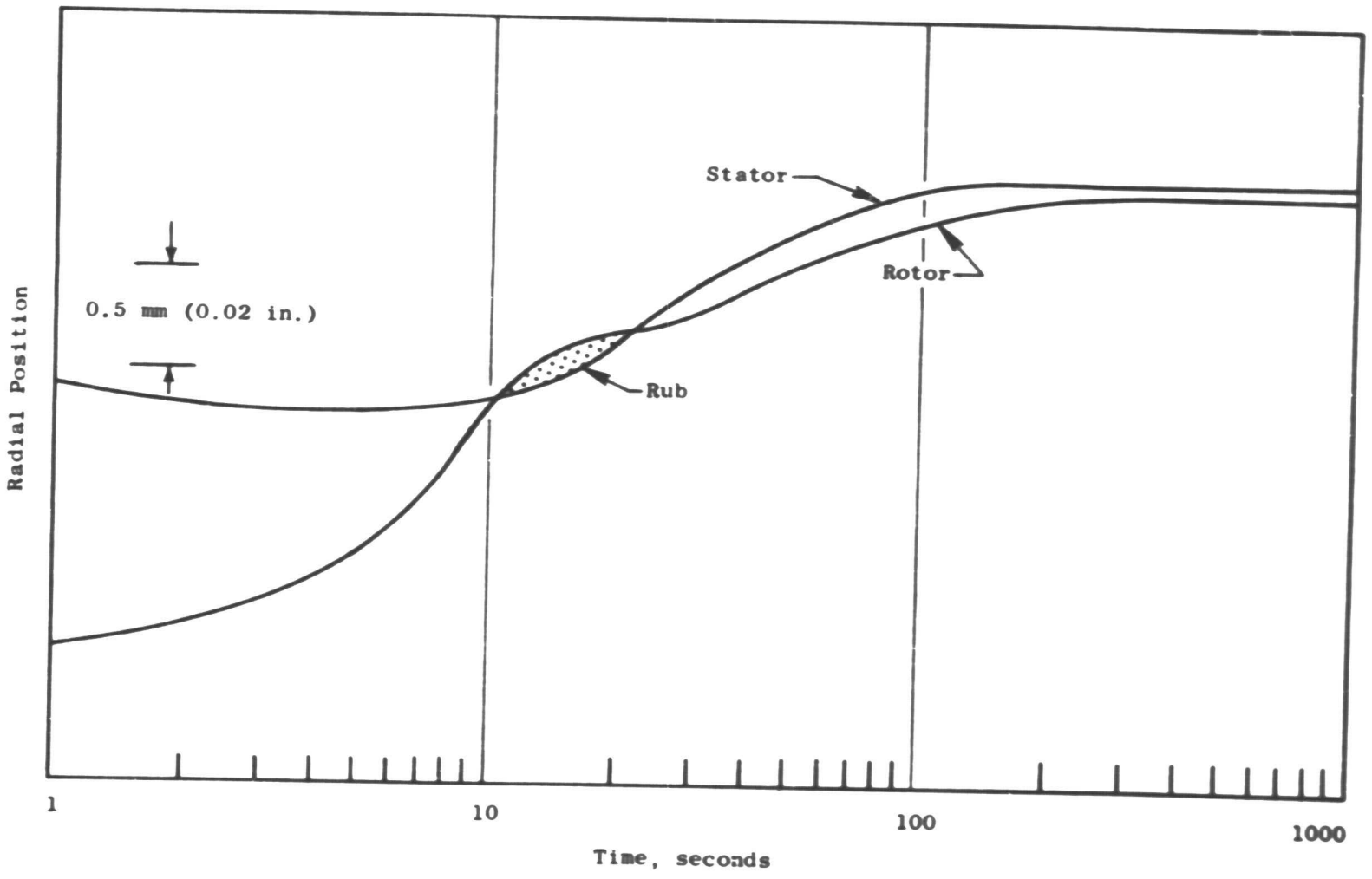

Figure 22. Typical 2 Minute Reburst - Stage 1 HPT I-903 Support Structure.

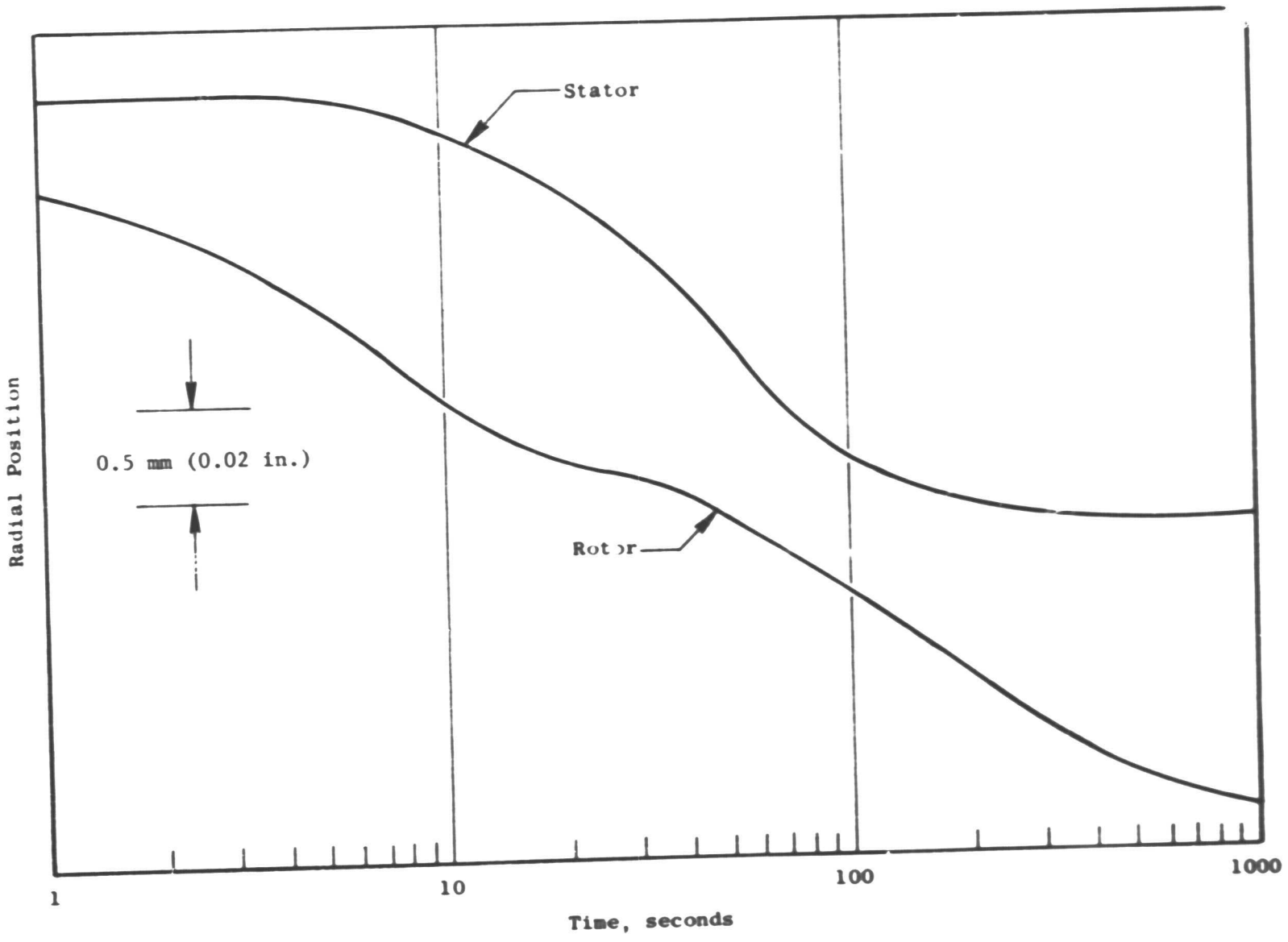

Figure 23. Current Configuration - Inco 718, Chop.

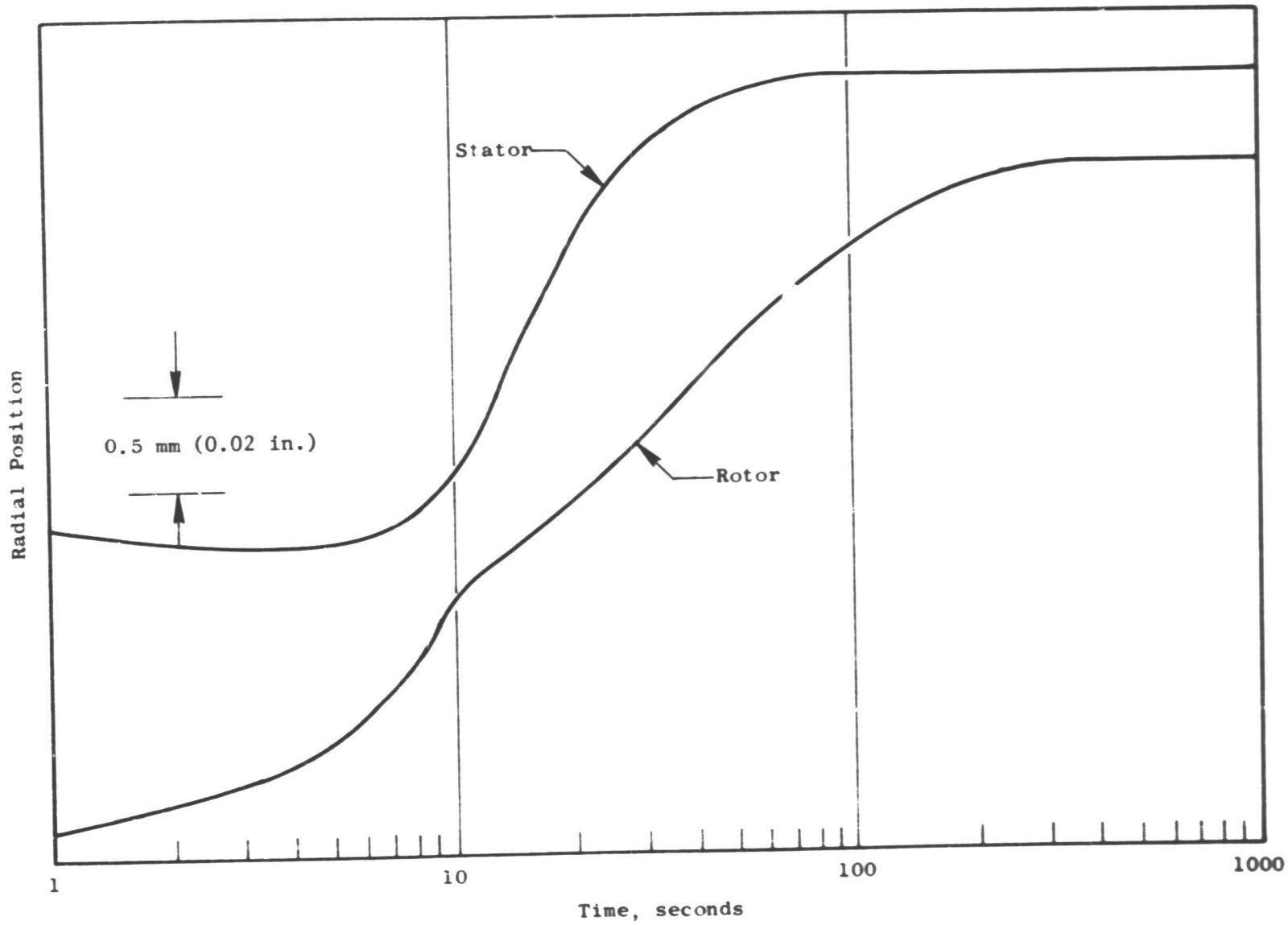

Figure 24. Current Configuration - Inco 718, Burst.

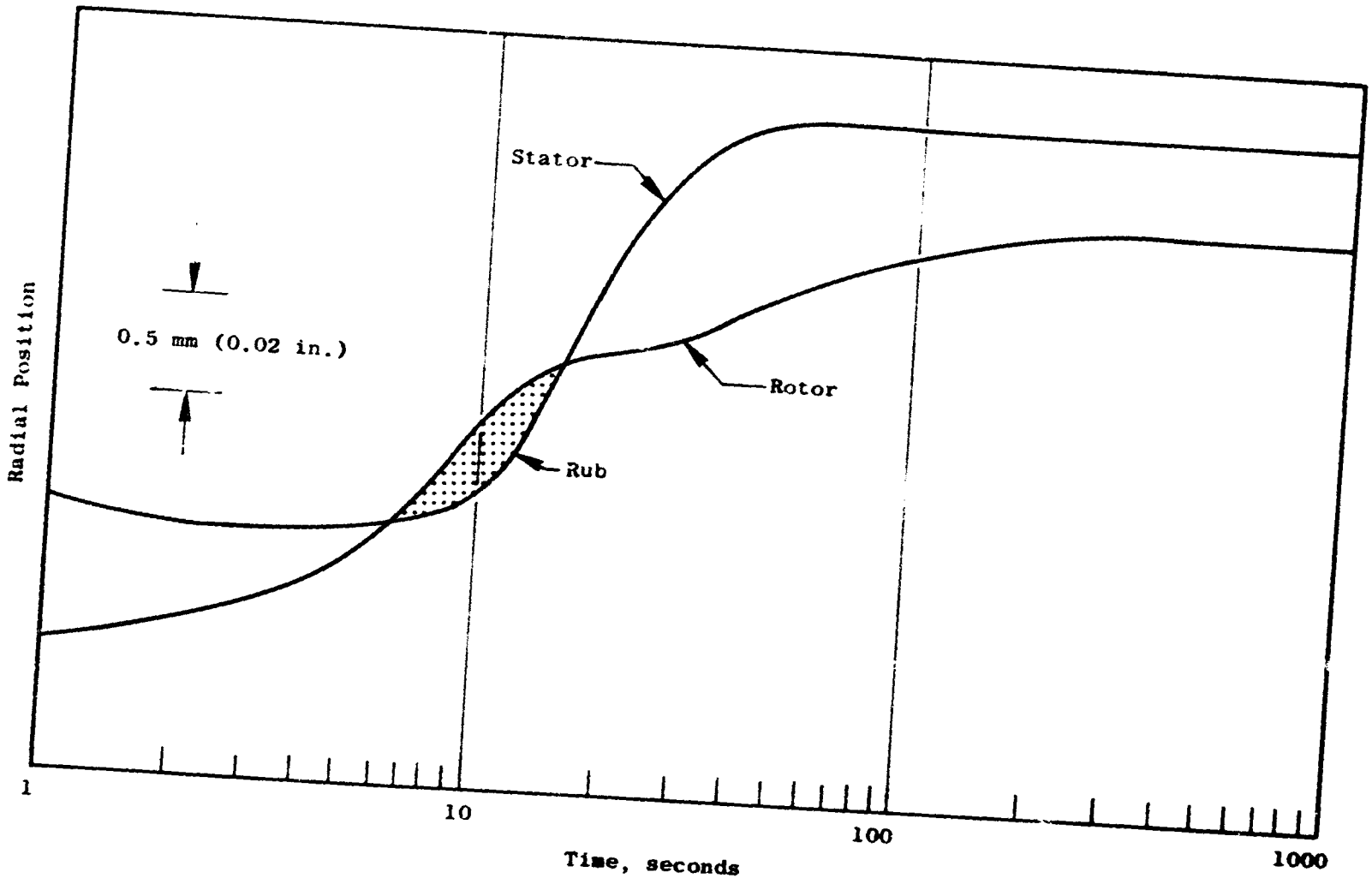

Figure 25. Current Configuration - Inco 718, Reburst.

The following improvements are possible using the controlled thermal expansion alloy:

Cruise: 0.53 mm (0.021 in) less clearance
Takeoff: 0.38 mm (0.015 in) less clearance
Reburst margin improvement: 0.25 mm (0.010 in)

The controlled thermal expansion coefficient alloys, IN903 and CTX1, that were studied during the preliminary design phase of this program, unfortunately have some rather severe limitations. Material testing showed that these alloys exhibited both notch sensitivity and a "stress corrosion" phenomenon. Another concern was that because these are materials which do not contain chromium, coating would be required to provide oxidation protection in most environments where their use would be beneficial.

The stress corrosion phenomenon manifested itself in a failure mode which is analogous to stress corrosion cracking in, for example, titanium alloys. Both IN903 and CTX1 when exposed to moderate stresses and high temperatures 480-700° C (900° to 1300° F), failed by intergranular failure. This phenomenon is called stress-accelerated grain boundary oxidation.

Although other materials with the controlled thermal expansion coefficient characteristics desired, such as CTX2, were under development at design "freeze" time for procurement purposes, it was decided not to use IN903, CTX1 or CTX2 in this engine improvement program. The long lead times required to obtain material, manufacture hardware, instrument hardware, assemble, etc., necessitated this decision.

However, it was decided to change the material of the shroud supporting structure from IN718 to WASPALOY. The coefficient of thermal expansion of WASPALOY allows some improvement in the decel response rate of the structure and when coupled with added mass, baffling, and cavity heat transfer improvements, provides a definitely improved shroud supporting structure.

The response of the WASPALOY structure is shown in Figure 26 for a decel from steady state takeoff to ground idle, in Figure 27 for an accel from ground idle and in Figure 28 for a two-minute reburst.

A comparison of the pretest analytical results for the current design to the redesigned WASPALOY stator is presented in Table 1, which assumes a constant 0.38 mm (0.015 in) rub resulting from a reburst.

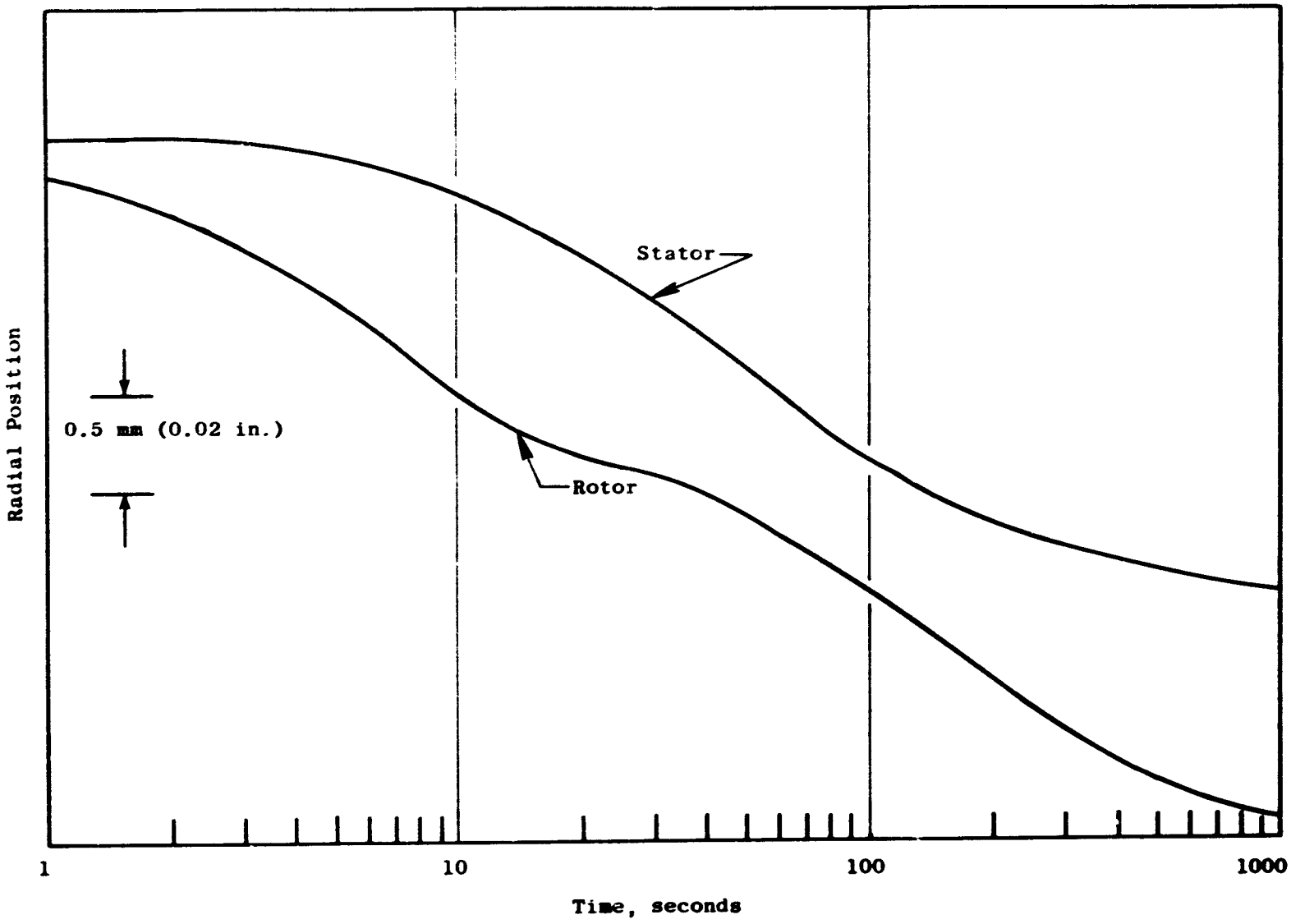

Figure 26. Square Support - Waspaloy, Decel.

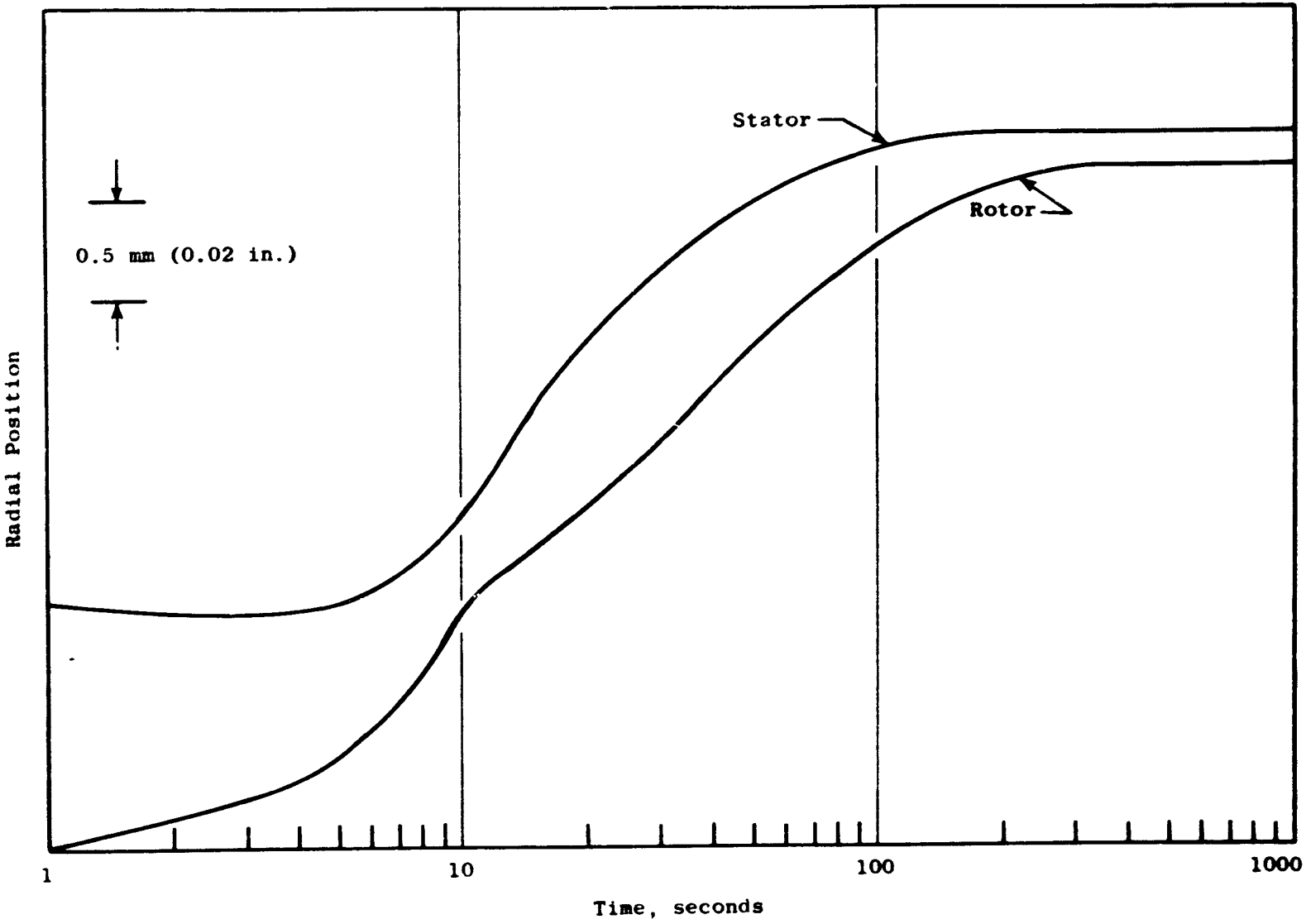

Figure 27. Square Support - Waspaloy, Accel.

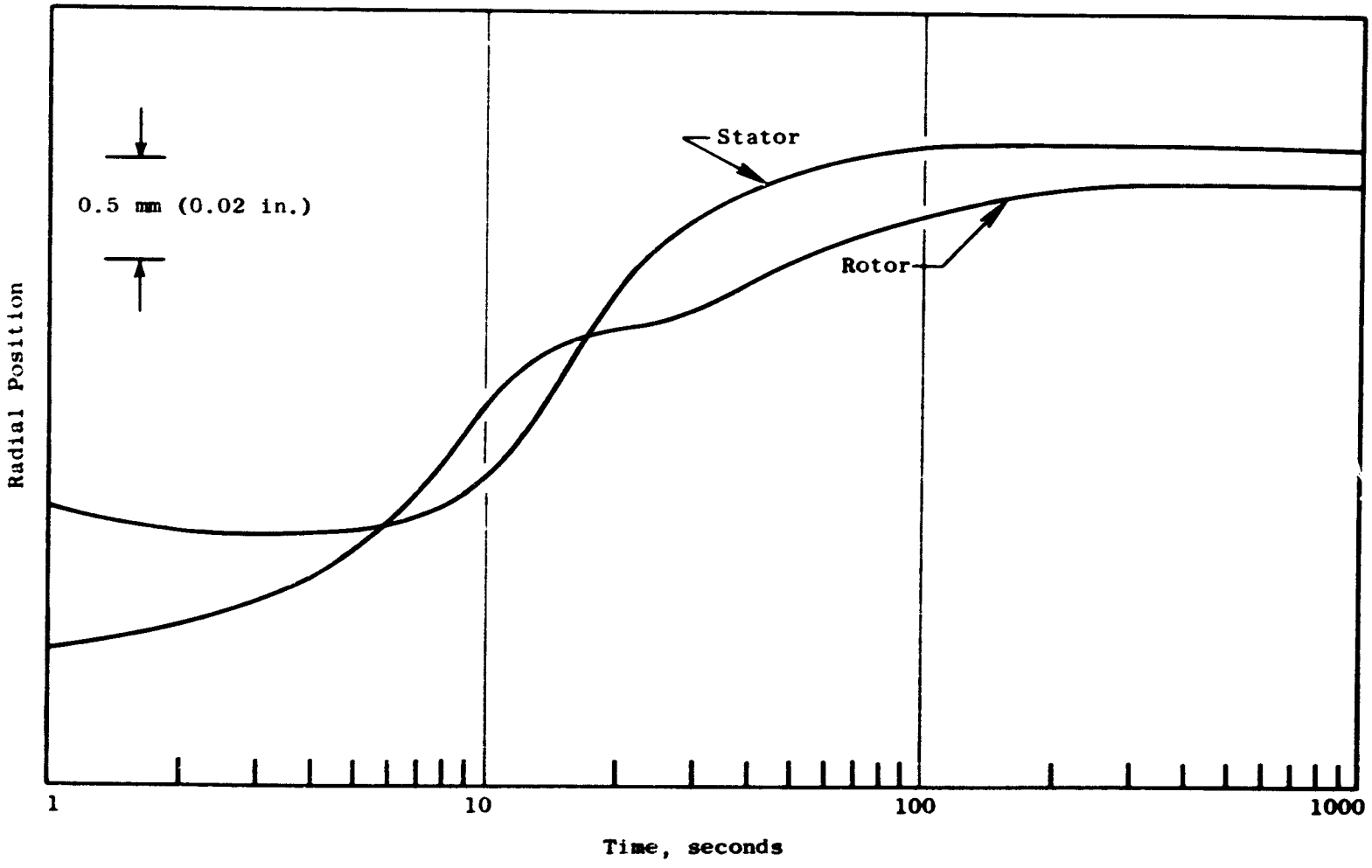

Figure 28. Square Support - Waspaloy, Reburst.

Table I. Clearance Predictions, mm (in).

	Cruise	Takeoff	Min. Accel	Min. Decel	Reburst	Cold Clearance
Current Design	0.74 (0.029)	0.46 (0.018)	0.64 (0.025)	0.71 (0.028)	-0.38 (-0.015)*	2.03 (0.080)
Redesign WASPALOY	0.33 (0.013)	0.28 (0.011)	0.46 (0.018)	0.69 (0.027)	-0.38 (-0.015)*	1.85 (0.073)

* Indicates rub

4.0 INSTRUMENTED ENGINE TEST

The objectives of this test program were to evaluate the improved high pressure turbine stator and turbine midframe performance improvement due to reduced blade-to-shroud clearance.

4.1 TEST SETUP

The test vehicle was a CF6-50C engine S/N 455-507, Build 20. The component configuration is described below:

• Front Frame	A standard CF6-50C front frame with rake pad capability to record compressor inlet characteristic, if needed.
• Compressor Stator	Standard CF6-50C compressor stator.
• Compressor Rotor	Standard CF6-50C rotor.
• Compressor Rear Frame	A CF6-50C frame modified to receive clearanceometer probes, (Figure 29).
• Combustor	A CF6-50C combustor.
• Fuel Nozzles	CF6-50C fuel nozzles.
• Stage 1 High Pressure Turbine Nozzle Assembly (including mini-nozzle)	Improved roundness control CF6-50 assembly.
• Stage 2 High Pressure Turbine Nozzle Assembly	Improved roundness control CF6-50C configuration modified to receive clearanceometer probes (Figure 29).
• High Pressure Turbine Rotor	CF6-50C configuration.
• Turbine Midframe	Improved roundness control CF6-50C frame.
• Low Pressure Turbine Nozzle	CF6-50C configuration.
• Exhaust Nozzle	CF6-50C configuration.

4.2 INSTRUMENTATION

Instrumentation was used to measure engine performance and to monitor engine operation. The instrumentation is broken down into four groups:

general instrumentation, aerodynamic instrumentation, turbine structural instrumentation, and clearanceometer instrumentation.

General

- Barometric Pressure - The local barometric pressure measured using a recording microbarograph.
- Humidity - The absolute humidity measured in grains of moisture per pount of dry air using a humidity indicator.
- Cell Static Pressure (P_0) - Test cell static pressure measured at four locations in the cell.
- Fan Speed (XNL) - Low pressure rotor speed measured using two fan-case-mounted fan-speed sensors.
- Core Speed (XNH) - High pressure rotor speed measured using engine core-speed sensor driven off the end of the lube and scavenge pump.
- Main Fuel Flow (WFM) - Volumetric flowmeter, facility mounted.
- Verification Fuel Flow (WFV) - Second fuel flowmeter mounted in series with WFM.
- Fuel Temperature - Temperature of fuel measured at the facility flowmeters using a single chromel/alumel probe in the fuel line.
- Fuel Sample Specific Gravity (SGSAMP) - Specific gravity of the fuel sample measured using a hydrometer.
- Fuel Sample Temperature (TSAMP) - Fuel sample temperature measured during the specific gravity measurement.
- Fuel Lower Heating Value (LHV) - Lower heating value of the fuel sample as determined by a bomb calorimeter.
- Thrust (FG) - Thrust-frame, axial force measured using three strain-gage-type load cells for redundant measurement.
- Variable Stator Vane Position (VSV) - Readout of the Linear Variable Displacement Transducer (LVDT) attached to the high pressure compressor variable stator pump handle.
- Variable Bleed Valve Position (VBV) - Readout of the LVDT attached to the variable bleed valve actuation mechanism.

Aerodynamic Pressure and Temperature

The following rakes, probes, and static pressure taps were installed to measure airflow temperature and pressure as required to define component

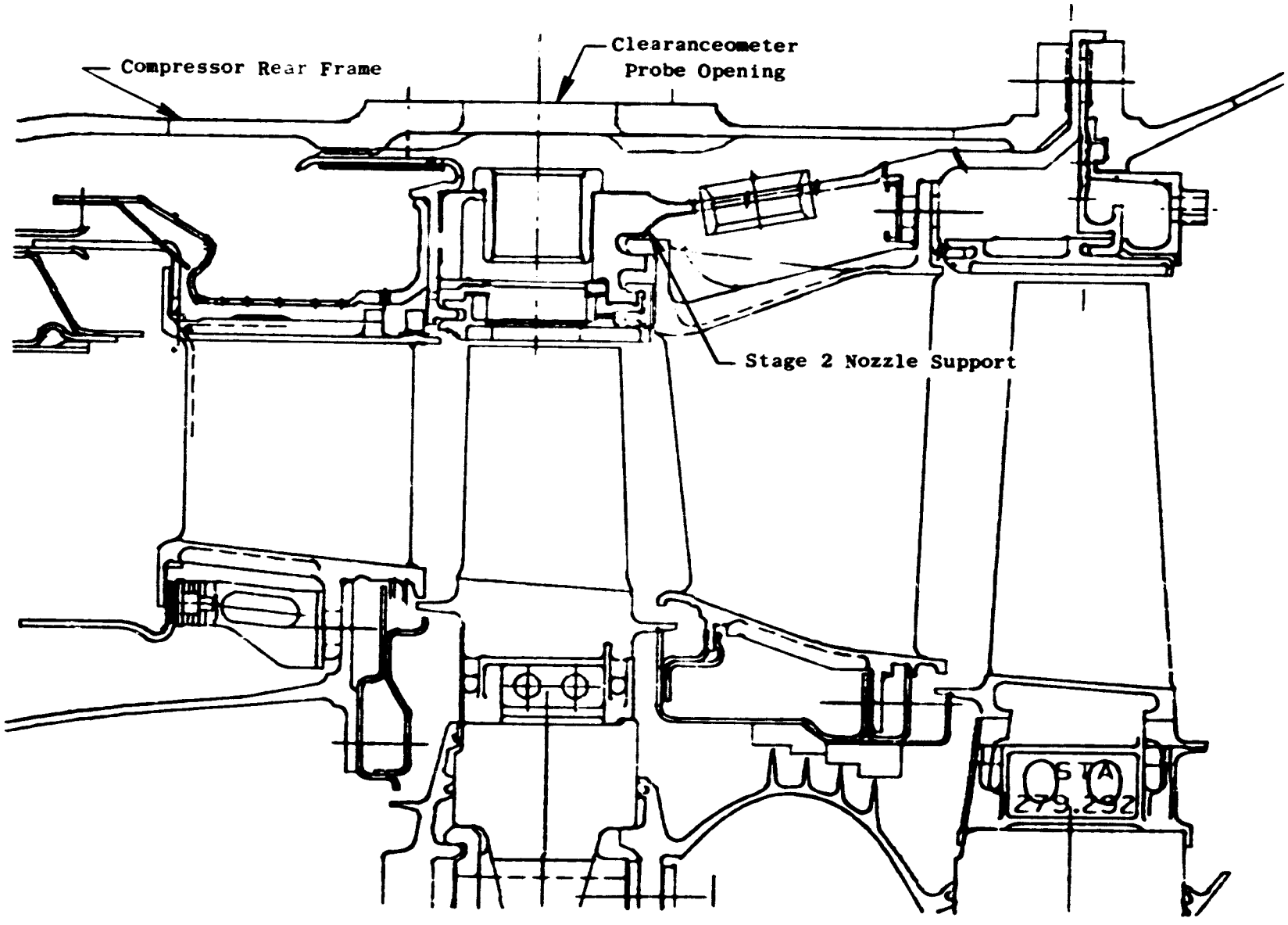

Figure 29. Improved Design Modified to Receive Clearanceometer Probes.

performance. (See Figure 30).

- Fan Inlet (Plane 1)

  Bellmouth rakes were installed to measure static pressure and total pressure at the fan inlet. Four rakes, each having six total pressure probes, six static pressure probes were used. Total temperature was obtained by averaging the output of 40 thermocouples mounted on the bellmouth FOD screen.

- Booster Discharge (Plane 23)

  Five arc rakes, each having six temperature and six pressure probes, were installed to measure booster discharge total temperature and total pressure. Ten taps were installed to measure booster discharge static pressure.

- Compressor Inlet (Plane 25)

  Five flow-path-wall static pressure taps were installed.

- Compressor Discharge (Plane 3)

  Five of the borescope port plugs in the compressor rear frame were modified to permit compressor discharge static pressure measurement. A single 5-element thermocouple probe was used to measure compressor discharge temperature.

- Low Pressure Turbine Inlet (Plane 49)

  Temperature in this plane was measured by eleven 5-element rakes with individual probe readout to permit monitoring of temperature profiles. Pressure was measured using five probes, each having five elements all feeding a single fitting.

- Low Pressure Turbine Discharge (Plane 50)

  Low pressure turbine discharge pressure was measured using four rakes having five elements each.

  Structures

  HPT stator thermocouples. 24 imbedded metal and 6 air thermocouples.
  HPT stator pressure probes. 4 basket-type pressure probes in the Stage 1 shroud cooling air supply cavity.
  Engine structure thermocouples.
  Engine structure cooling air temperatures and pressures.

- Low Pressure Turbine Interstage (Stage 1)

  Temperature and static pressure were measured at each of three circumferential locations at the Stage 1 stator exit.

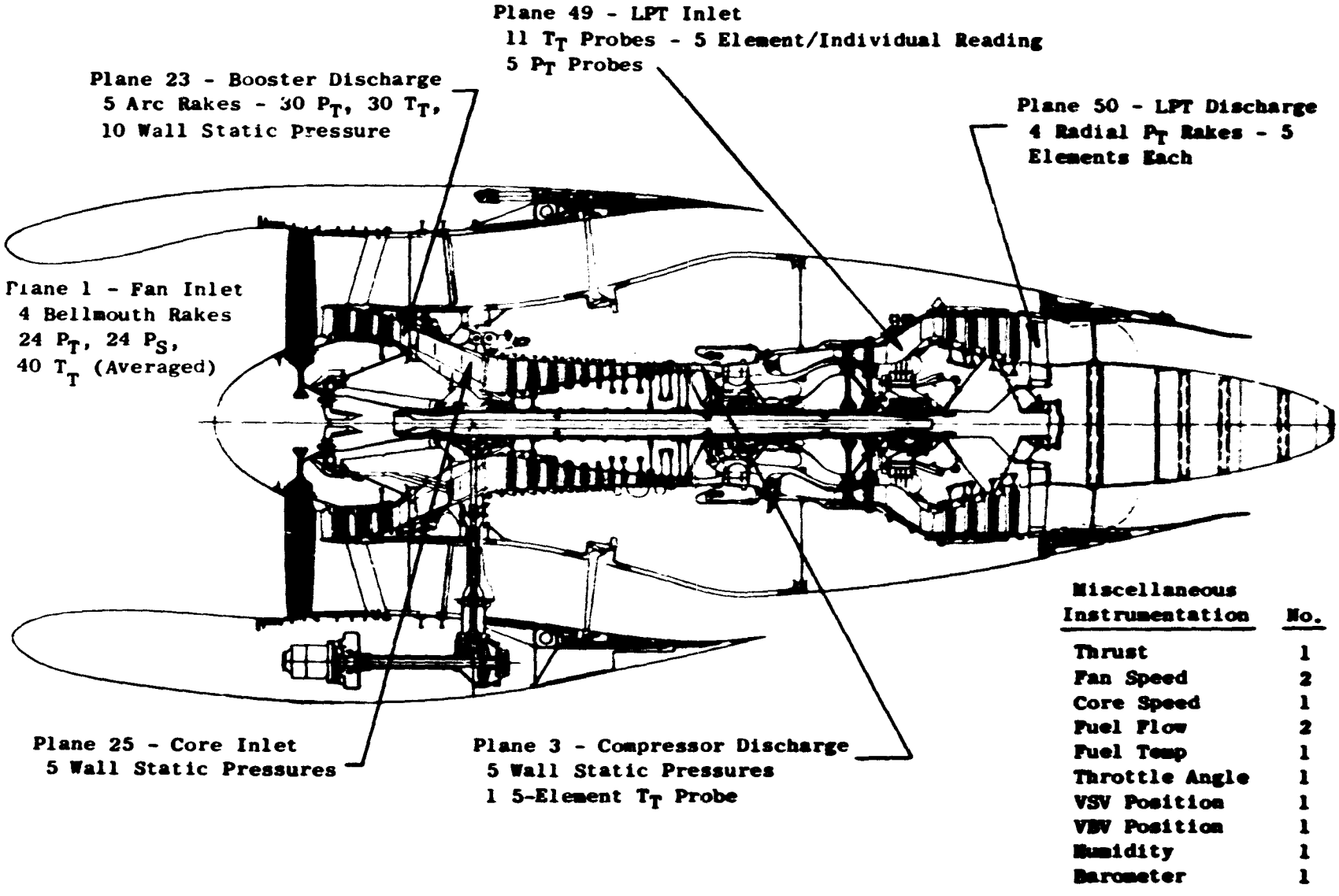

Miscellaneous Instrumentation	No.
Thrust	1
Fan Speed	2
Core Speed	1
Fuel Flow	2
Fuel Temp	1
Throttle Angle	1
VSV Position	1
VBV Position	1
Humidity	1
Barometer	1

Figure 30. Instrumented Engine Test Instrumentation.

- **LPT Case Thermocouples**

  A total of 32 embedded thermocouples were installed in the first two case hooks and 40 skin thermocouples were applied to the case exterior.

Clearanceometer Instrumentation

The clearanceometers were located at eight circumferential positions as shown in Figure 31. The high pressure turbine stator on the test vehicle was modified to receive the probes. The reworked stator components included: Stage 1 shrouds, Stage 2 nozzle support, Stage 1 nozzle impingement ring and 10th Stage air seal as shown in Figure 29.

Each clearanceometer probe was individually calibrated and checked during assembly on the HPT stator. A final reference calibration was obtained during initial cold rotation and motoring of the engine.

A proven light-beam triangulation technique was utilized for the clearance measuring sensors. Data were collected for fixed-time intervals and individual blade clearances were obtained from each probe. Individual probe processors were used to store data from blade tips and the processor calculated blade minimum, maximum and average clearances from the total collected data. A high speed data tape recorder was also used to independently record individual blade clearances.

4.3 TEST FACILITY

All testing was conducted in Test Cell 2, Building 500, at the General Electric Company plant in Evendale, Ohio. The engine was mounted in an overhead frame consistent with all CF6-50 engines. A photograph of the engine installed in the test cell is shown in Figure 32.

Like most Building 500 cells, Cell 2 has access to the data recording systems in the Instrumentation Data Room. In addition to the standard test cell equipment, a clearanceometer probe cooling system was provided which utilized engine compressor bleed air. A microcomputer and high speed signal processor were used to collect and record the clearanceometer data.

The data acquisition and processing system used in Evendale consists of a Cell System and a Site System. The Cell System performs steady-state and transient data acquisition, conversion to engineering units, quick-look performance calculations, and short-term storage. Converted data is automatically transmitted to the Site System for further on-line processing and hard-copy output. The Site System utilizes a data-base concept for efficient storage, retrieval, and reprocessing of current and historical data. In addition, data may be transmitted to the General Electric Evendale Time - Sharing Computer Center for further processing such as cycle deck analysis and comparison.

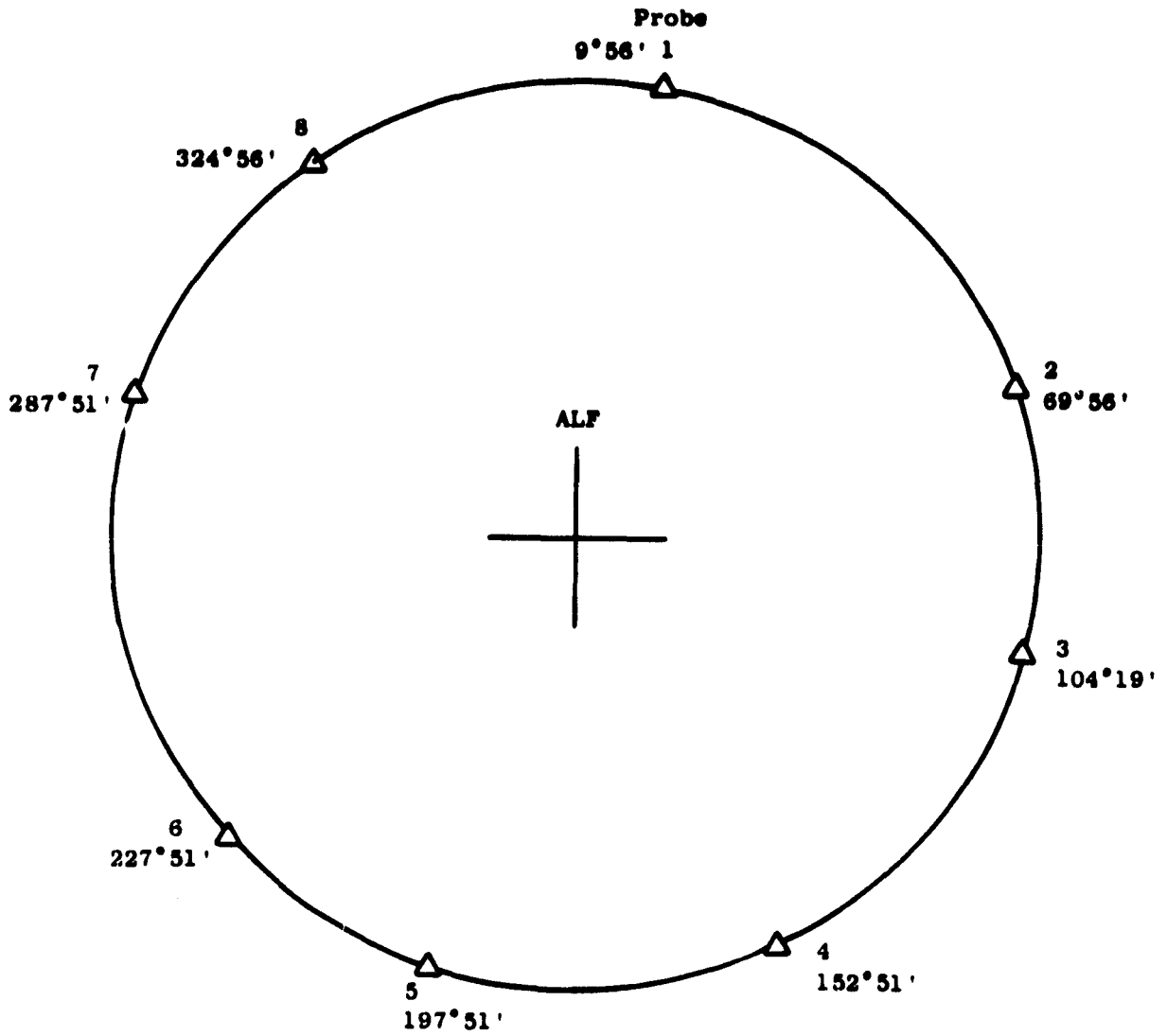

Figure 31. Probe Angular Position, Aft Looking Forward.

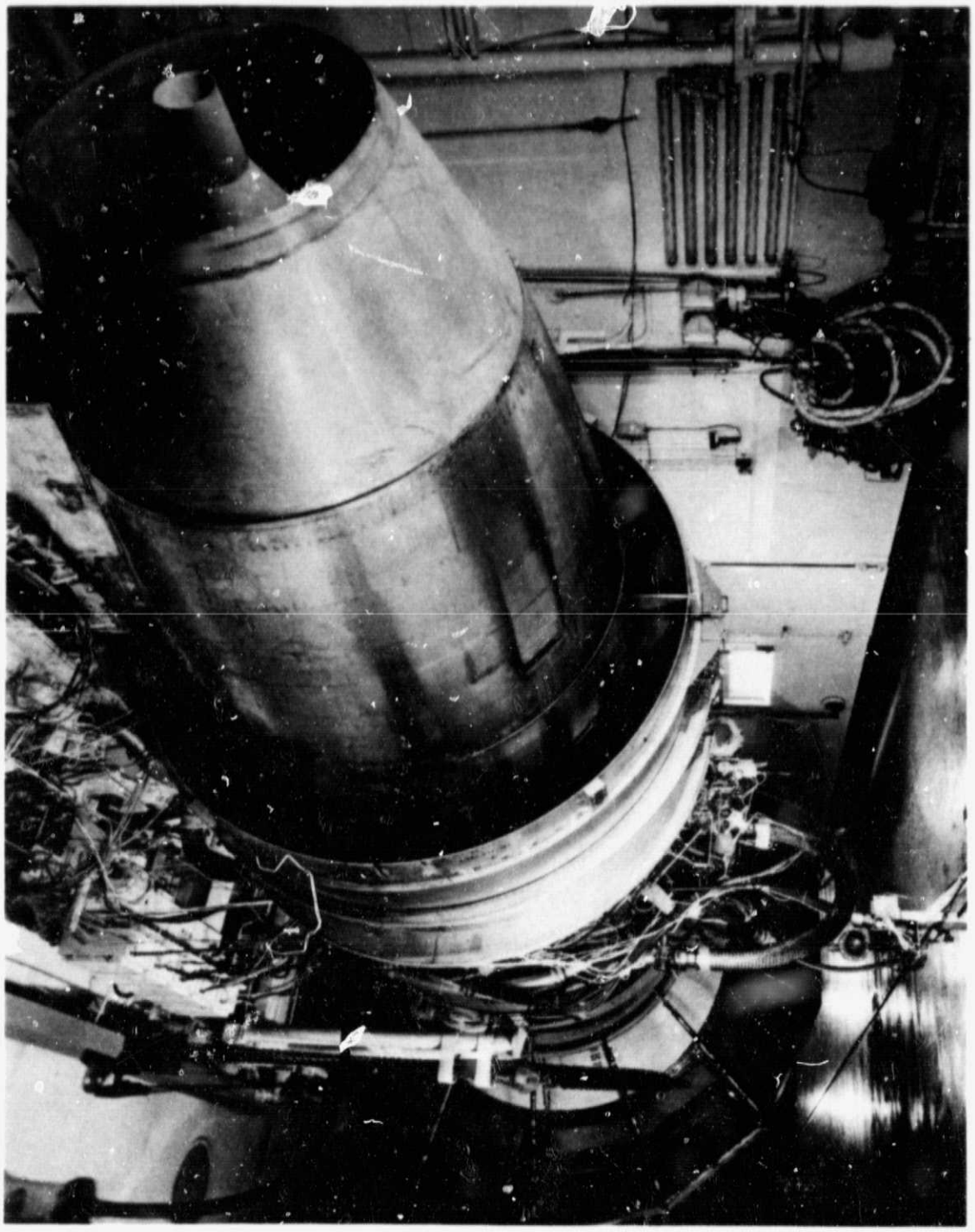

Figure 32. CF6 Engine Installed in Evendale Test Cell

Data acquisition capability consists of 400 pressure channels, 400 temperature channels, 10 frequency channels, and 28 d.c. voltages such as load cells, individual pressure transducers, position potentiometers, etc. The pressure system consists of ten 40-port scannivalves with available pressure ranges from ± 6.9 N/cm^2 (10 psig) through ± 344.7 N/cm^2 (500 psig). The system incorporates autoranging and multiple sampling capability for all data channels to assure optimal resolution and precision in addition to variable averaging time for frequency measurements. Data may be obtained and processed in either a steady-state or transient mode. Typical steady-state acquisition time is 30 seconds with each parameter sampled 49 times over the 30-second time period. Transient acquisition rates are variable from one sample per second per channel to 250 samples per second per channel. Redundant measurements are made of key parameters such as fuel, flow, fan speed, and thrust. Automatic data rejection techniques, ratio of redundant measurements, and on-line system-verification analysis further enhance overall data quality.

All data are converted to engineering units on the Cell System and automatically transferred to the Site System. These are then used to run various data-analysis computer programs. Quick-look programs are available on the Cell System to provide on-line hard copy of overall engine performance and health calculations. Simultaneously, these data are available at the Site System for hard copy and plotting of corrected overall and interstage performance characteristics. Engineering units and/or calculated data may be transmitted to the General Electric Evendale Time-Sharing Computer Center for archival storage and additional analysis such as cycle deck comparison.

4.4 TEST PROCEDURE

The actual test consisted of operating the test engine through the following engine test runs:

- Cold motoring.
- Ground idle.
- Slow accels and decels to and from takeoff power.
- Steady-state operation at takeoff power.
- Several bursts and chops to and from takeoff power with specified time intervals at takeoff.
- Several rebursts to takeoff power after specified time intervals at ground idle.
- Engine speed settings of sufficient numbers to establish the performance power calibration.

A schematic presentation of the test sequence, showing power levels and times is given in Figure 33.

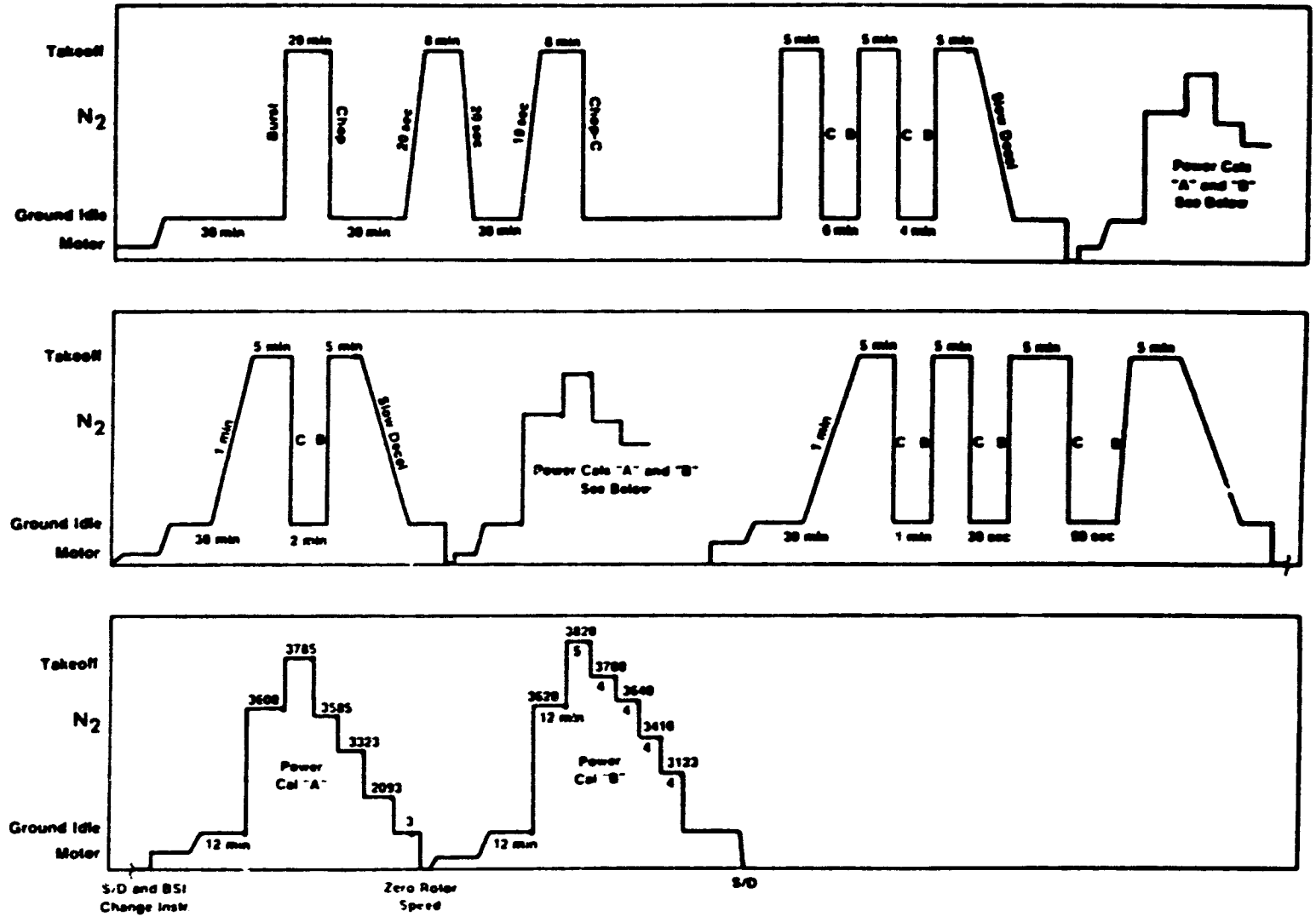

Figure 33. Test Sequence.

4.4.1 Performance Evaluation

The performance portion of the test program was designed to evaluate the performance over a range of power settings after the engine reached steady-state conditions. Each power calibration consisted of two sets of power levels in descending order of fan speed with a short shutdown in between. The shutdown is included to assure testing repeatability.

The data were analyzed using the General Electric Phase II computer program. This program has for its basis a status cycle deck representative of the particular engine model being tested. Some of the key features of this data analysis program are:

(a) For each test reading a pretest prediction point is run on the cycle deck at the tested conditions (ambient temperature, pressure, humidity, etc.), and this pretest point is used to check the measurements for outliers.

(b) Several alternate analysis paths are built in for determination of core flow, low-pressure system work, etc. In addition, it is possible for the user to select his own analysis setup. All of these analysis paths guarantee a balanced cycle; that is, the solution is self-consistent and satisfies the continuity, momentum, and energy equations.

(c) The built-in analysis options feature mission-data protection. When a measurement is missing, a suitable assumption is made to replace the measurement in the analysis; for example, when compressor discharge temperature is unavailable, compressor efficiency is held at the predicted level to effectively take its place. For a few key measurements, the analysis is terminated when they are unavailable, but for the majority of the measurements, an alternate analysis is performed instead.

(d) At the conclusion of the analysis, the cycle deck is matched to the test data; that is, the cycle deck maps, etc., have been rescaled to be consistent with the measurements.

(e) The data is adjusted to dry, sea-level, static, standard-day condition by running the rescaled cycle deck at the standard condition. This method for correcting the data eliminated the problem, encountered in the past, of trying to select a single number to represent, for example, the temperature effect on fuel flow independent of power setting or type of day. This is particularly significant in modern engines because they employ more and more variable geometry.

4.5 TEST RESULTS

4.5.1 High Pressure Turbine Stator Roundness

The objective of this test was to demonstrate the roundness improvement of the redesigned hardware. The roundness improvement of the turbine midframe and HPT stator will be discussed first and then the roundness during a throttle burst, chop and a 90-second reburst will be presented.

The demonstration of the roundness improvement associated with the redesigned hardware was accomplished by measurement of TMF temperature variations, TMF/CRF flange temperatures, HPT stator support temperatures and engine operating parameters affecting TMF mechanical loads at specific engine operating conditions with the redesigned TMF. These measurements were then used to calculate the TMF distortion and resultant HPT stator out-of-roundness at the same condition. Comparisons of the TMF-caused HPT stator out-of-roundness from this test with the redesigned TMF to that determined from the previous diagnostics testing (Ref. 2) with the production TMF were used to show the effectiveness of the TMF redesign.

Temperatures of the structural elements in the TMF were measured at steady-state takeoff power at the same time the clearances in the high pressure turbine were being recorded. The significant engine parameters recorded at this condition, which are used to determine the mechanical loading on the TMF, are as follows:

Fan Speed (RPM)	3762
Core Speed (RPM)	10150
Engine Thrust (N/lb)	217072/48800
HPT exit temp (^{o} C)	868
HPT exit pressure (N/cm^2/ PSIA)	60.2/87.3

The measured temperatures in the TMF structural elements are shown on Figures 34 and 35. The hub temperature was measured at several circumferential locations. As no significant variation was noted, only the average temperature is shown on Figure 34. The temperature of both the forward and aft structural Hat sections was measured at the base and apex of the Hat sections at several circumferential locations. These measurements were used to calculate the area weighted average and radial gradient at each circumferential location. This is the data shown on Figure 35.

Temperatures on the CRF/TMF flange were measured at the radial midpoint on the CRF and TMF flange as a measure of the average flange temperatures which are shown on Figure 36.

Temperatures were also measured at three locations on the HPT stator at the same engine operating points. These results are shown on Figures 37, a, b, and c.

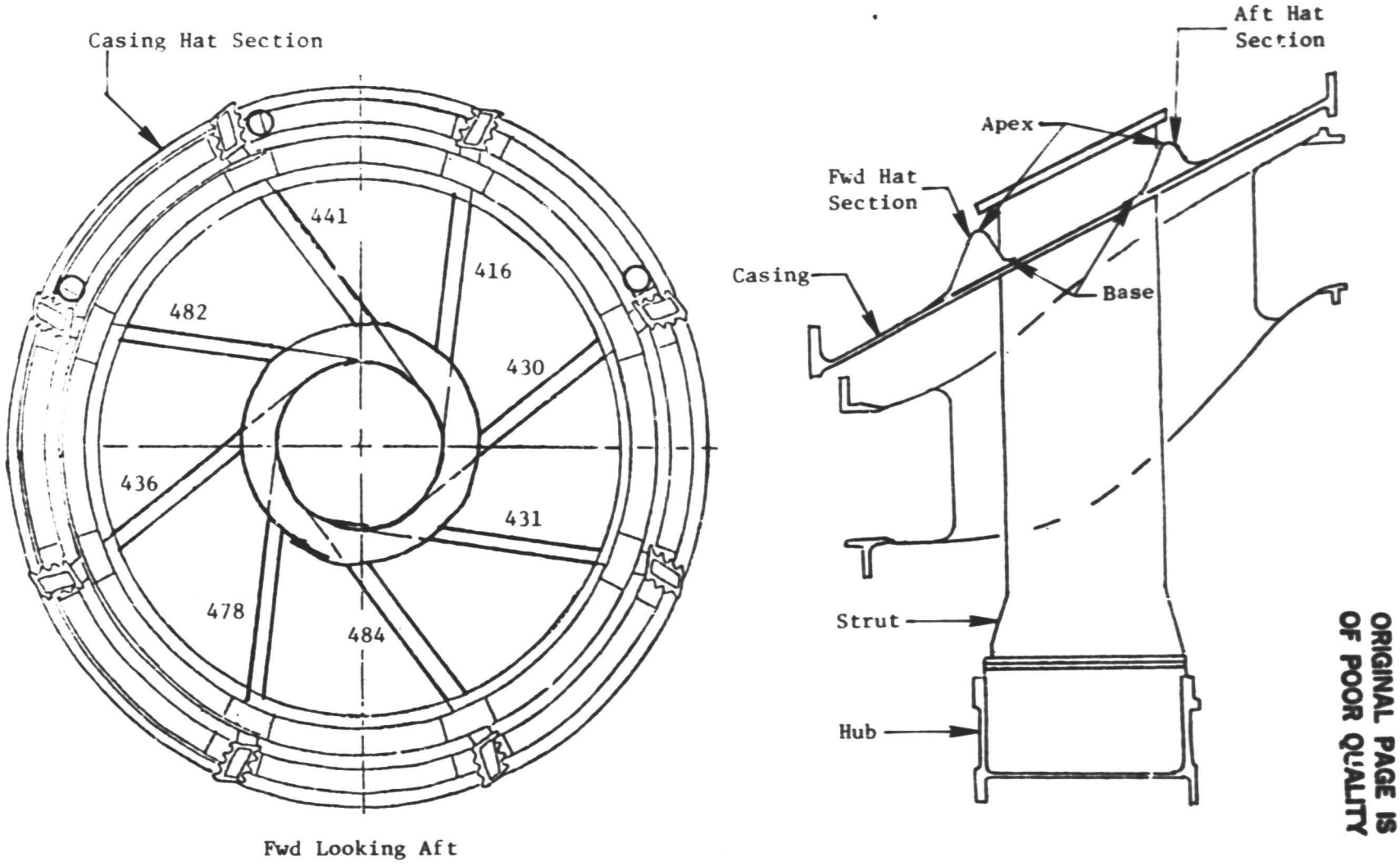

Figure 34. Turbine Midframe Strut Average Temperatures, Takeoff.

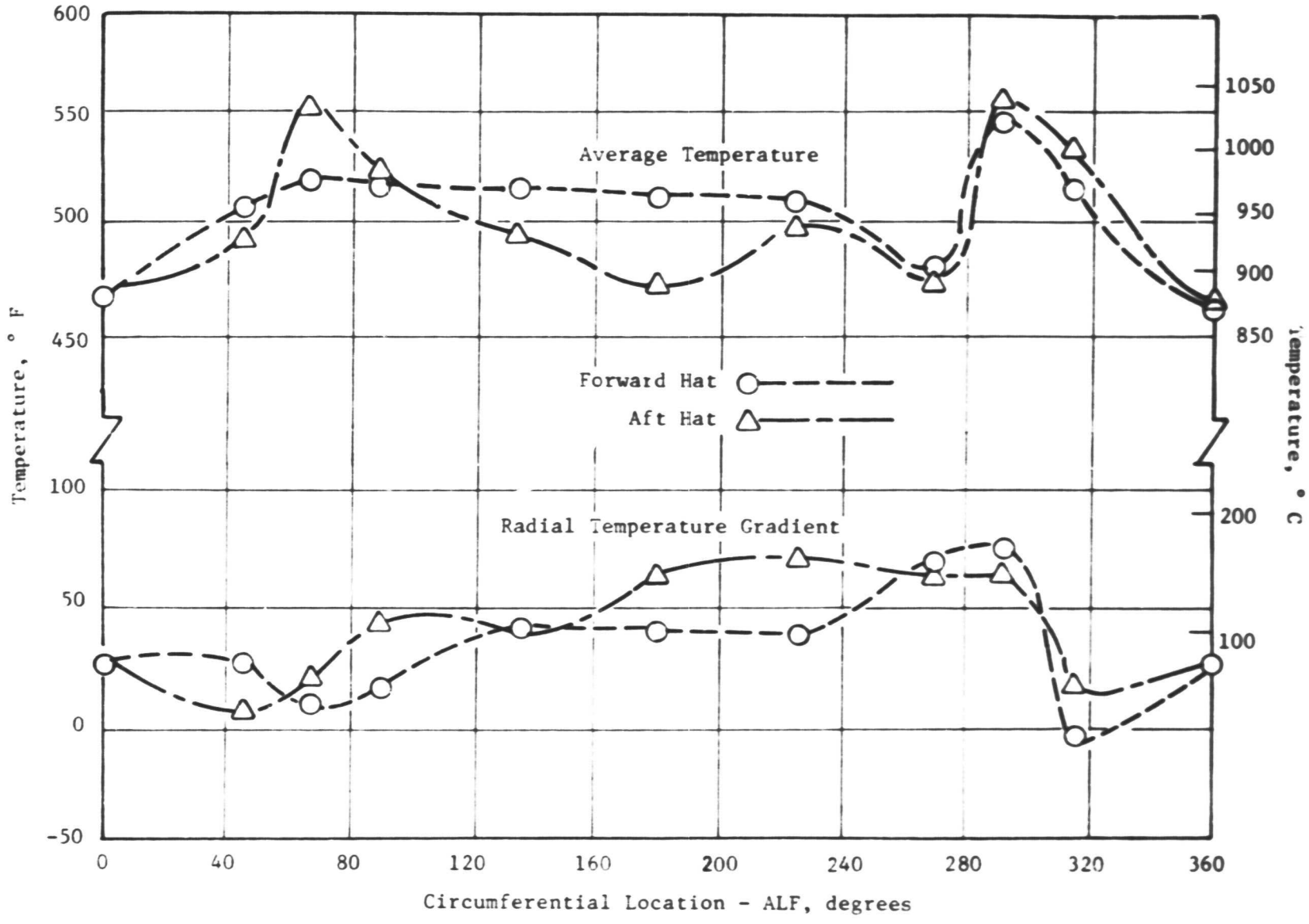

Figure 35. TMF Casing Hat-Section Temperature, Takeoff.

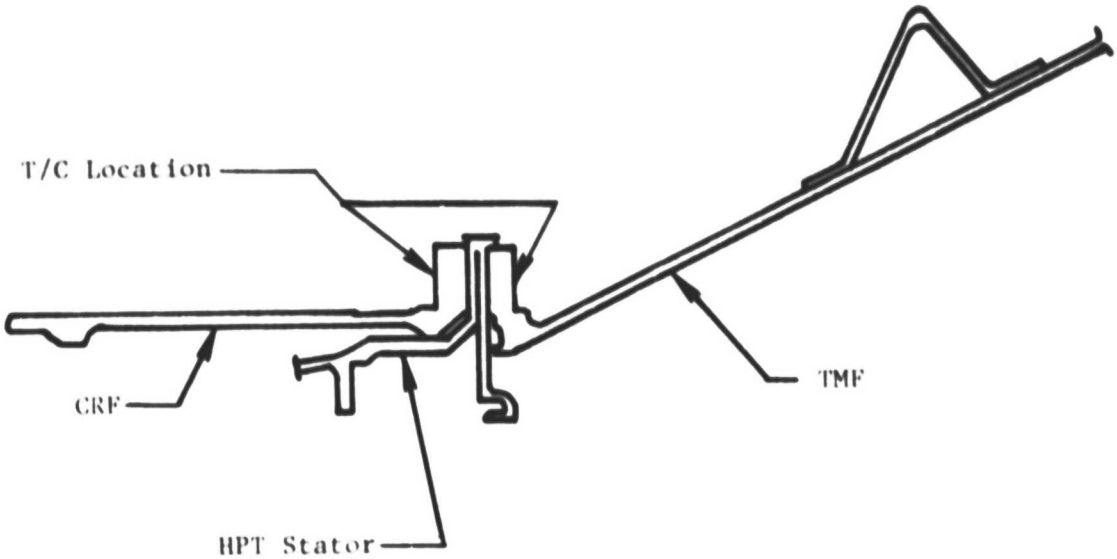

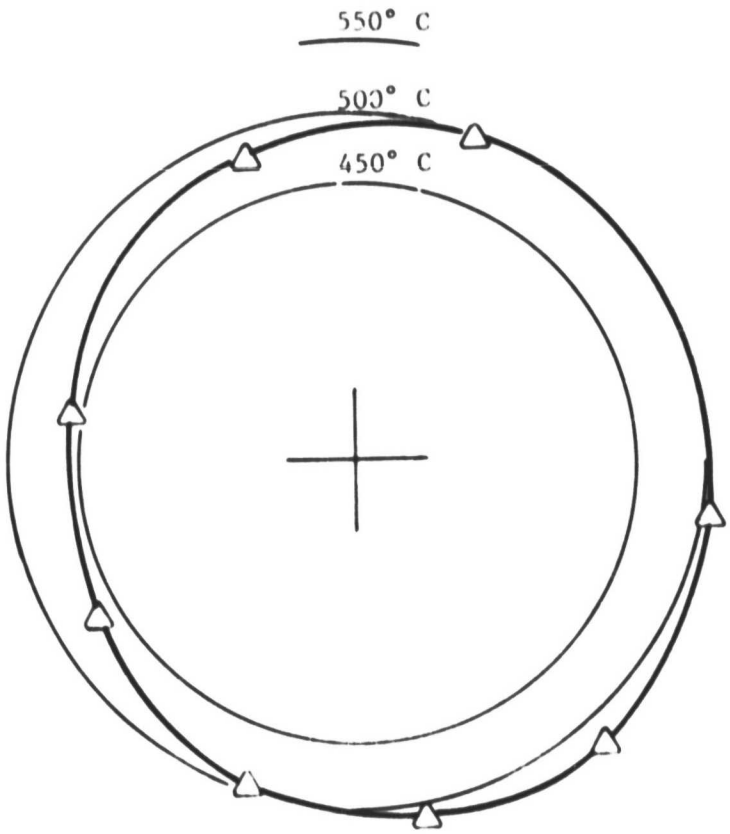

Figure 36. Compressor Rear Frame/Turbine Midframe Average Temperature, Takeoff.

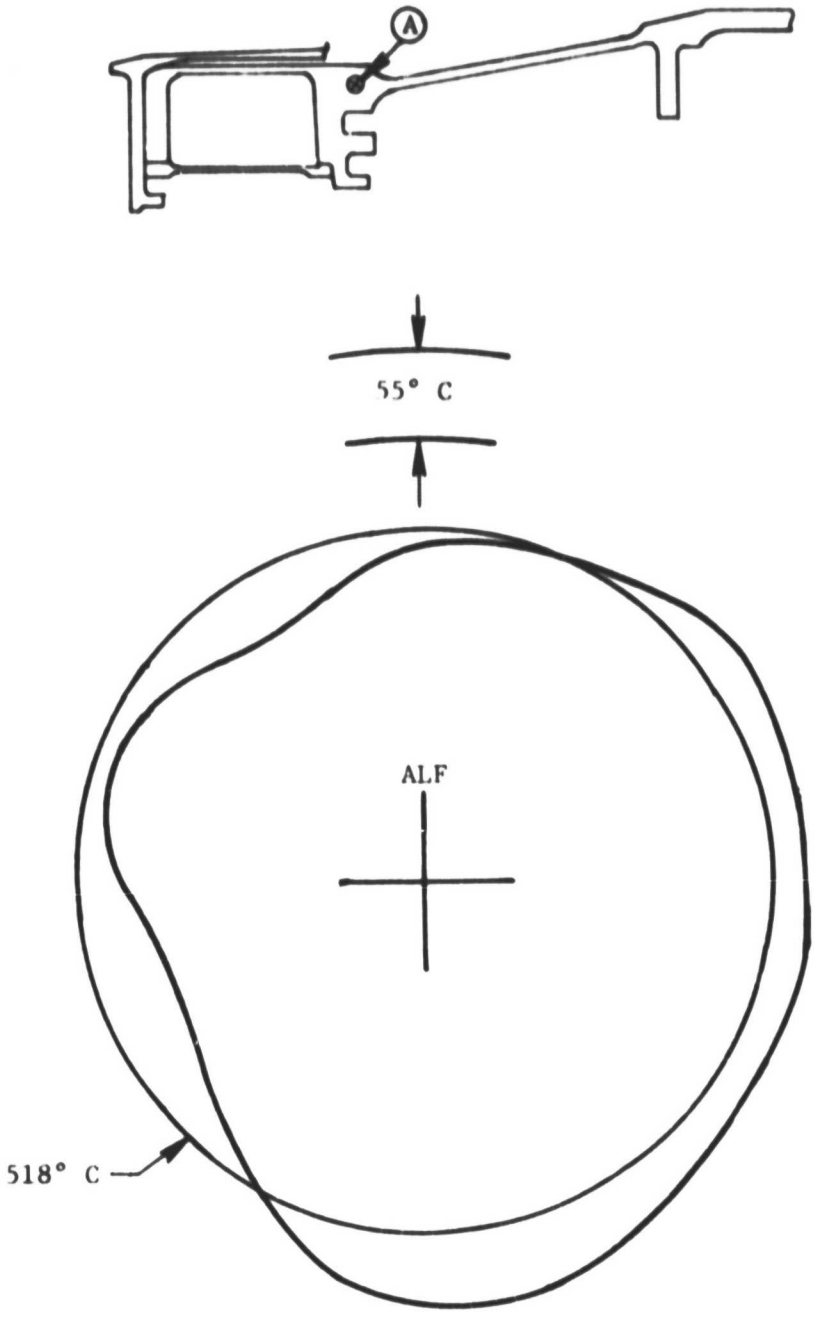

Figure 37a. H' Turbine Stator Temperature Varation, Thermocouple A.

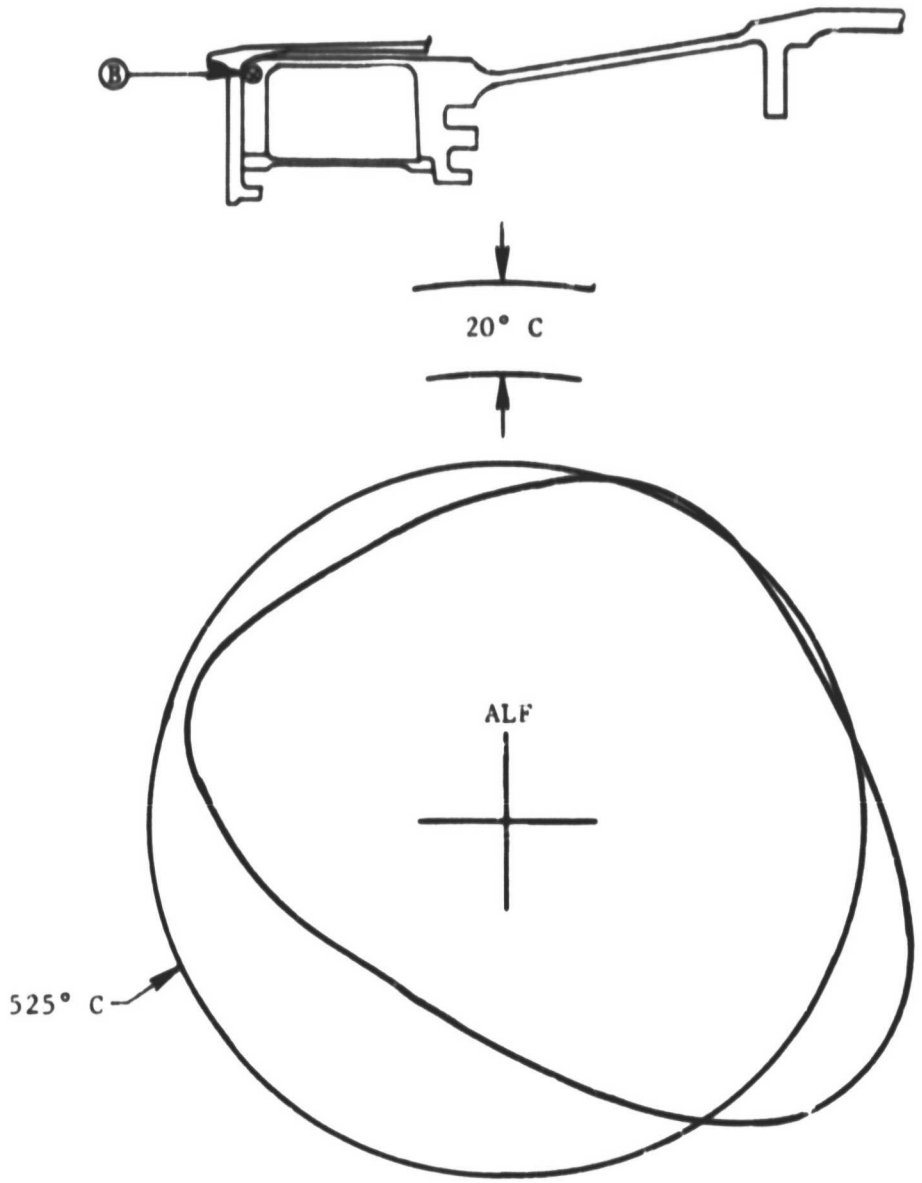

Figure 37b. HP Turbine Stator Temperature Varation, Thermocouple B.

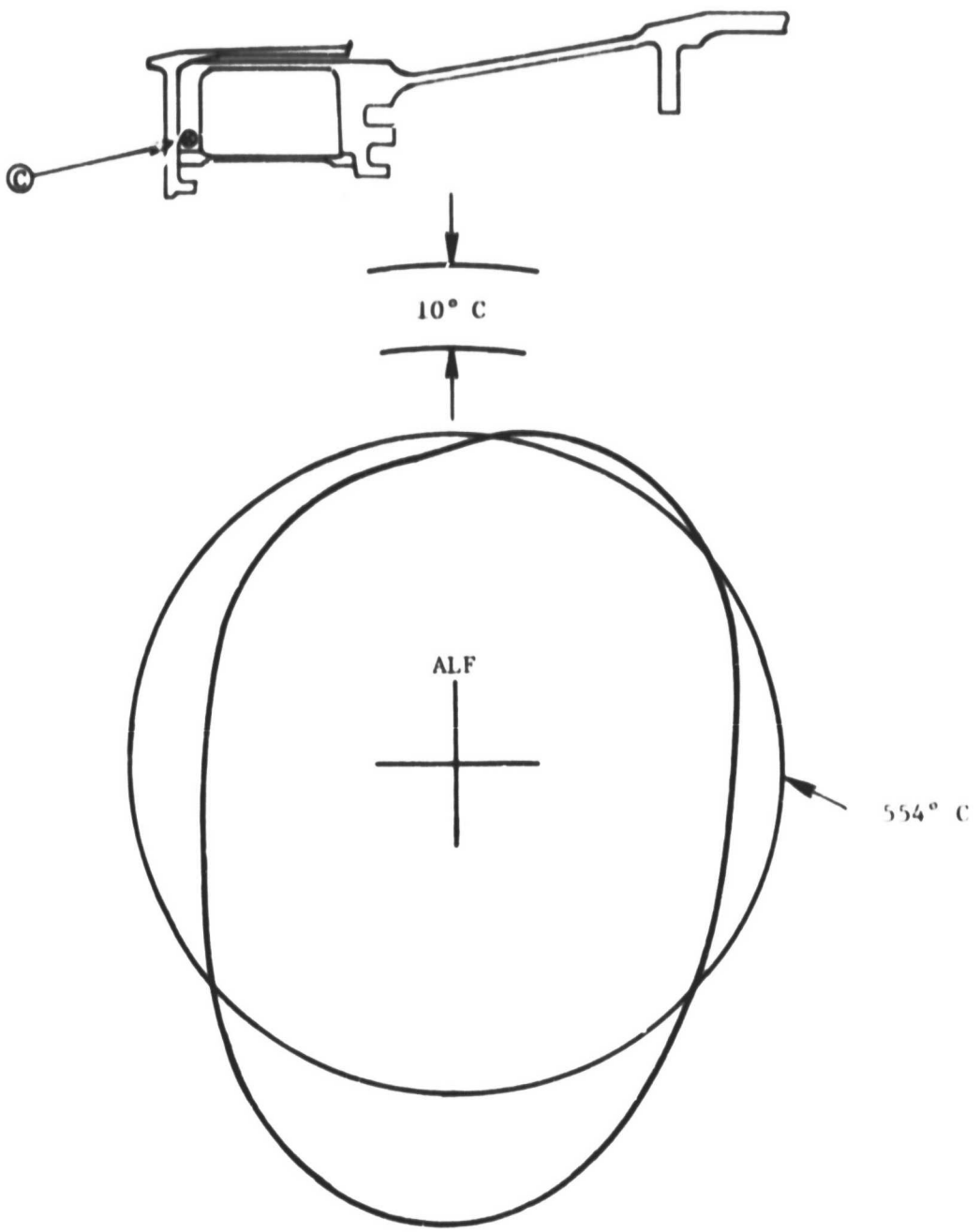

Figure 37c. HP Turbine Stator Temperature Varation, Thermocouple C.

Calculated HPT Stator Out-of-Roundness

The measured engine data were used to calculate the HPT stator out-of-roundness at steady state take-off. The out-of-roundness resulting from the thermally and mechanically induced TMF out-of-roundness is shown in Figure 38. The out-of-roundness caused by the HPT stator temperature variation is shown in Figure 39.

Measured HPT Stator Out-of-Roundness

The measured HPT stator out-of-roundness is determined by removing the manufacturing and assembly-caused out-of-roundness from the clearance probe measurements at each circumferential location for a given operating condition and then plotting this data as deviation from an average or round engine clearance.

The manufacturing and assembly-caused out-of-roundness is obtained from cold motoring data. Cold motoring data is clearance probe data acquired by rotating a cold engine with the air driven starter motor. The clearance data obtained show the out-of-roundness caused by manufacturing and assembly. The probe-to-probe deviation from an average or round shape is then used to correct any other roundness data. The cold motoring data is also used to establish the actual round engine cold clearance used in the clearance response work. This data is shown in Figure 40.

The measured out-of-roundness at the steady-state takeoff power point previously mentioned is shown in Figure 41 as corrected for the manufacturing and assembly-caused out-of-roundness.

Comparison of Calculated and Measured Results

Figure 42 shows the total calculated HPT stator out-of-roundness and that measured during the test at the same engine operating condition. Reasonable agreement exists between the measured and calculated out-of-roundness. Examination of Figures 38, 39, 40 and 42 shows that the major contribution to the total out-of-roundness is the TMF.

The changes made to the TMF were expected to produce less HPT out-of-roundness than shown in Figure 38. Examination of the temperature data shown in Figures 34 through 36 shows that there are two reasons why this did not occur:

1) The effectiveness of the insulating liners in the struts was not as great as anticipated; therefore, not as much of the mechanical load caused distortion was cancelled out by the strut-to-strut temperature variation.

2) The flange heat shield was more effective than anticipated resulting in a greater change in distortion due to the CRF/TMF flange temperature variation than was anticipated.

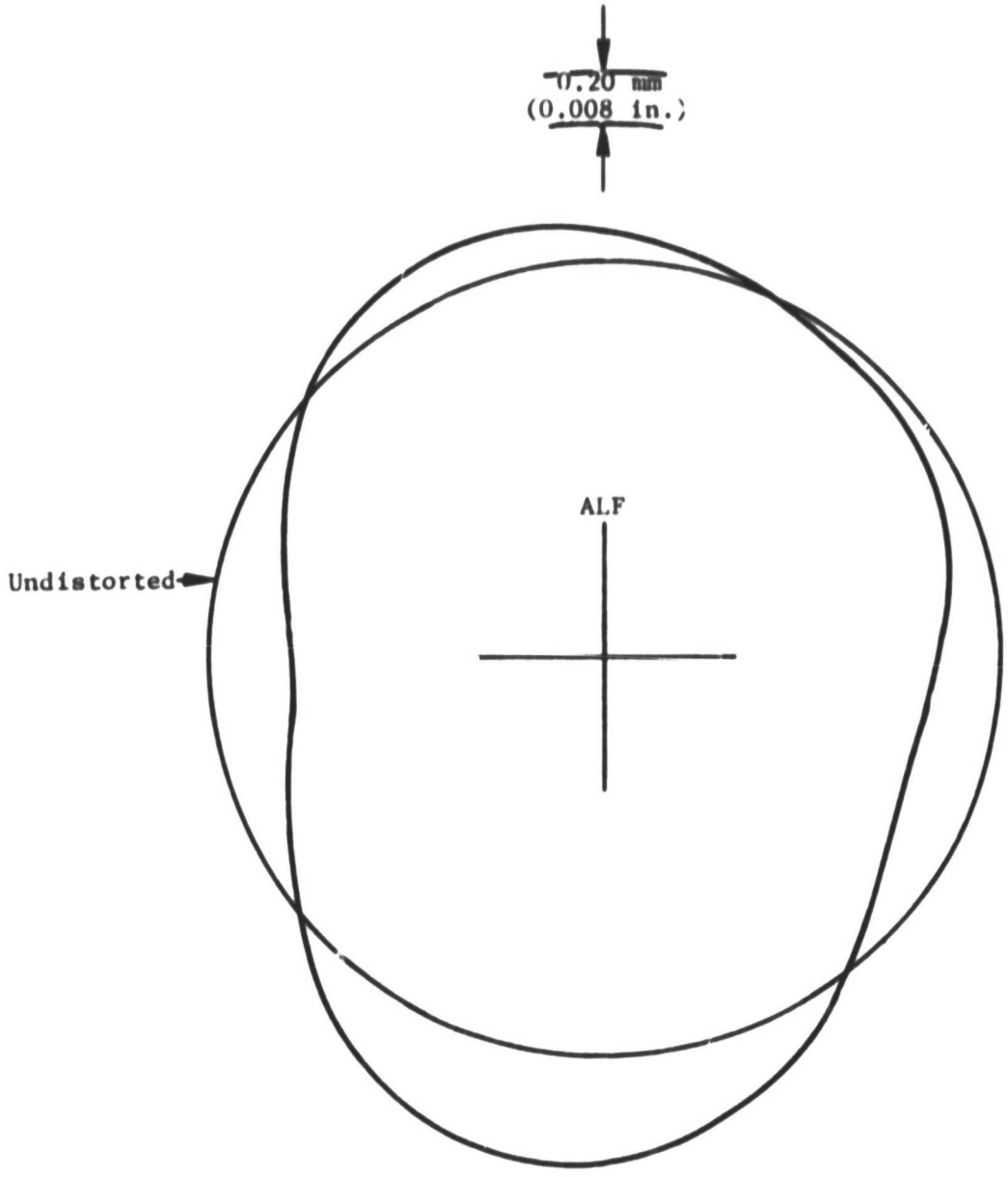

Figure 38. Calculated HPT Stator Out-of-Roundness Due to TMF, Takeoff (Based on Measured Data).

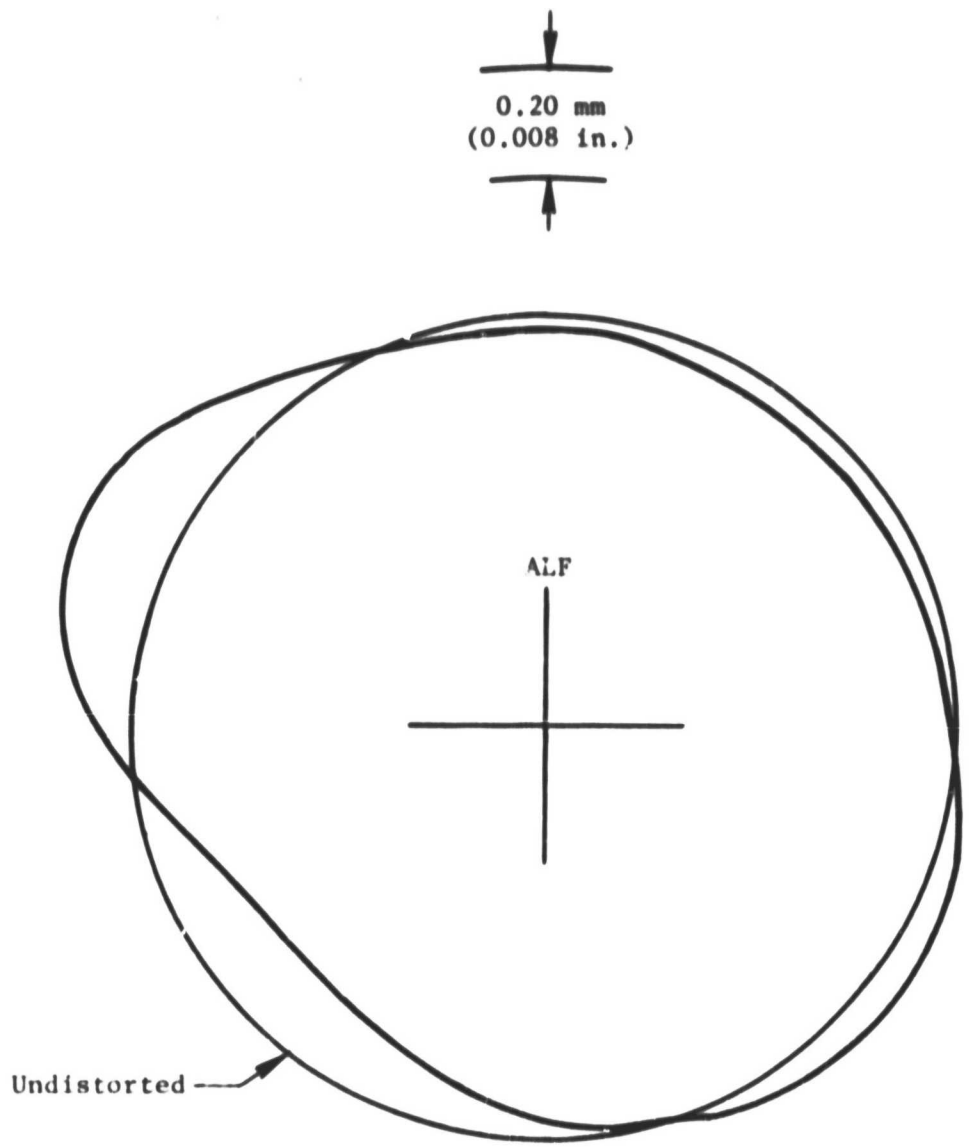

Figure 39. Calculated HPT Stator Out-of-Roundness Due to Stator Temperature Variation, Takeoff (Based on Measured Data).

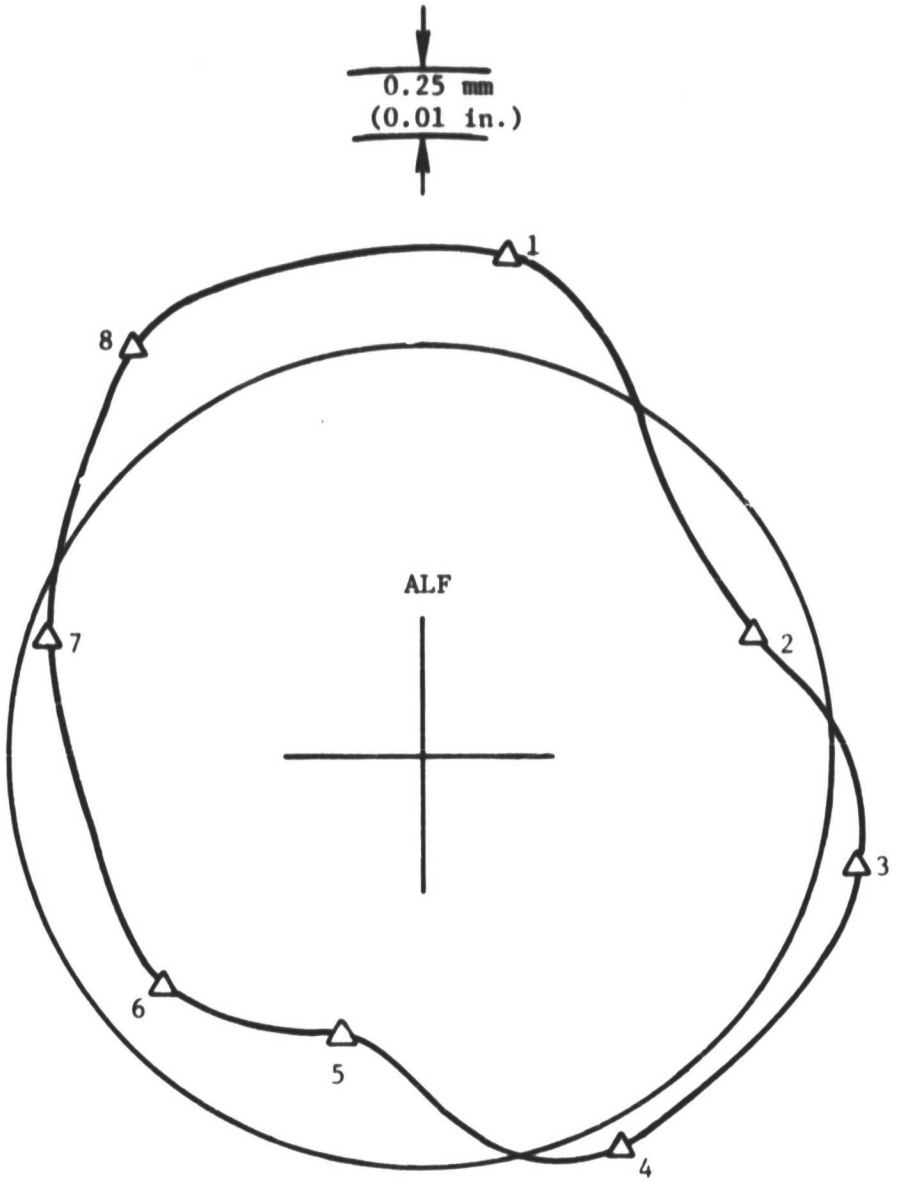

Figure 40. Cold Monitoring Roundness Shape.

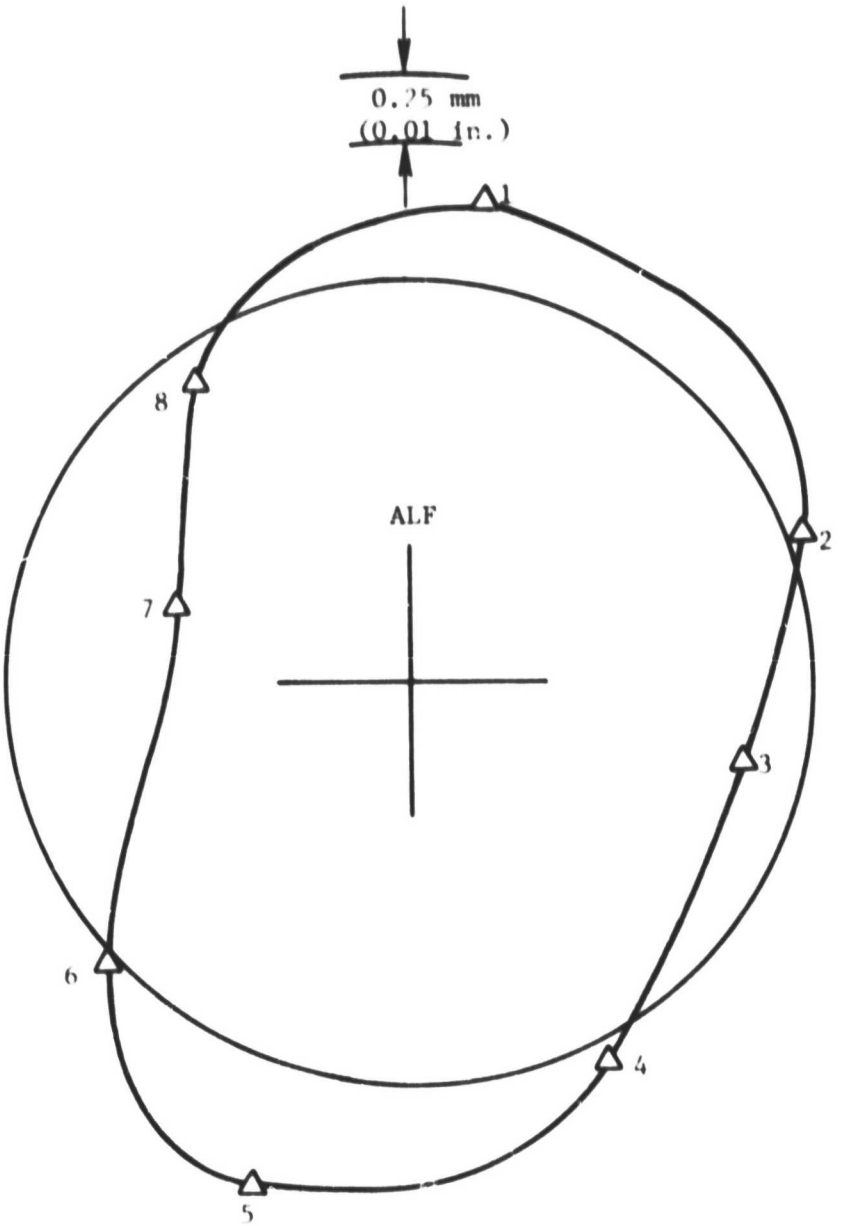

Figure 41. Measured Roundness at Steady State Takeoff Corrected for Manufacturing and Assembly - Caused Out-of-Roundness.

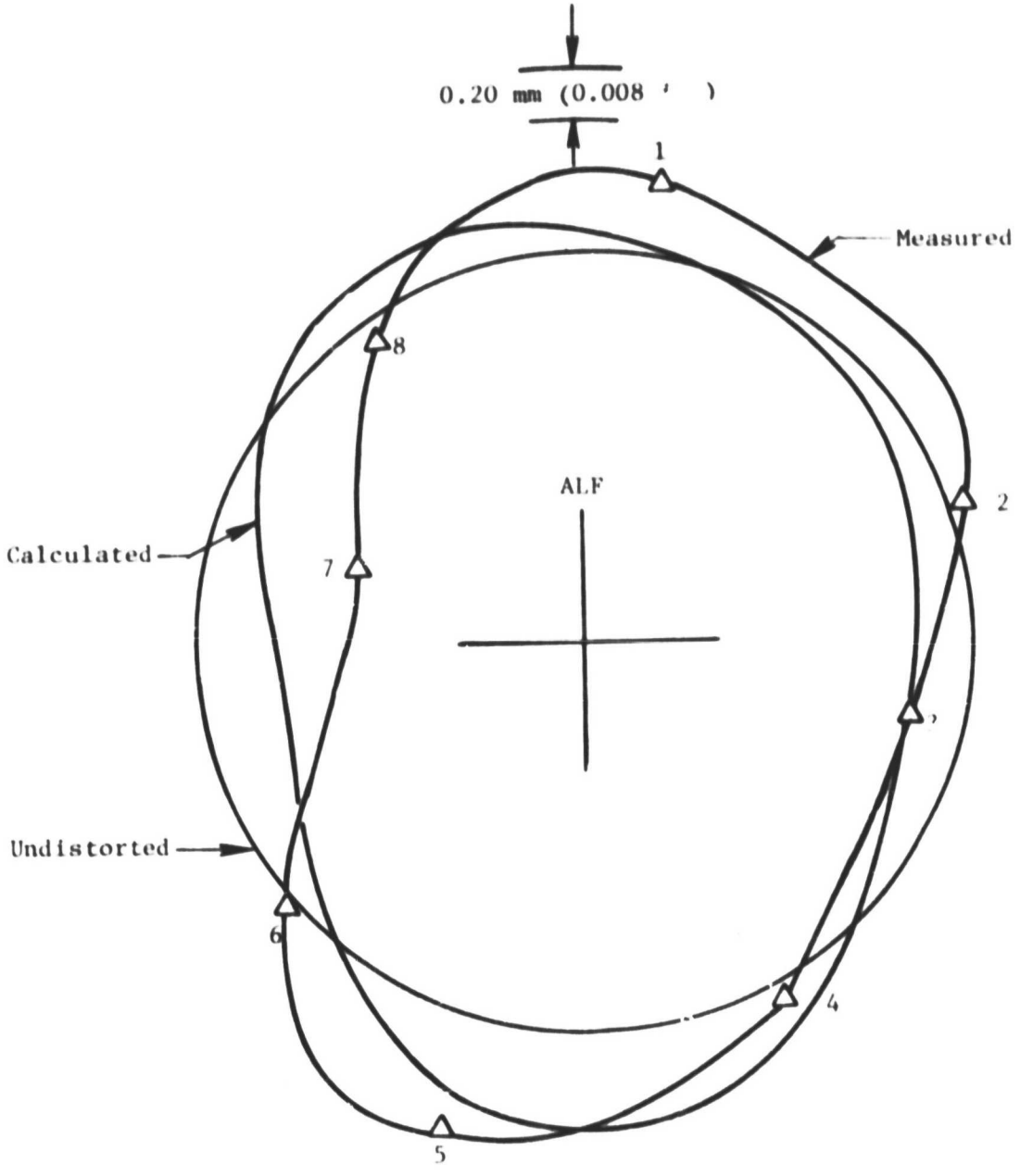

Figure 42. HPT Stator Out-of-Roundness, Takeoff.

Figure 43 compares the calculated HPT stator out-of-roundness caused by the TMF for the production and redesigned TMF at steady-state takeoff. Both of the curves shown on this figure were calculated using measured TMF temperatures and loading at comparable engine operating conditions. This data shows that the TMF redesign does have a significant effect on HPT out-of-roundness and that the TMF caused out-of-roundness can be minimized by a readjustment of the elements of the redesign (i.e., improving effectiveness of strut insulating liners and taking advantage of the increased effectiveness of the flange heat shield).

Roundness During Transient Operation

The roundness of the Stage 1 shrouds is presented for an accel from stabilized ground idle to steady-state takeoff (Figures 44 through 53); a decel from steady-state takeoff to stabilized ground idle (Figures 54 through 65); and a reburst after 90 seconds at ground idle (Figures 66 through 74).

The clearance probes were very intermittant during the 2-minute reburst and, therefore, the out-of-roundness could not be established. These 90-second reburst plots show the immediate effect upon roundness of the mechanical loads and the slow effect of the thermal loading. It should be noted that this out-of-roundness is not worse than the out-of-roundness at the minimum point during an accel from stabilized ground idle (Figure 48) or a decel from steady-state takeoff (Figure 60). Therefore, any rubs resulting from rebursts are caused by an average clearance response problem and not from out-of-roundness.

4.5.2 Clearance Transient Response

The clearance response characteristics of the shroud and the rotor structure, after roundness has been established, are the criteria that established the turbine operating clearances. These clearances are primarily established by the response characteristics during a decel although those of accel and rebursts must also be considered.

The clearance response data shown were obtained by averaging the clearances measured by the eight circumferentially spread clearance probes. These average curves were then modified, since all of the tests were not performed on the same day, to reflect those ambient conditions considered to be standard. The predicted values that correspond to these measured clearances are also plotted. The clearances shown are those of the instrumented engine which contains certain modifications necessary to accommodate the clearance probes and other instrumentation. The clearance responses are, however, very similar to those of a production configuration CF6-50 engine.

Decel from Steady-State Takeoff to Stabilized Ground Idle

The measured and predicted clearance response during a decel are presented in Figure 75. The agreement between the measured curve and the

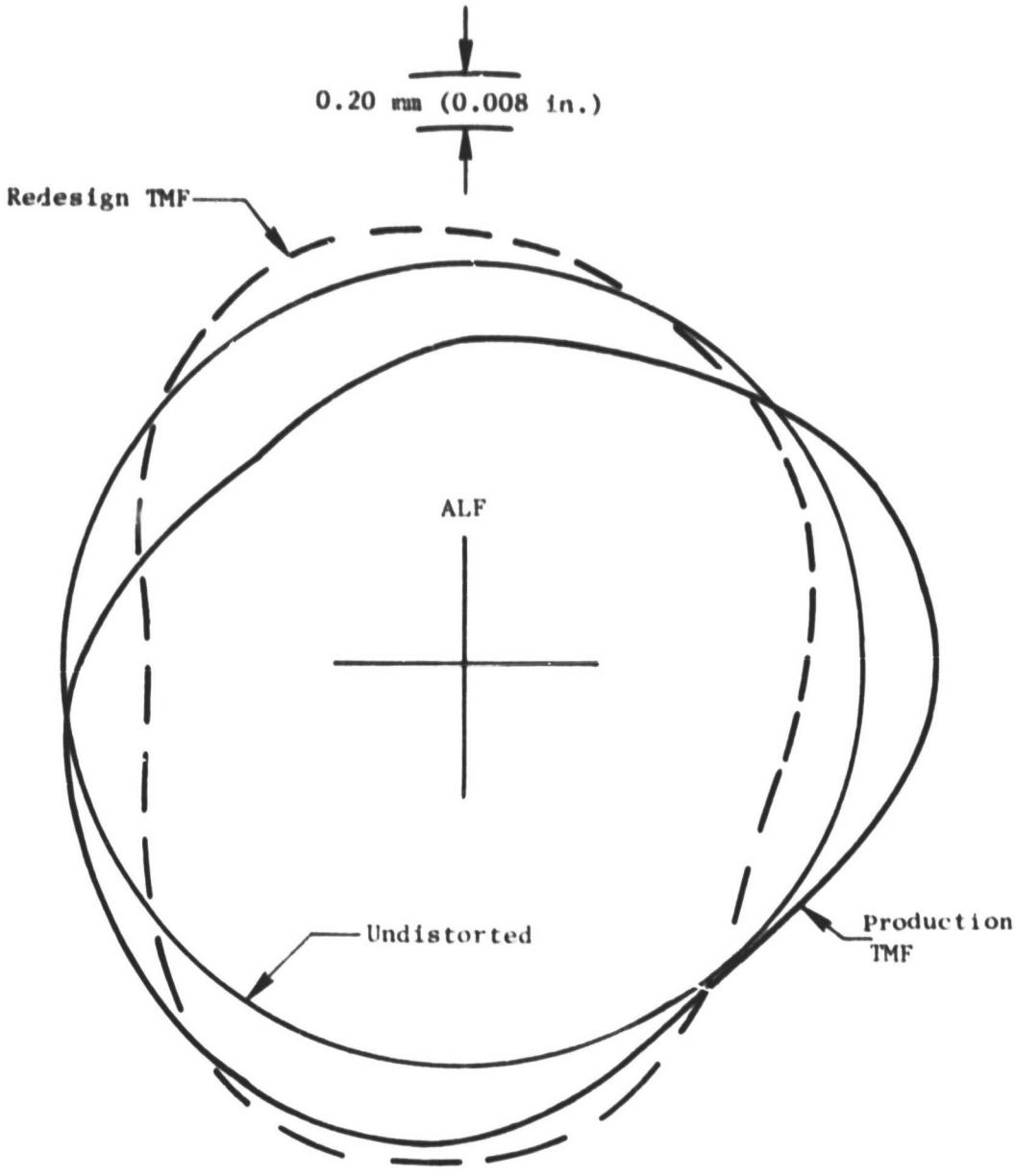

Figure 43. Calculated HPT Stator Out-of-Roundness Due to TMF, Takeoff.

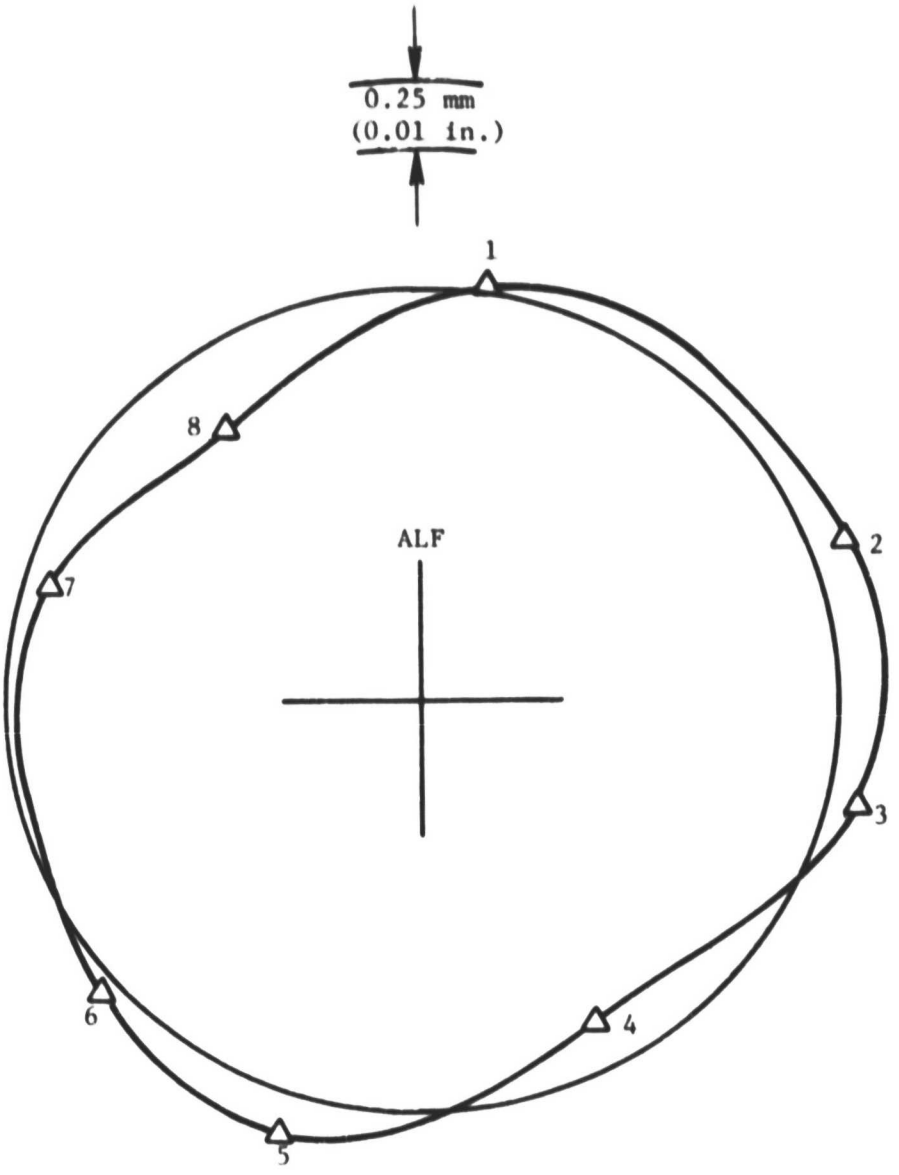

Figure 44. HP Turbine Stator Out-of-Roundness, 1 Second into Accel.

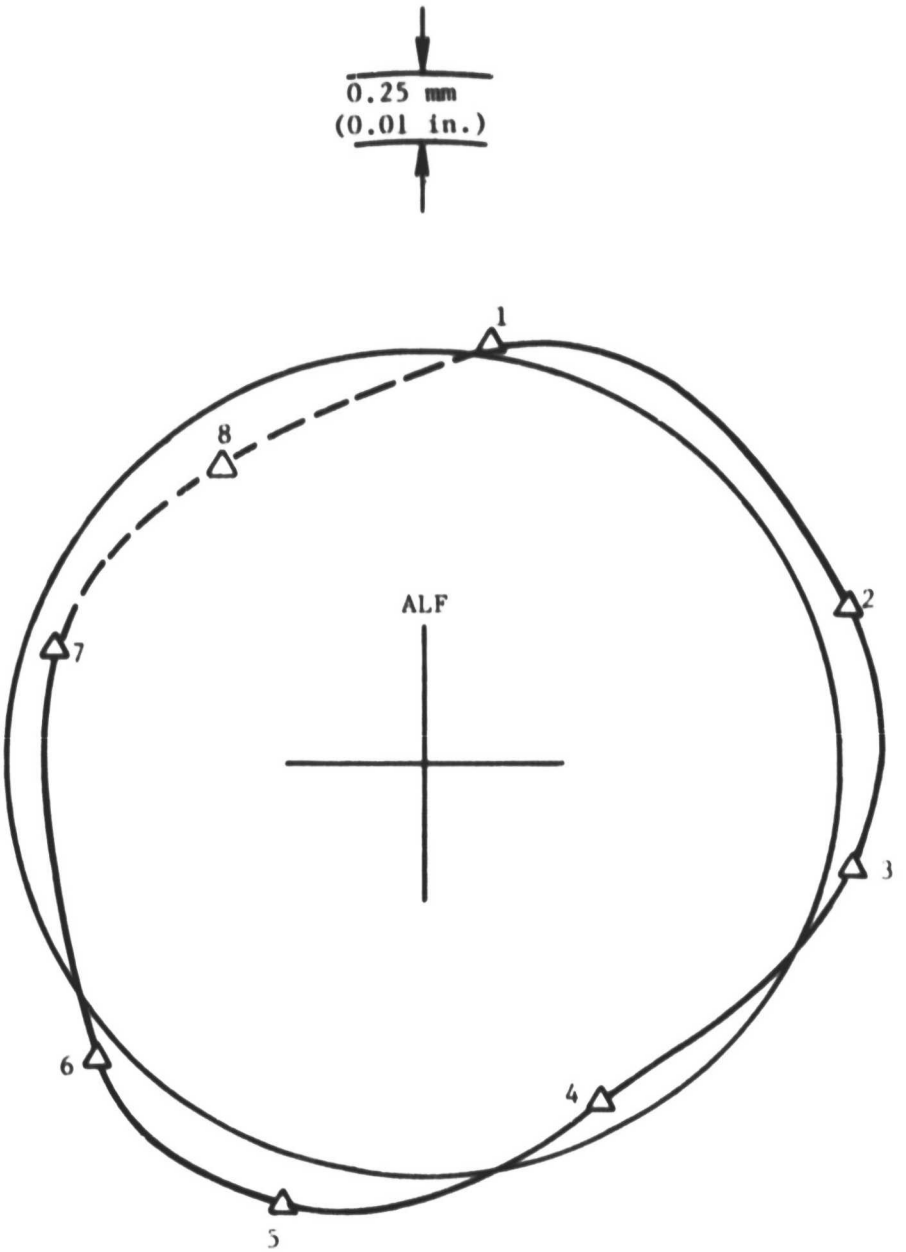

Figure 45. HP Turbine Stator Out-of-Roundness, 2 Seconds into Accel.

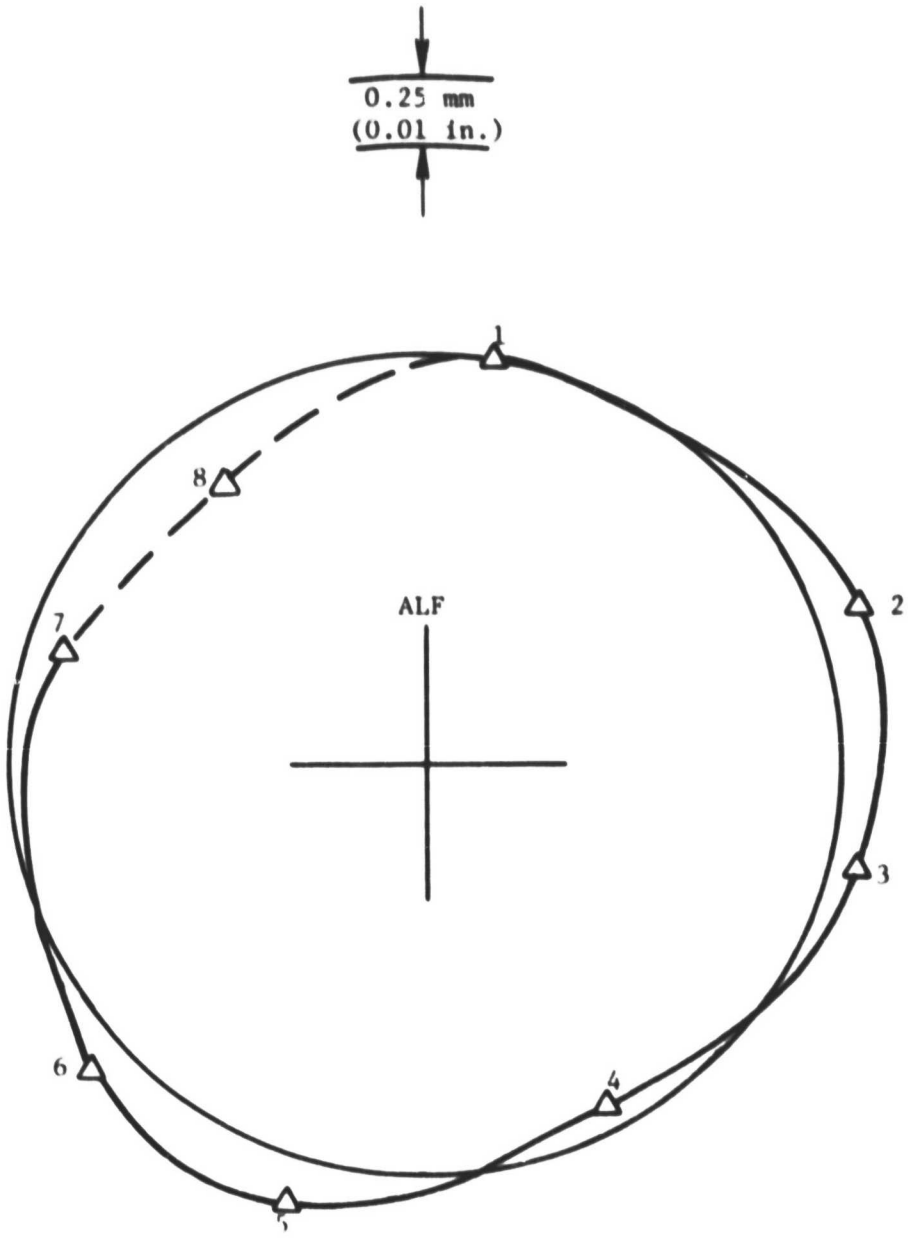

Figure 46. HP Turbine Stator Out-of-Roundness, 4 Seconds into Accel.

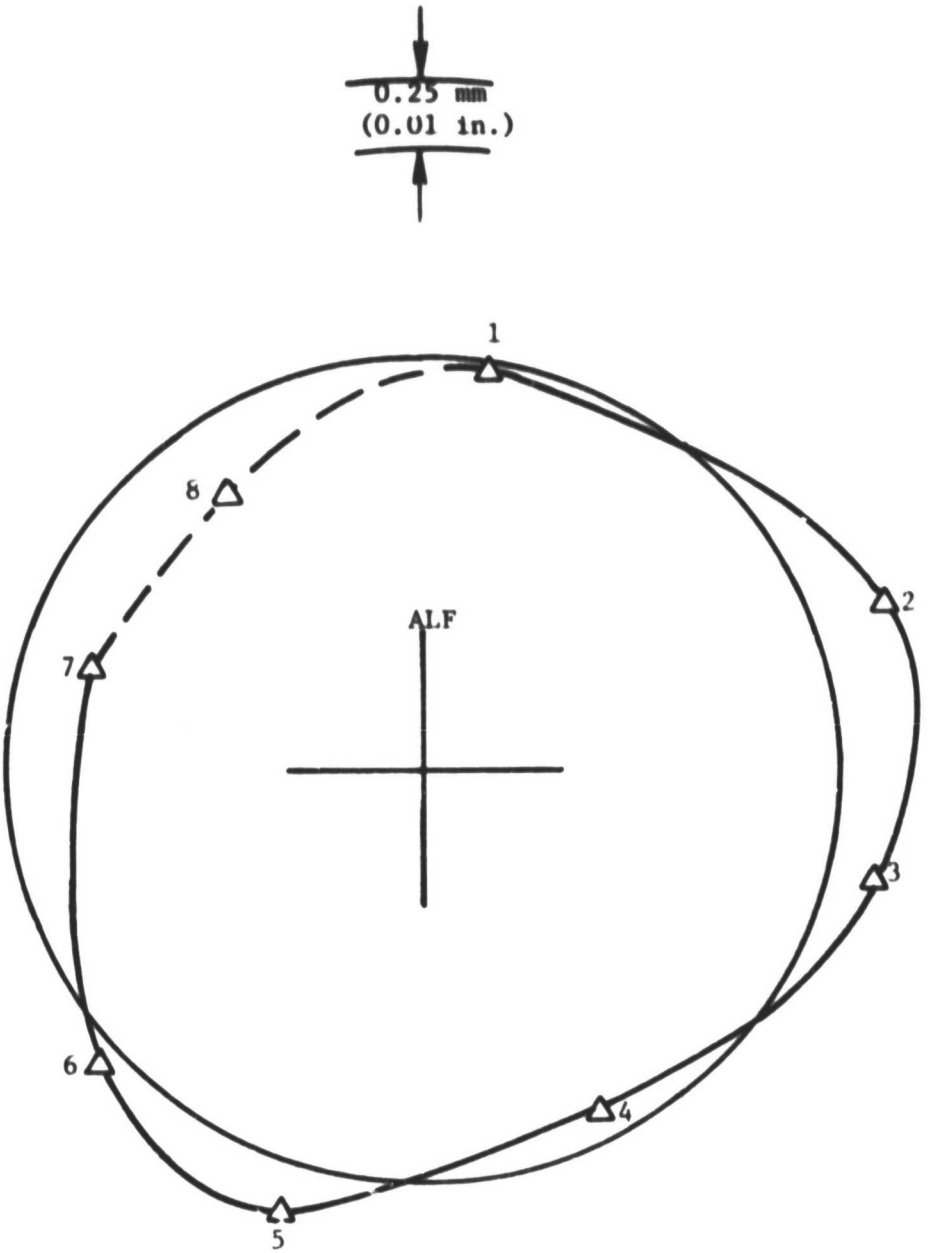

Figure 47. HP Turbine Stator Out-of-Roundness, 10 Seconds into Accel.

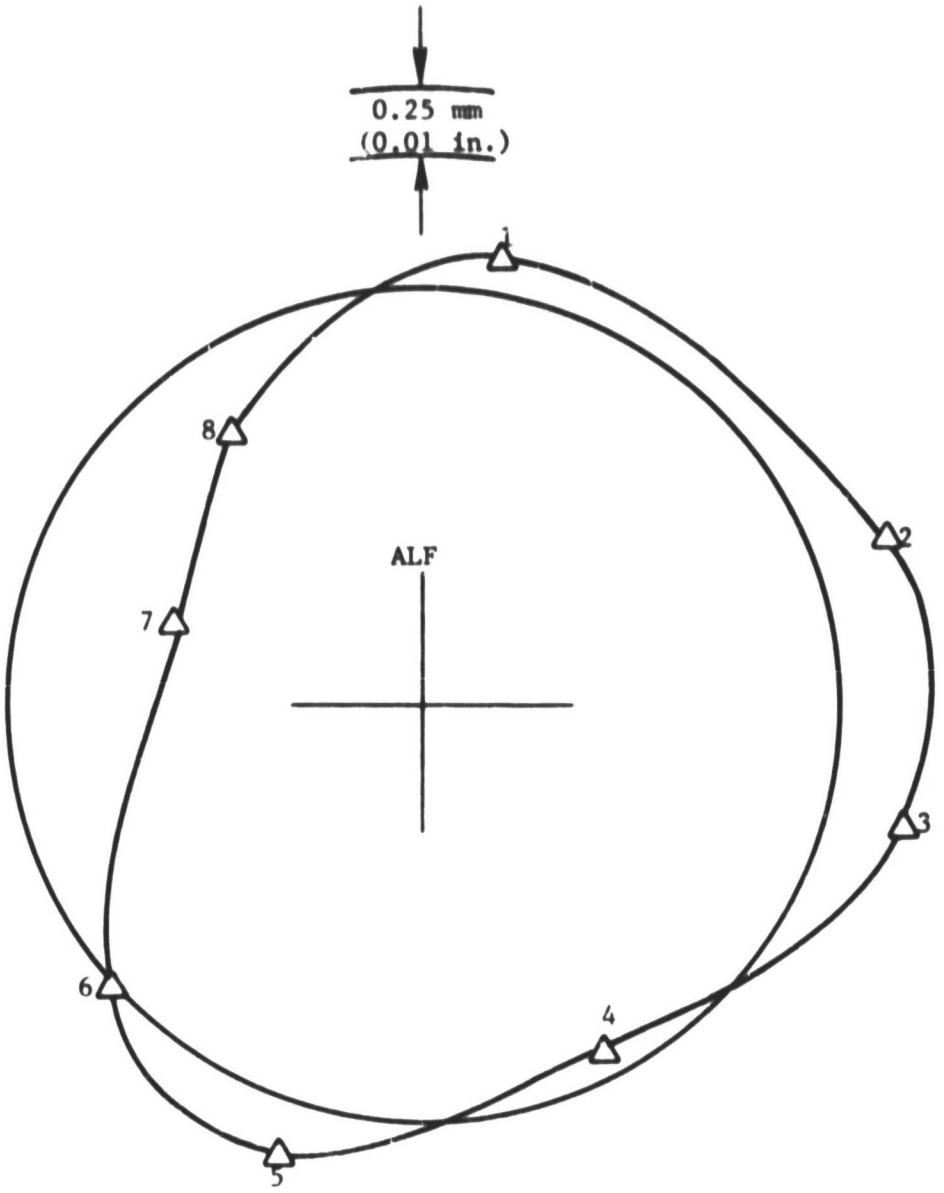

Figure 48. HP Turbine Stator Out-of-Roundness, 20 Seconds into Accel.

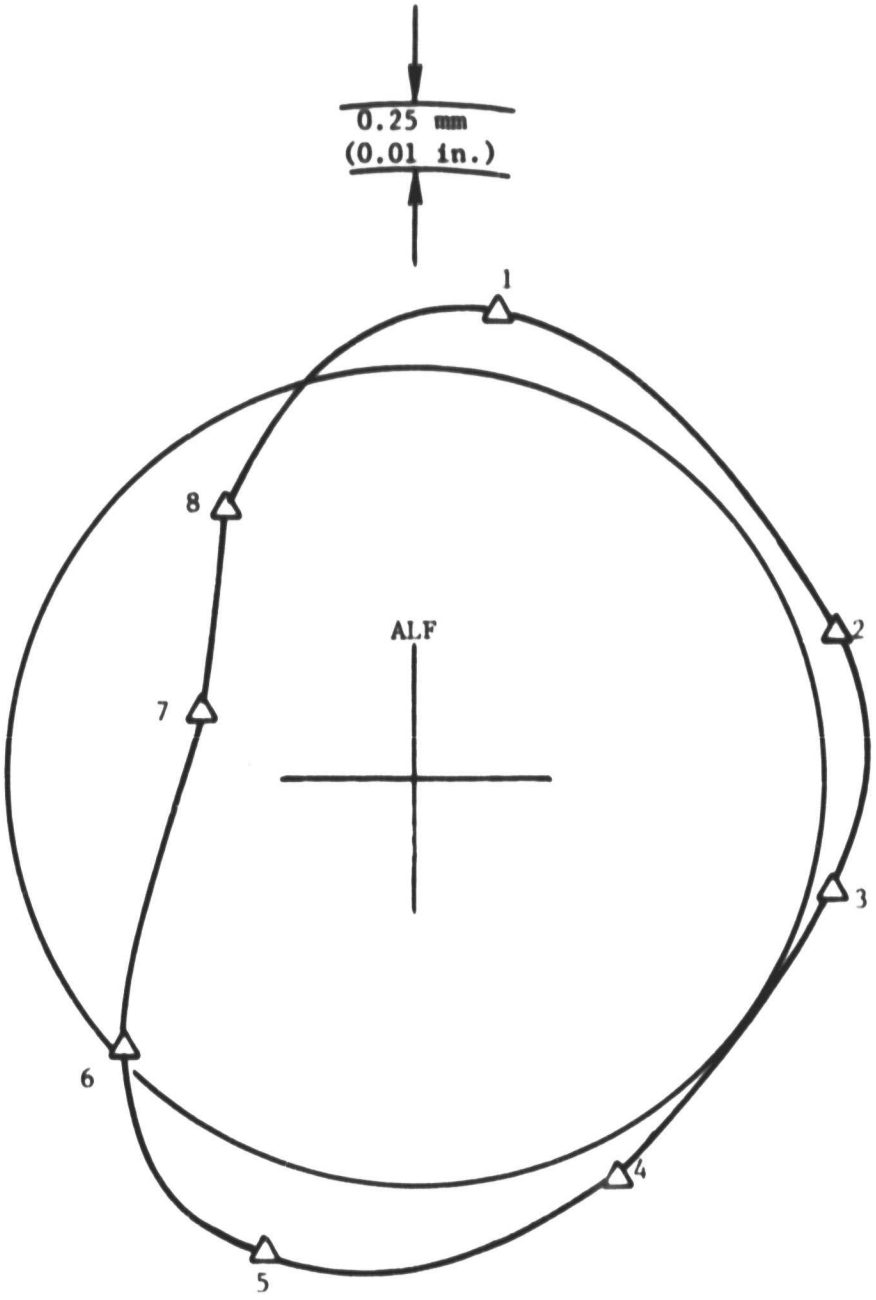

Figure 49. HP Turbine Stator Out-of-Roundness, 40 Seconds into Accel.

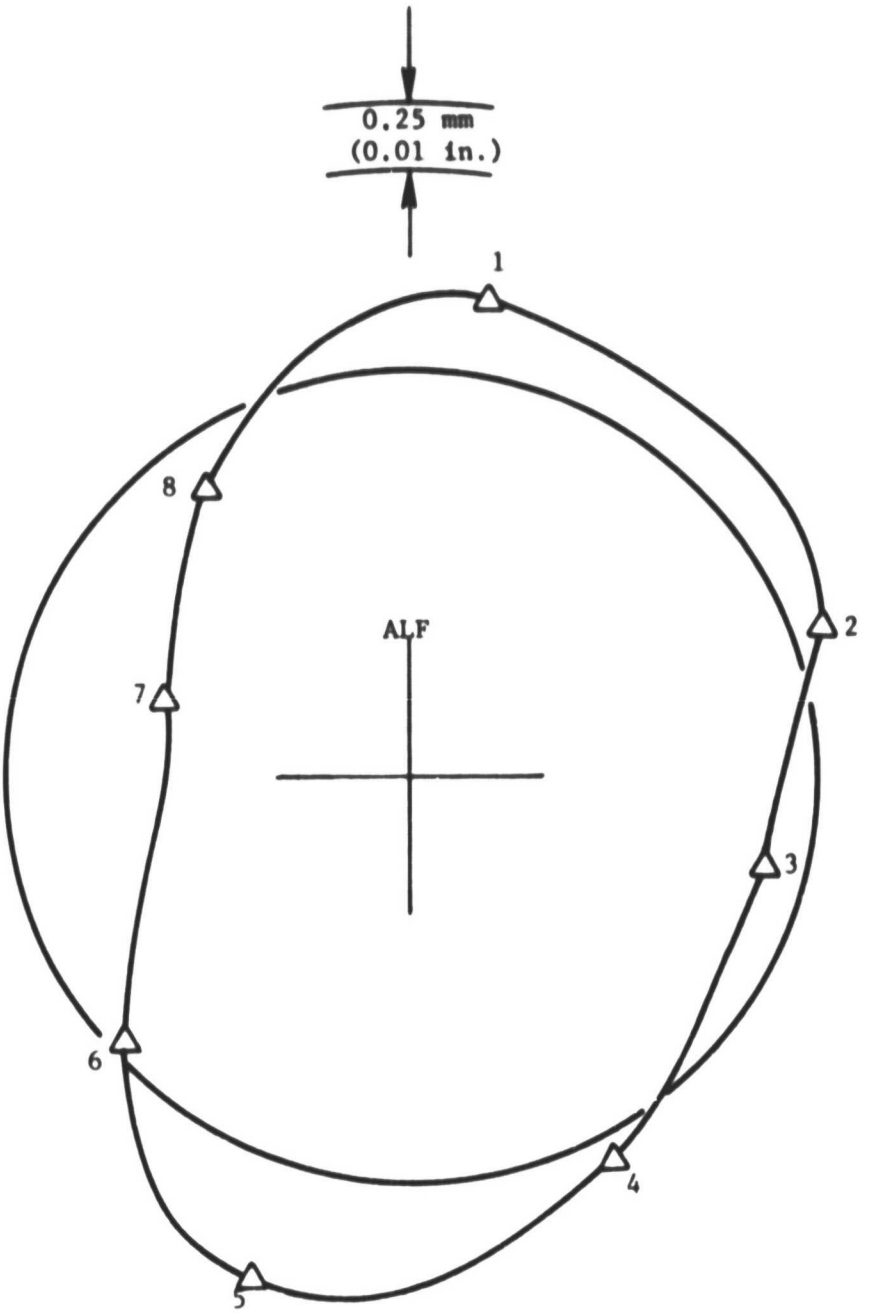

Figure 50. HP Turbine Stator Out-of-Roundness, 100 Seconds into Accel.

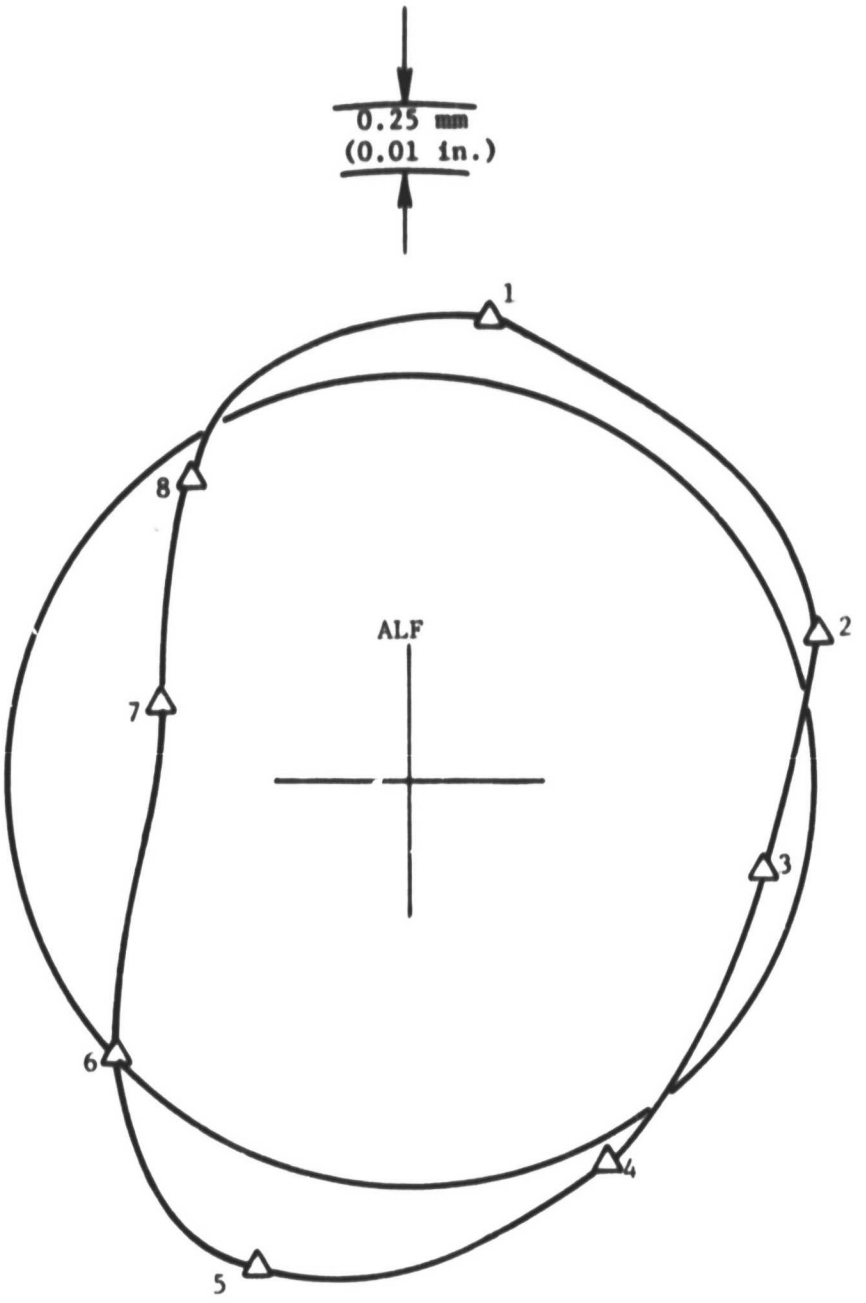

Figure 51. HP Turbine Stator Out-of-Roundness, 200 Seconds into Accel.

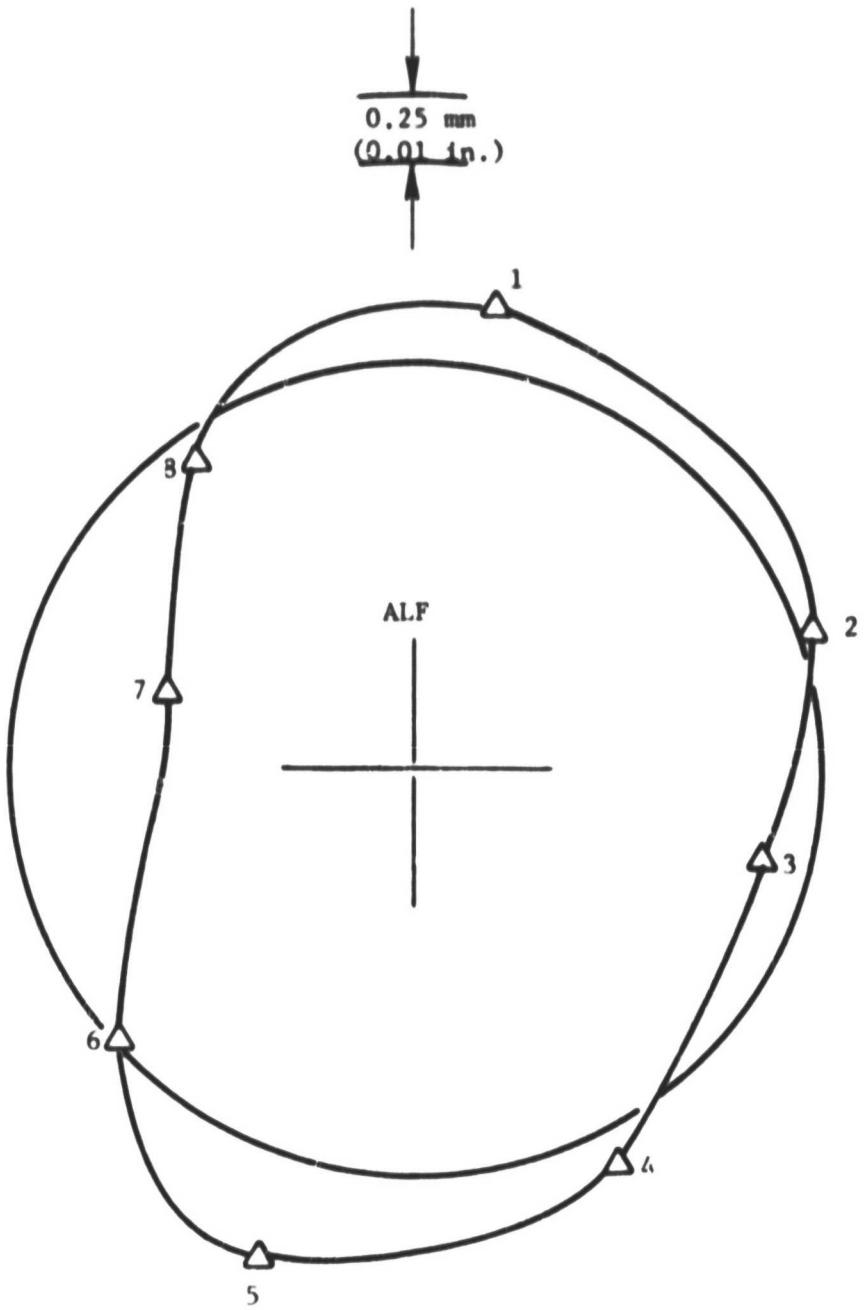

Figure 52. HP Turbine Stator Out-of-Roundness, 400 Seconds into Accel.

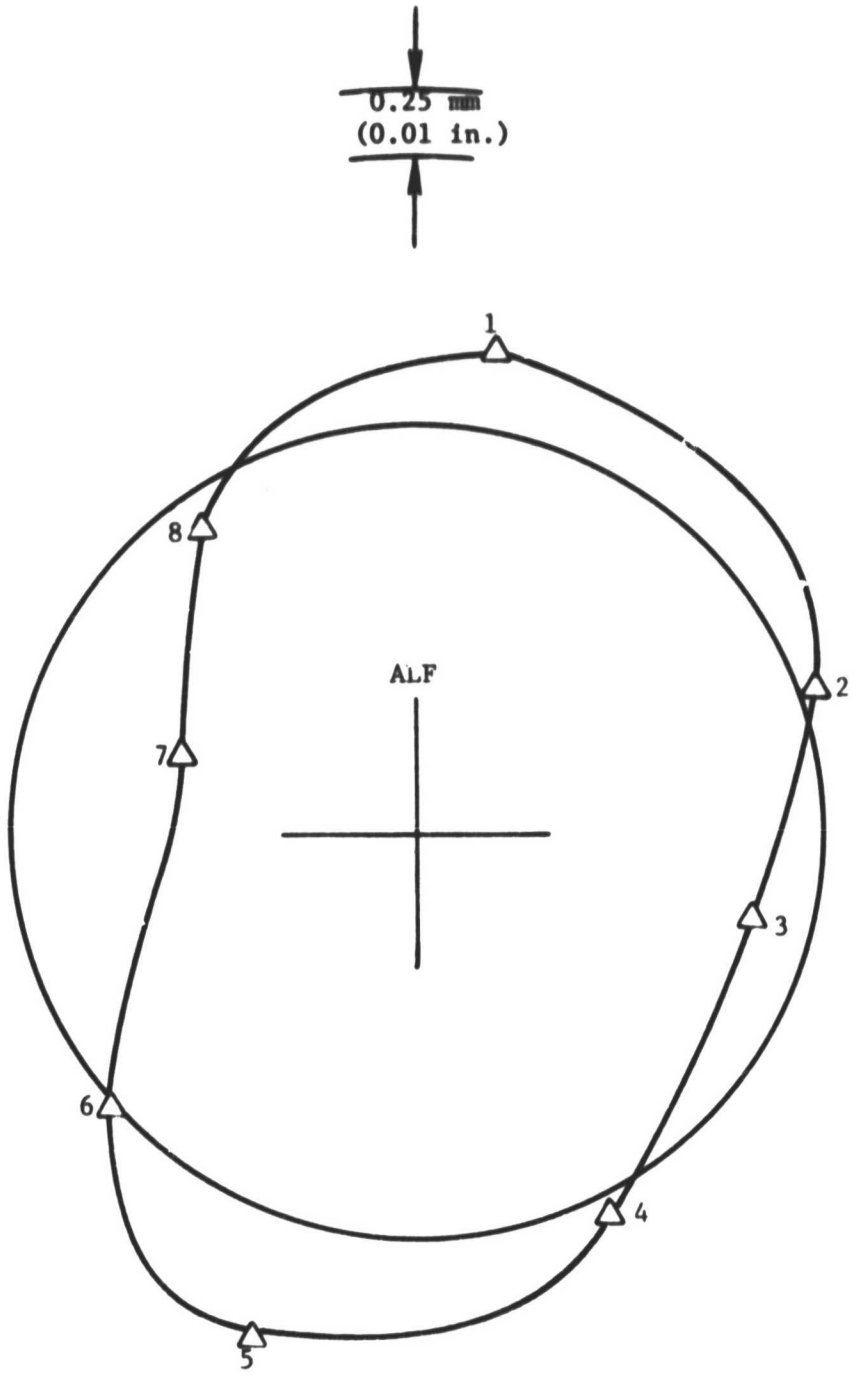

Figure 53. HP Turbine Stator Out-of-Roundness, 145 Seconds into Accel.

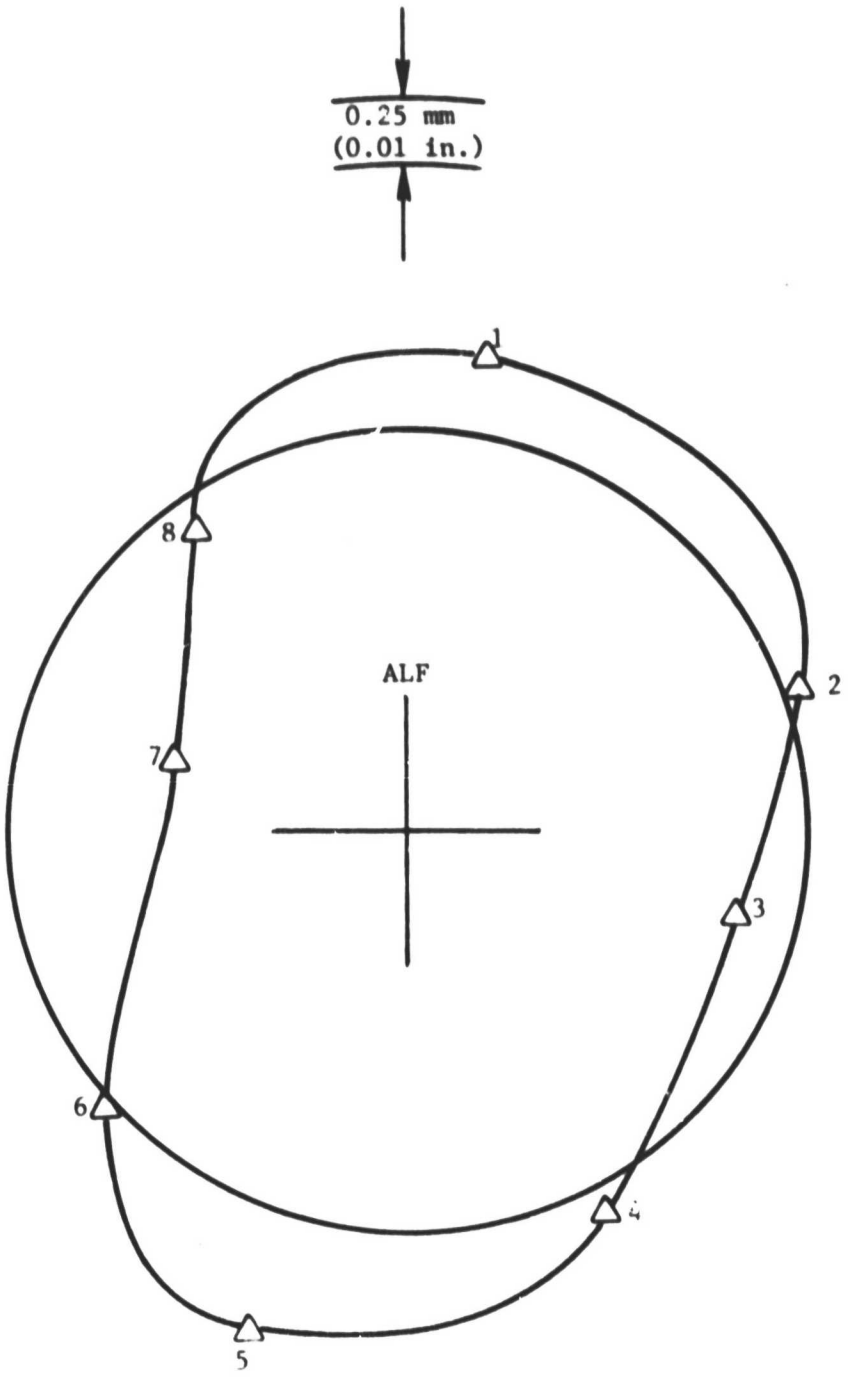

Figure 54. HP Turbine Stator Out-of-Roundness, 1 Second into Decel.

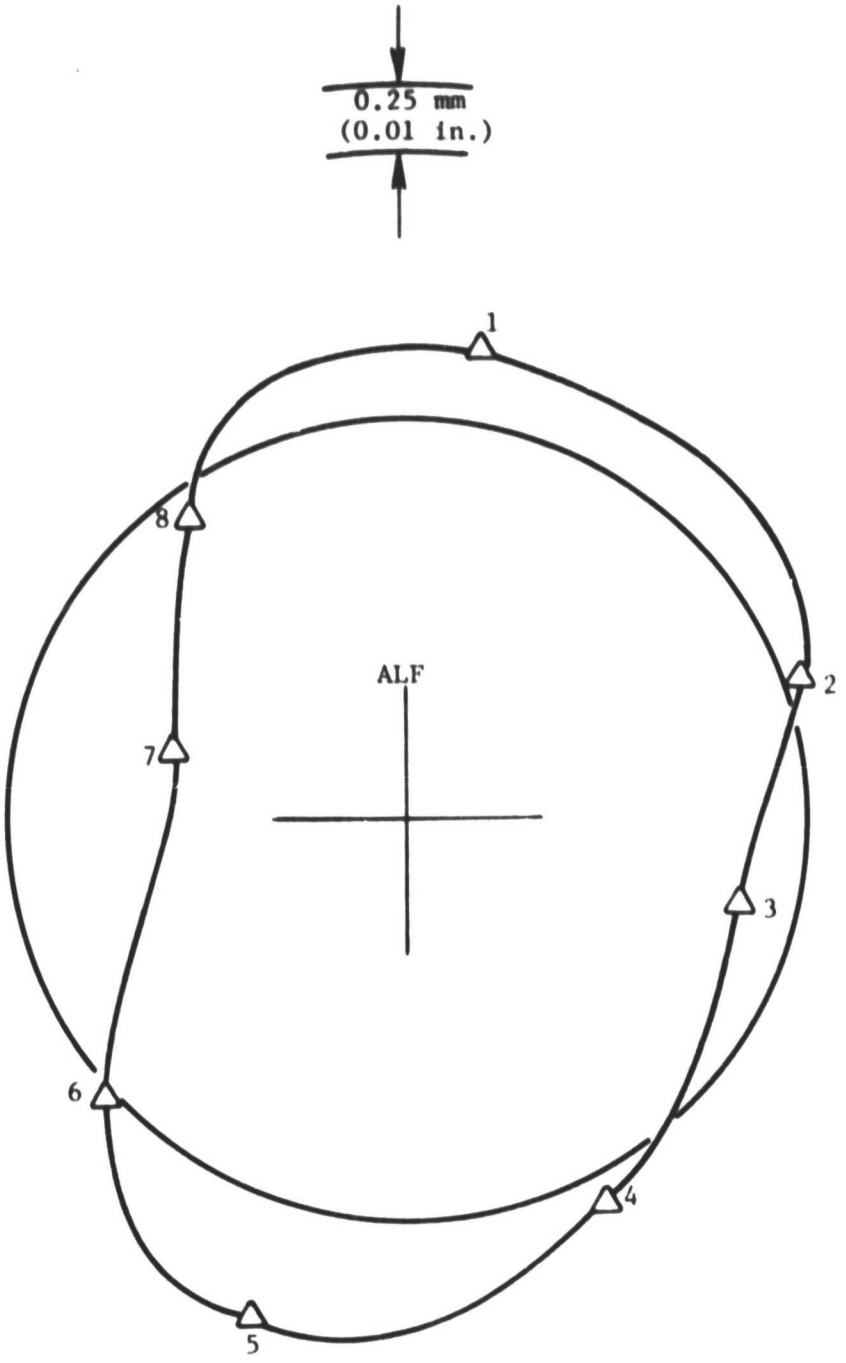

Figure 55. HP Turbine Stator Out-of-Roundness, 2 Seconds into Decel.

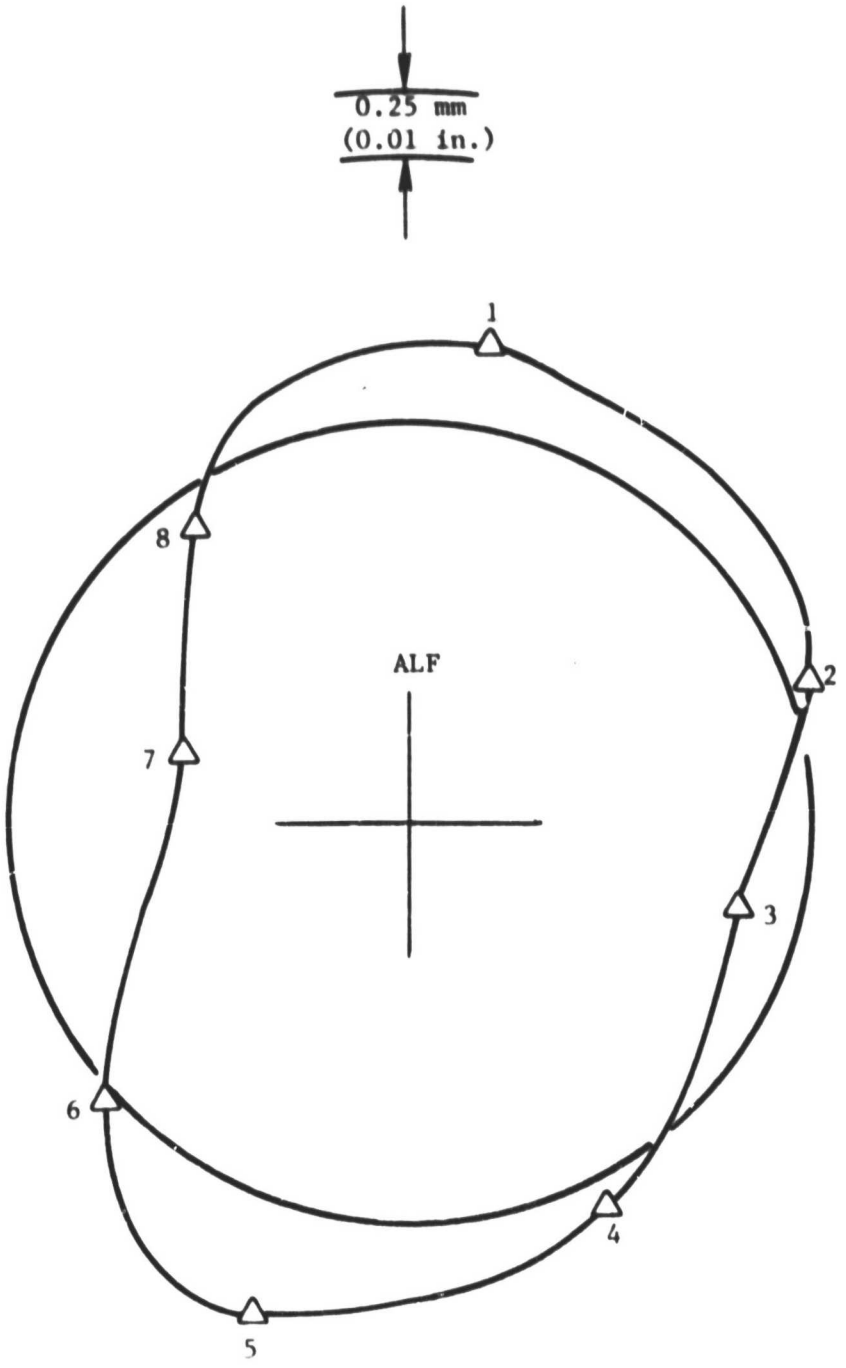

Figure 56. HP Turbine Stator Out-of-Roundness, 4 Seconds into Decel.

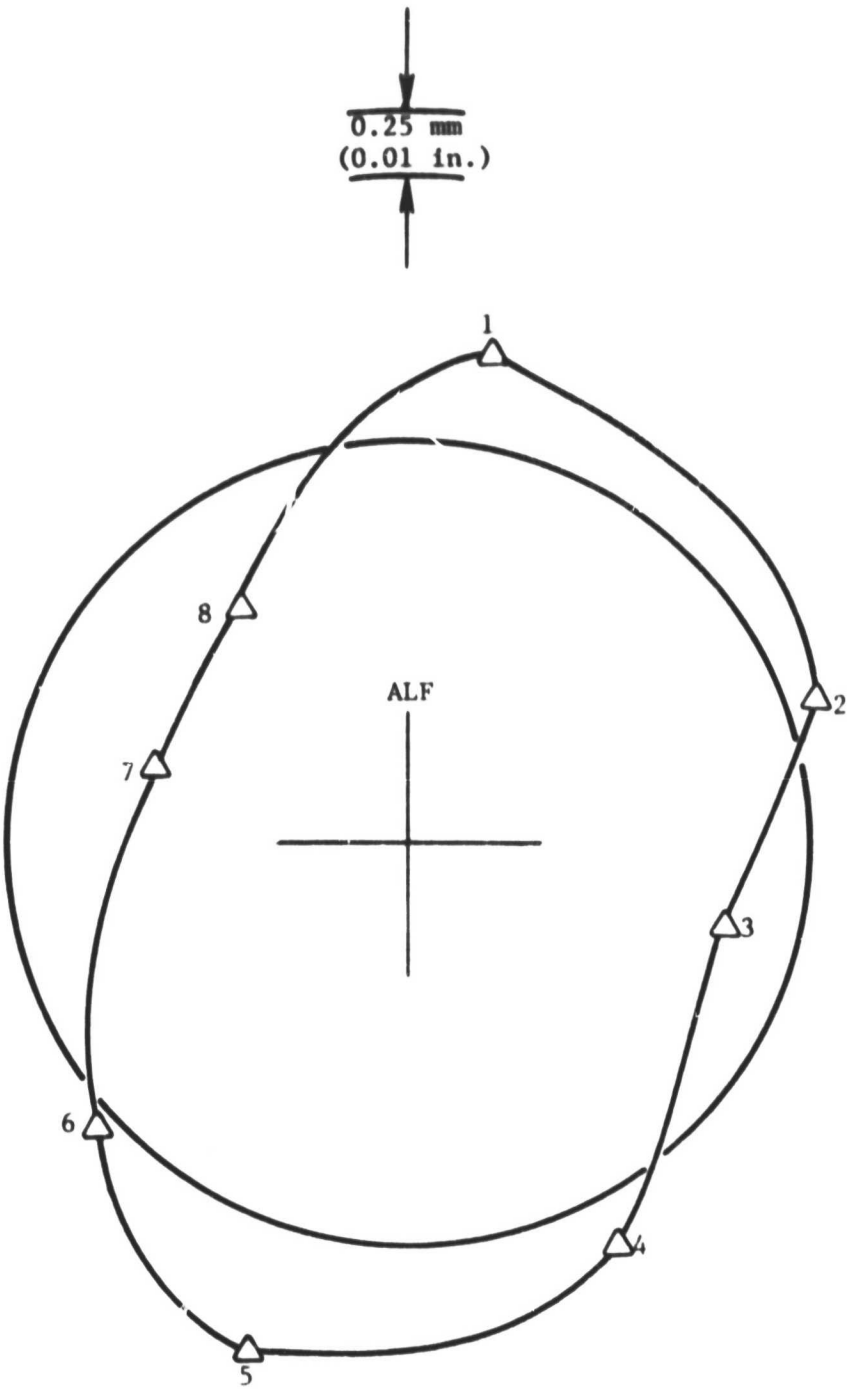

Figure 57. HP Turbine Stator Out-of-Roundness, 10 Seconds into Decel.

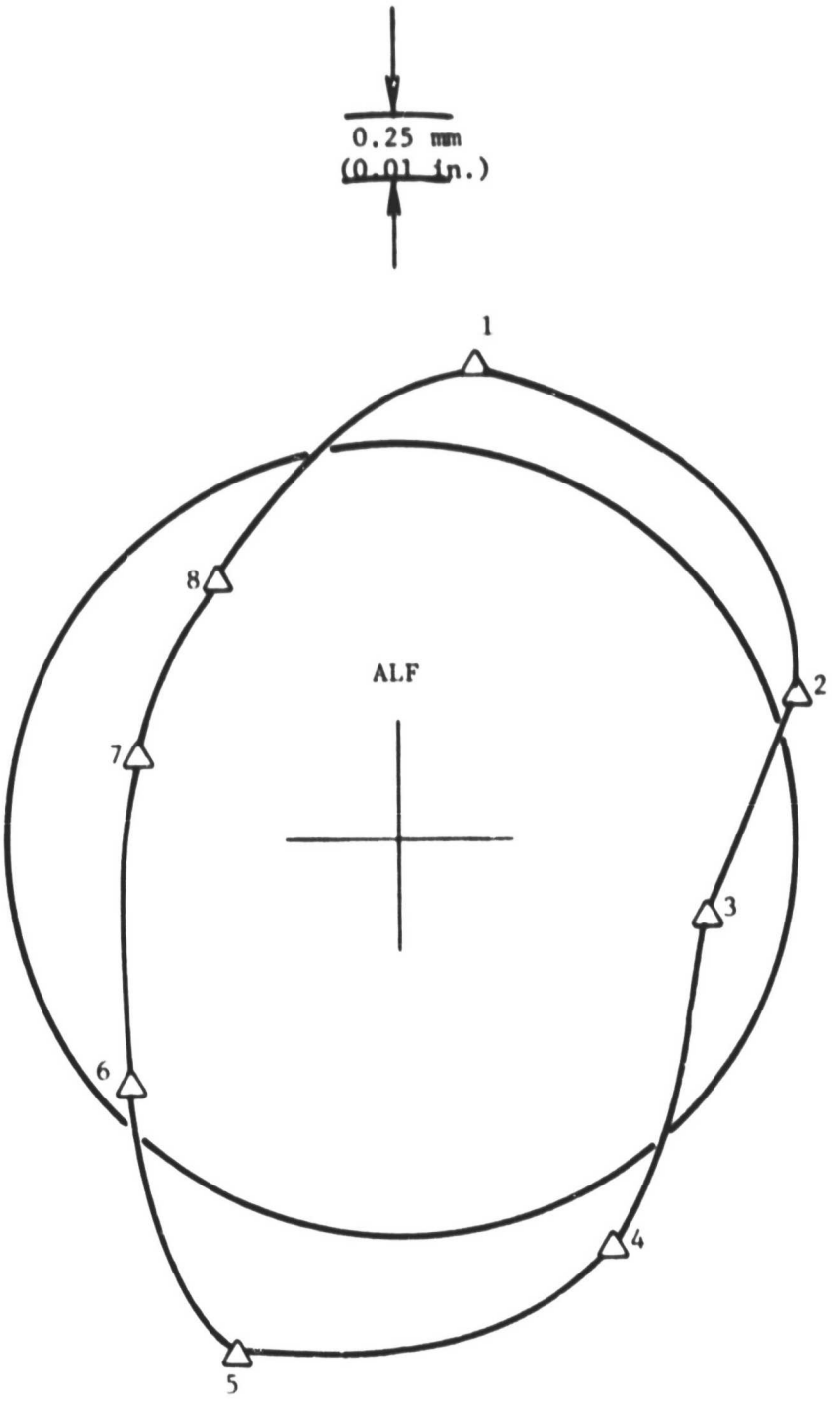

Figure 58. HP Turbine Stator Out-of-Roundness, 20 Seconds into Decel.

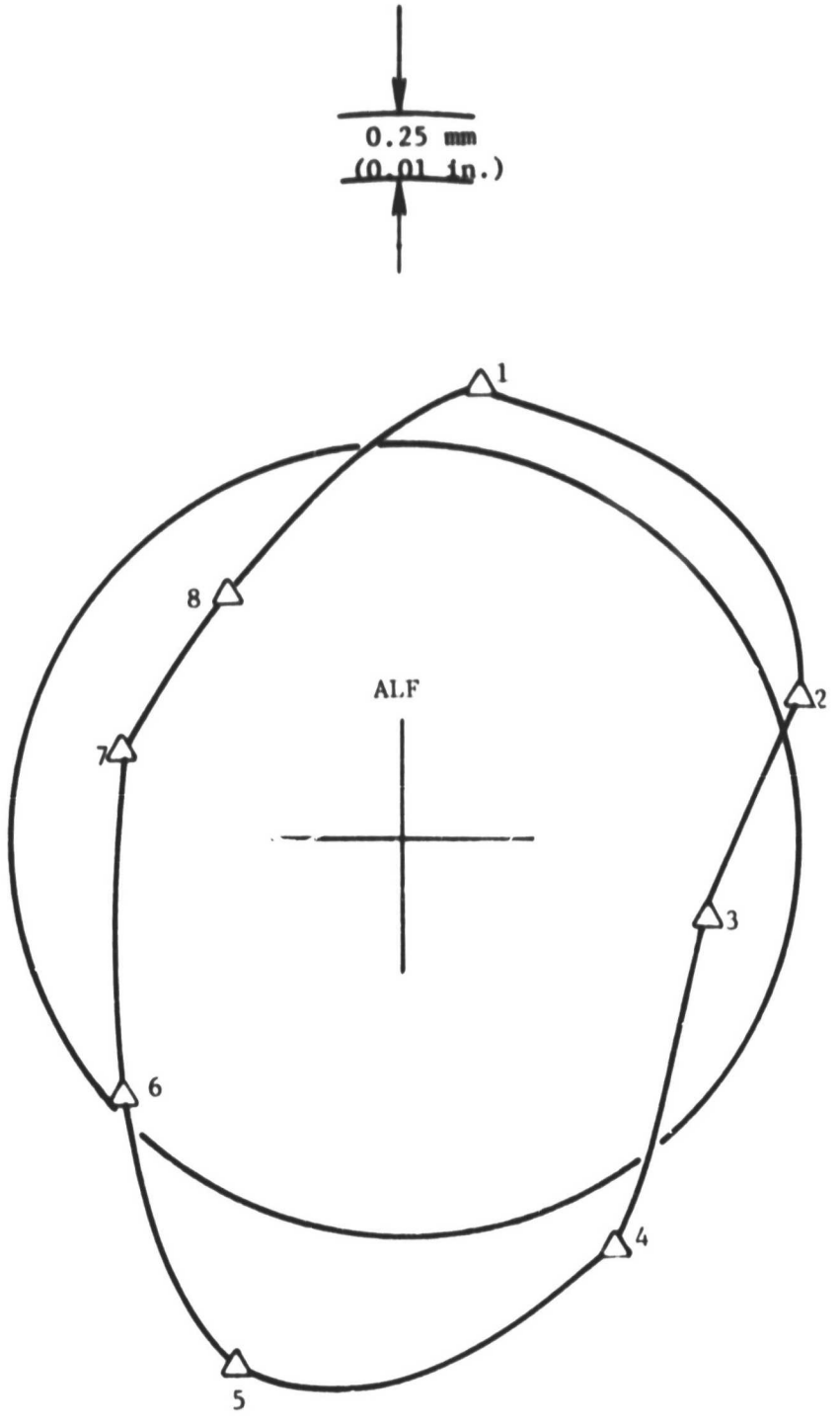

Figure 59. HP Turbine Stator Out-of-Roundness, 40 Seconds into Decel.

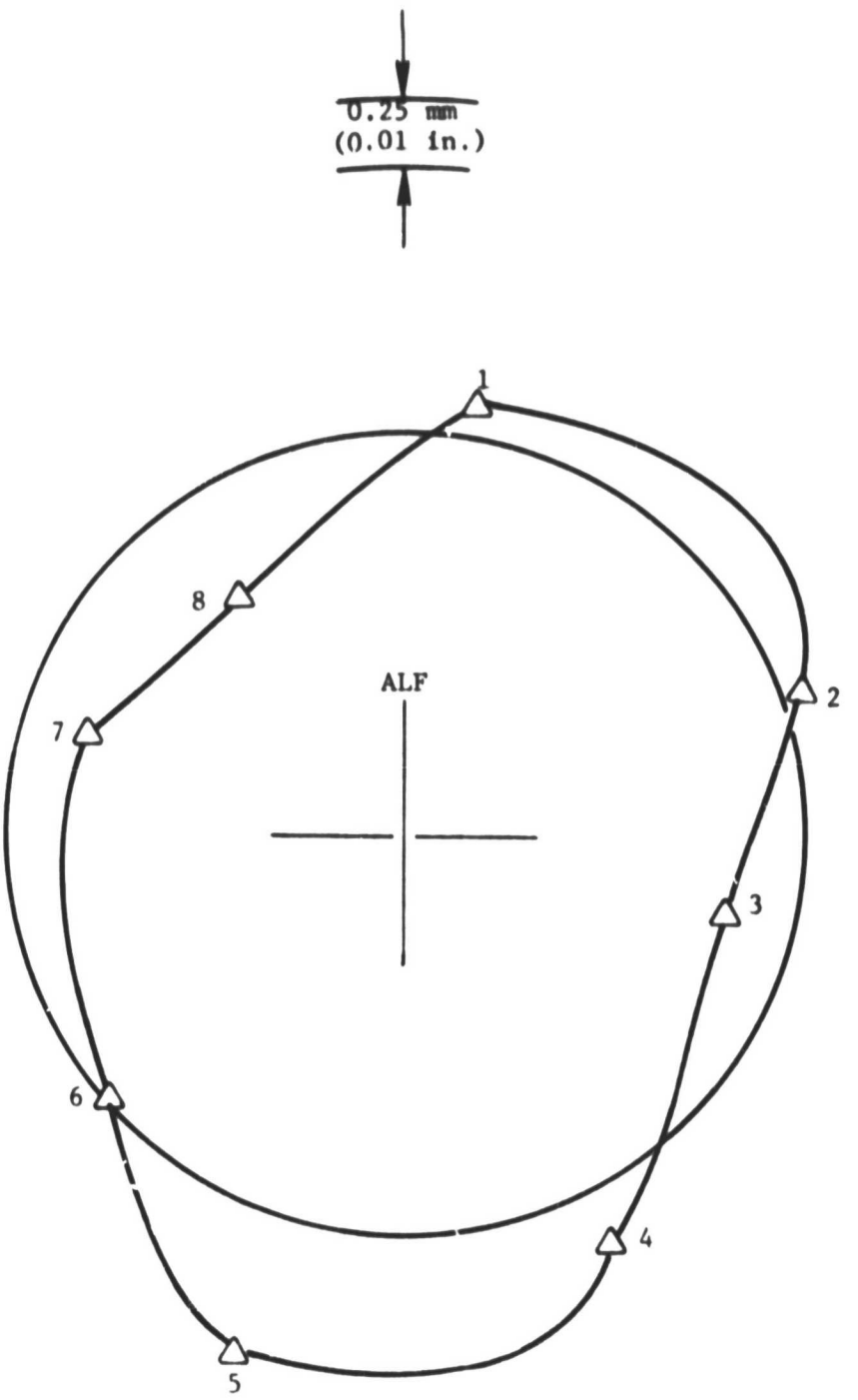

Figure 60. HP Turbine Stator Out-of-Roundness, 100 Seconds into Decel.

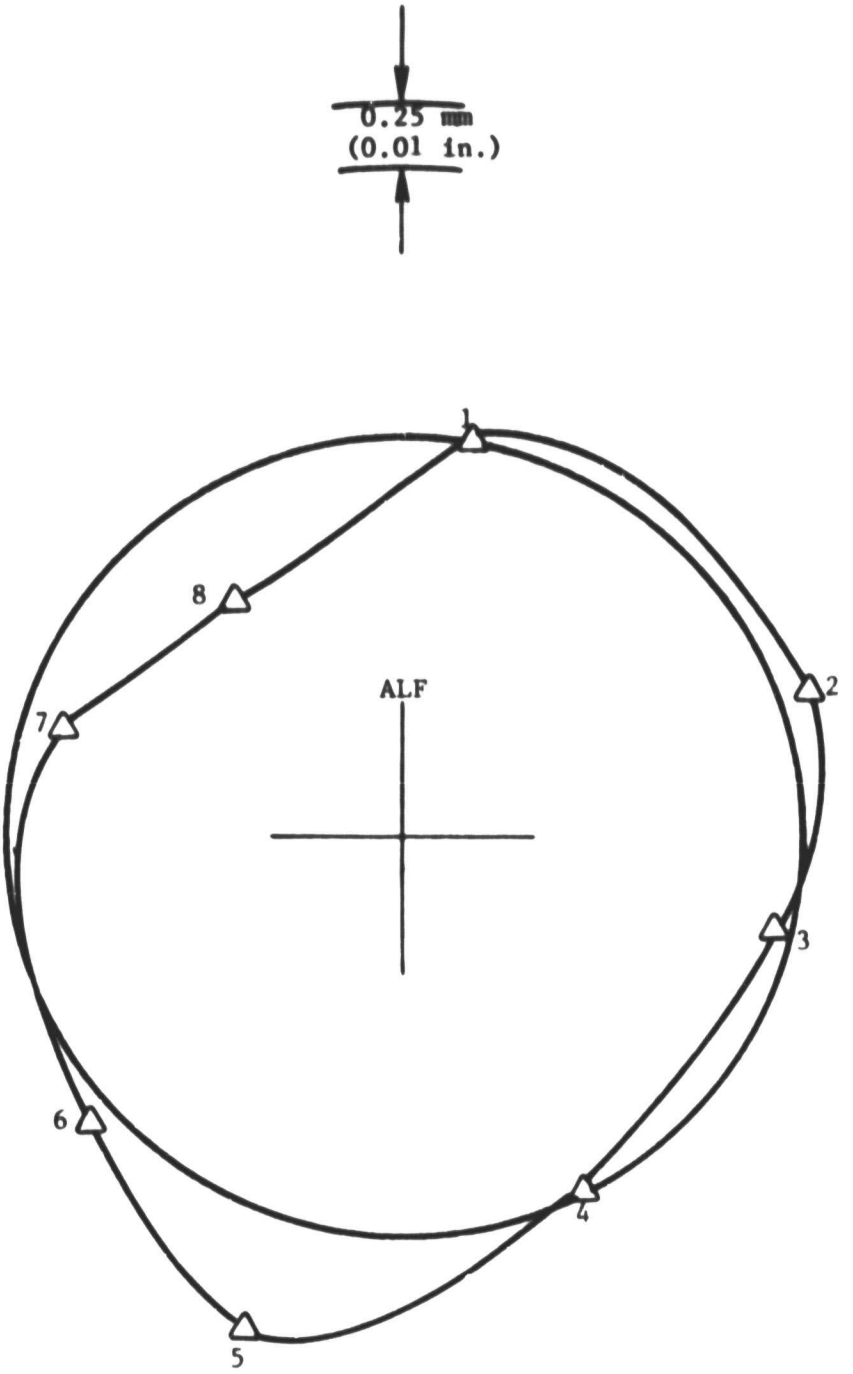

Figure 61. HP Turbine Stator Out-of-Roundness, 200 Seconds into Decel.

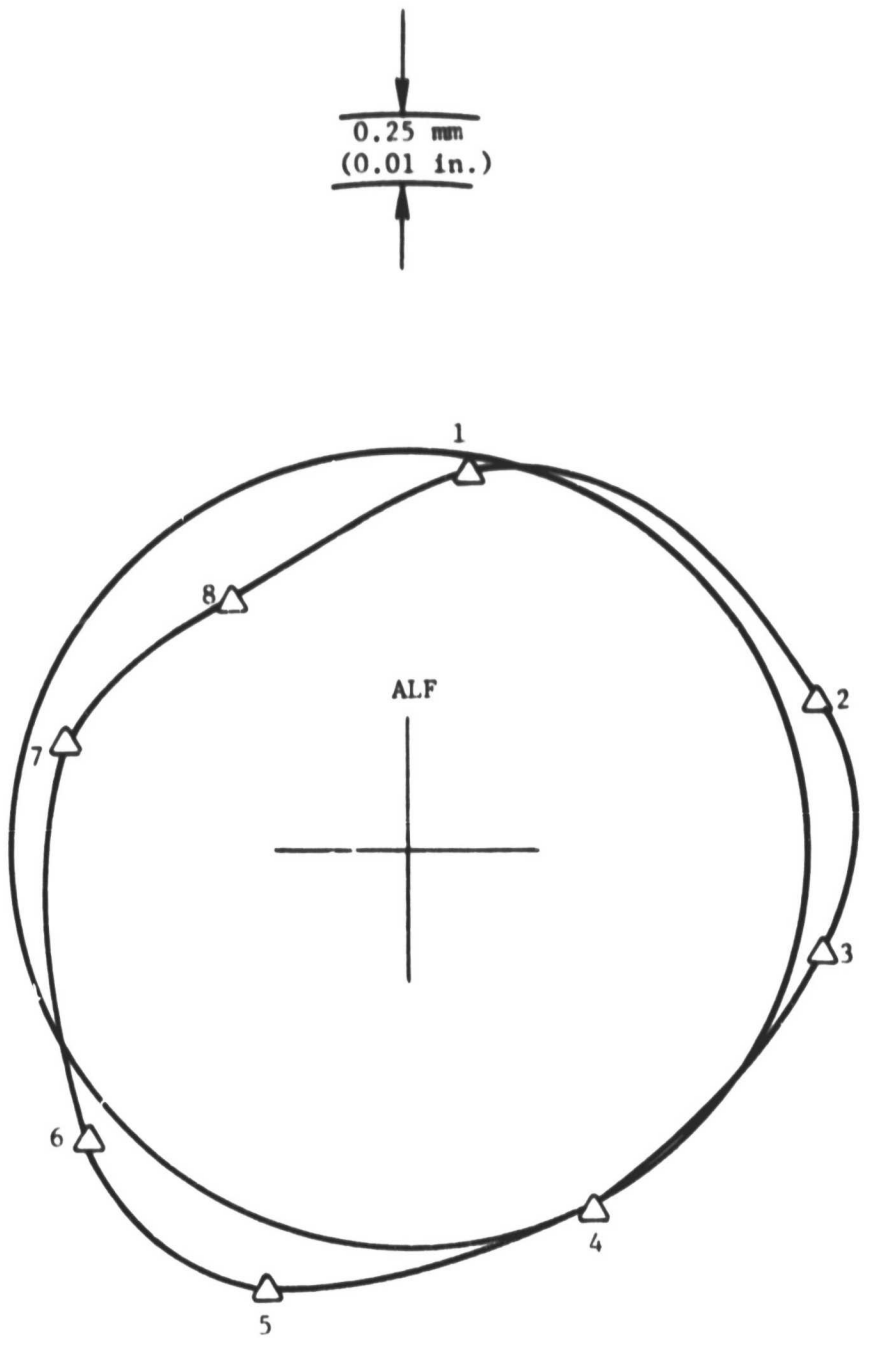

Figure 62. HP Turbine Stator Out-of-Roundness, 400 Seconds into Decel.

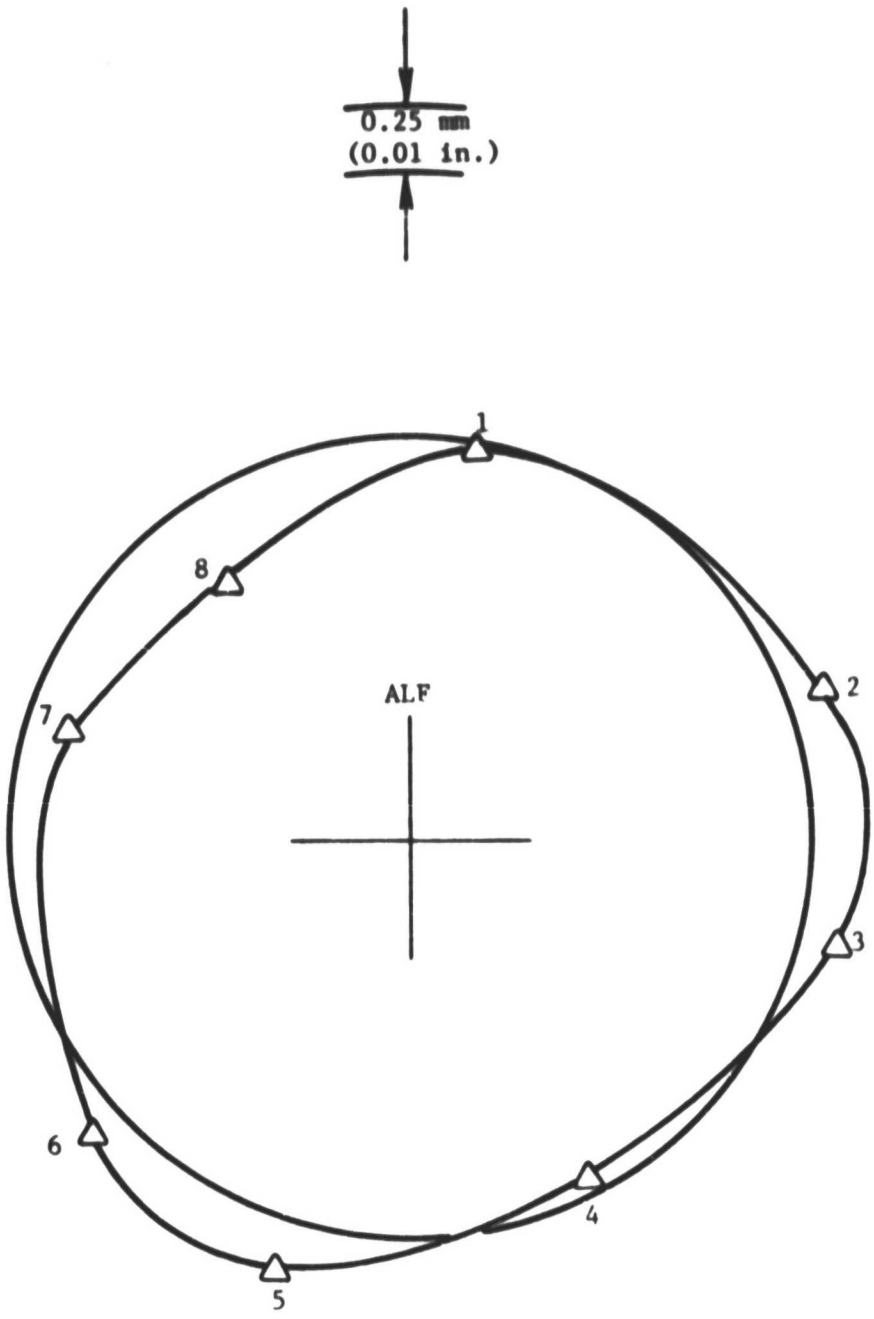

Figure 63. HP Turbine Stator Out-of-Roundness, 715 Seconds into Decel.

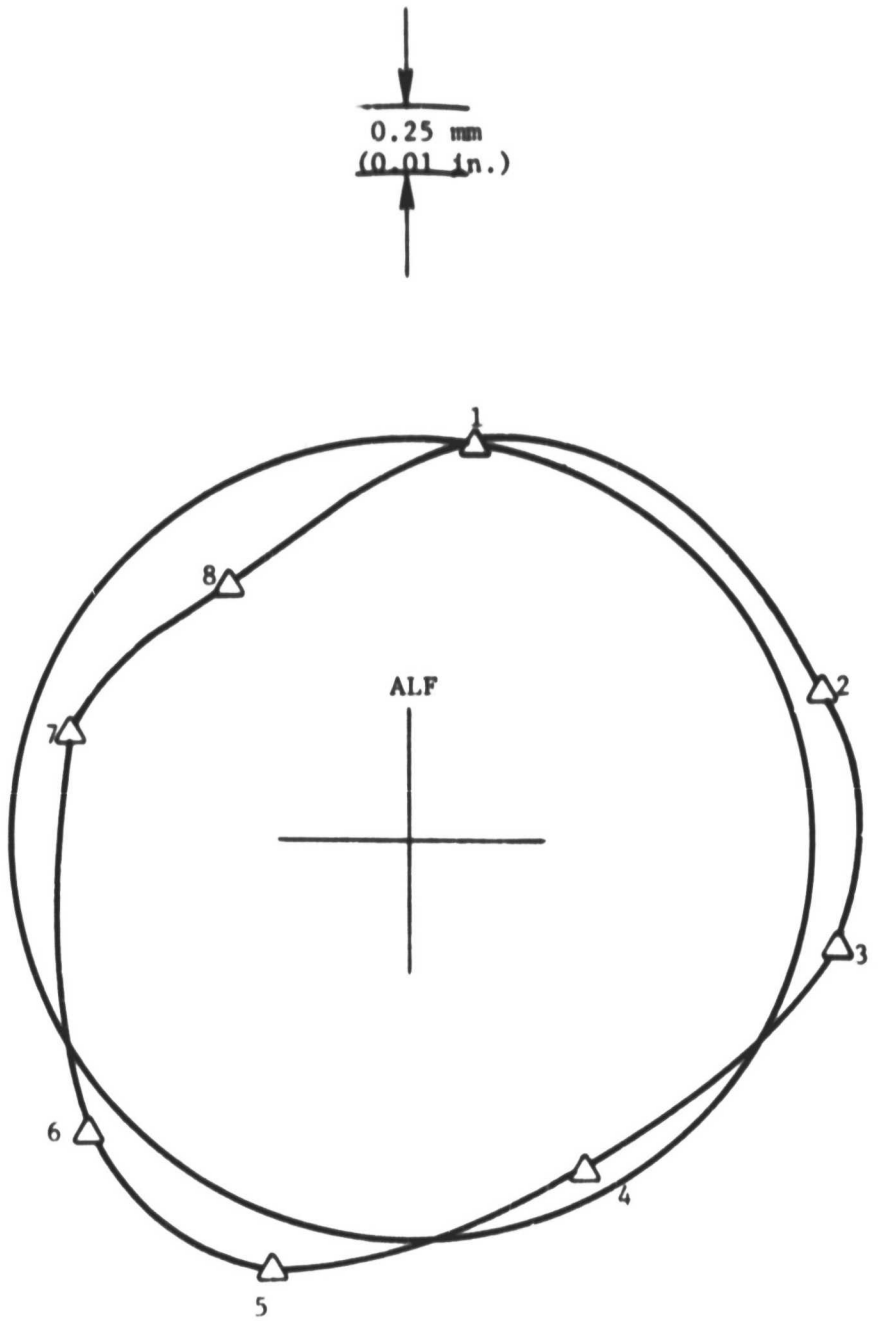

Figure 64. HP Turbine Stator Out-of-Roundness, 1031 Seconds into Decel.

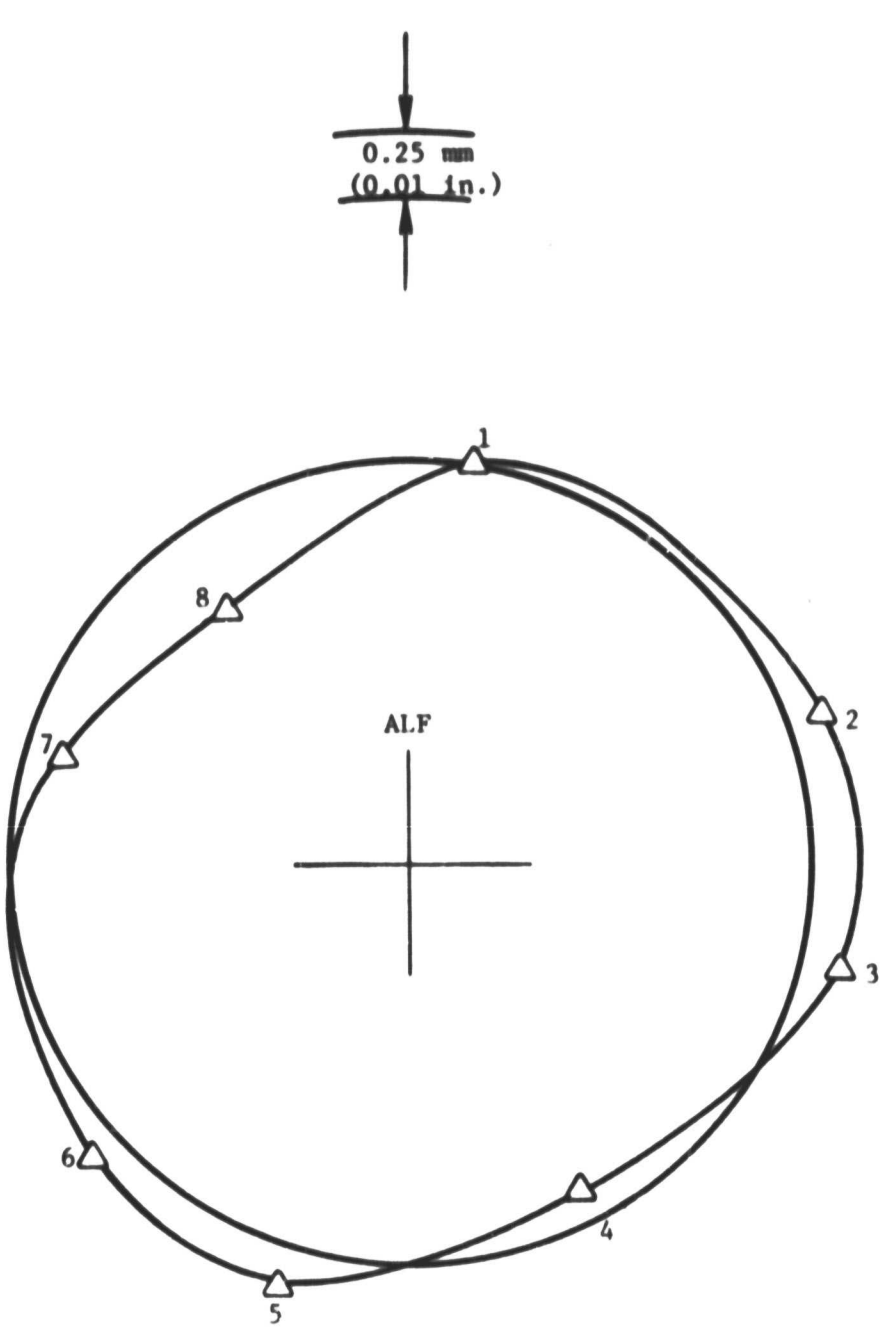

Figure 65. HP Turbine Stator Out-of-Roundness, 2199 Seconds into Decel.

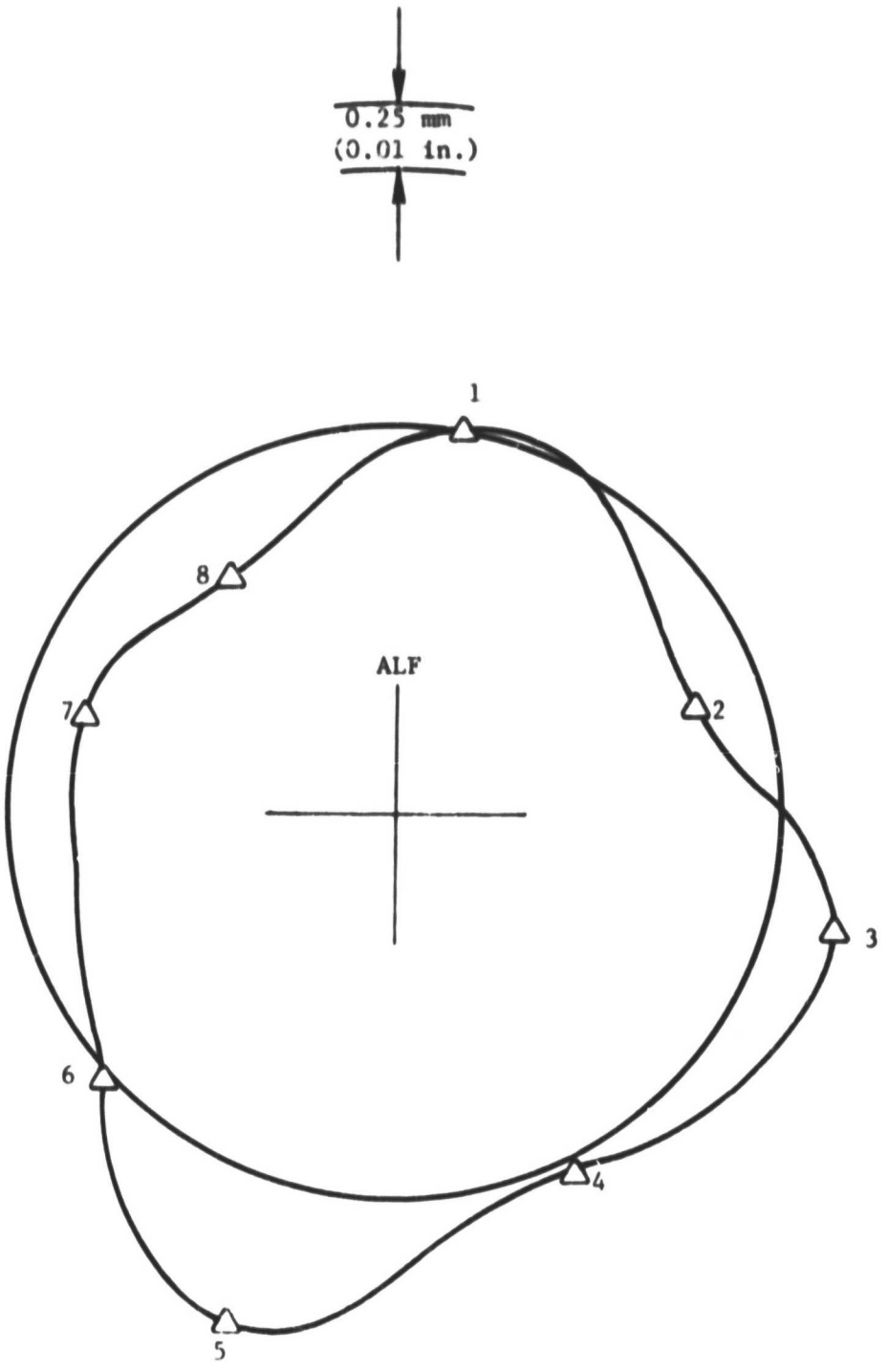

Figure 66. HP Turbine Stator Out-of-Roundness, 1 Second into Reburst.

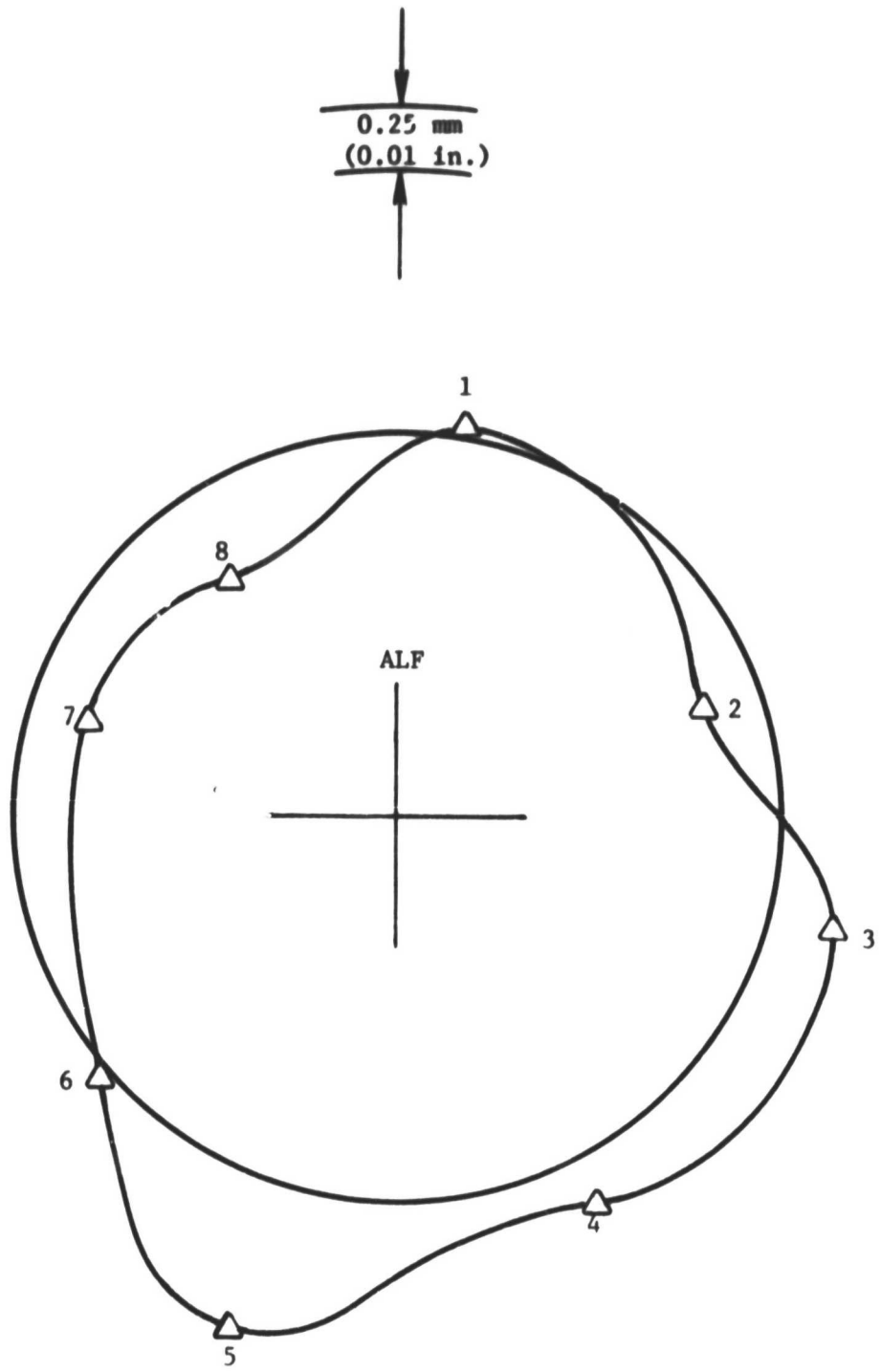

Figure 67. HP Turbine Stator Out-of-Roundness, 2 Seconds into Reburst.

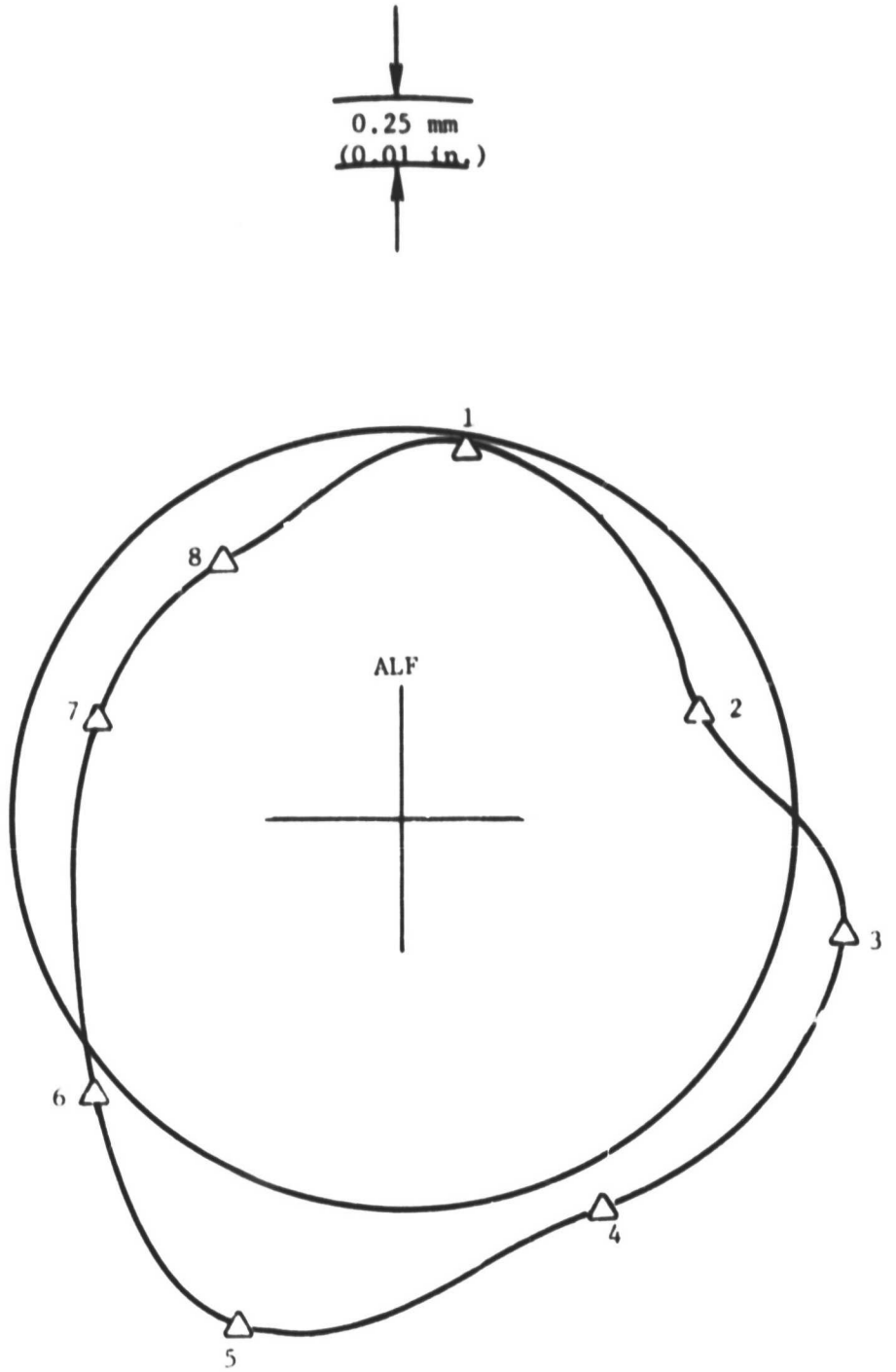

Figure 68. HP Turbine Stator Out-of-Roundness, 3 Seconds into Reburst.

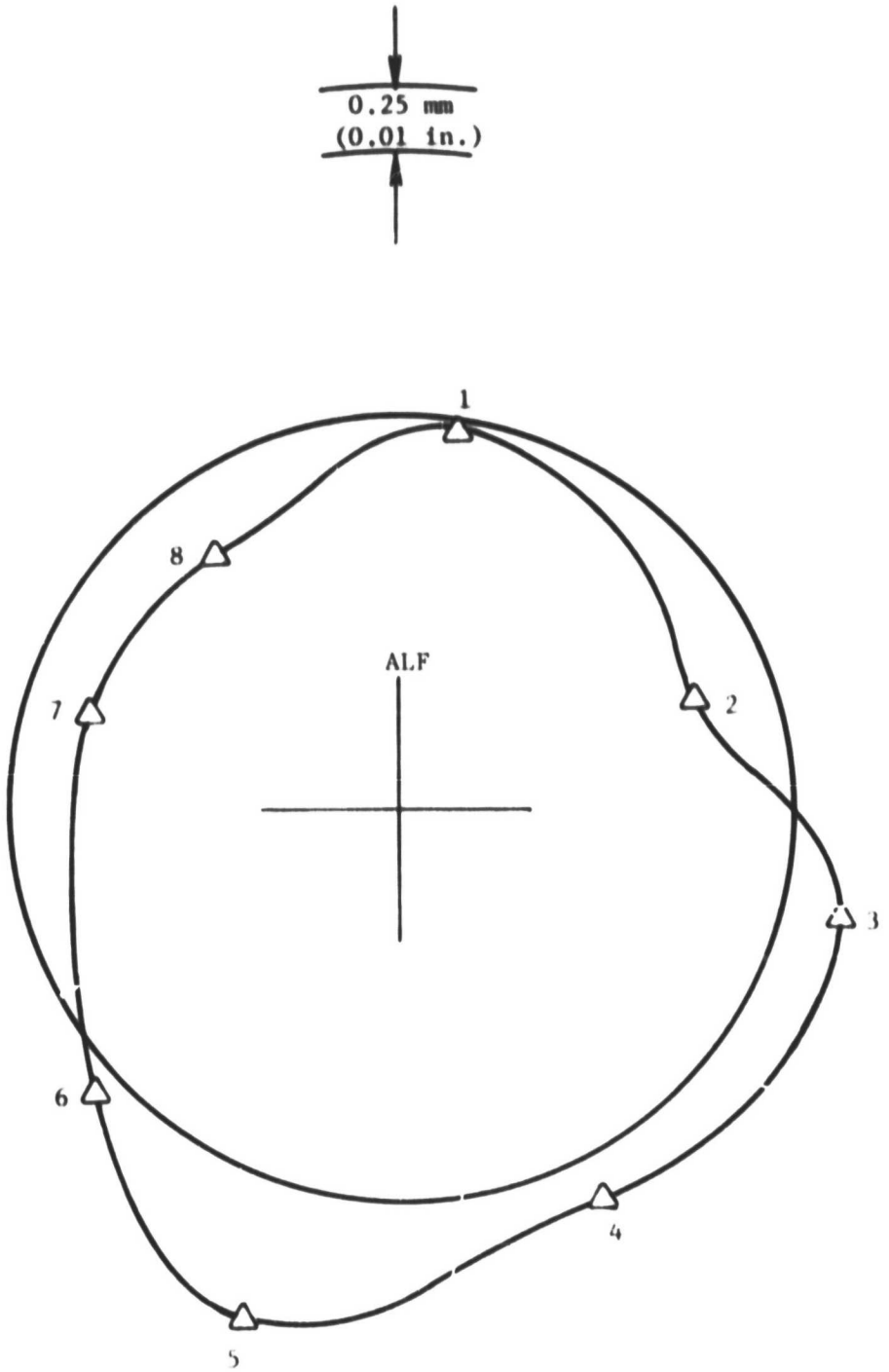

Figure 69. HP Turbine Stator Out-of-Roundness, 5 Seconds into Reburst.

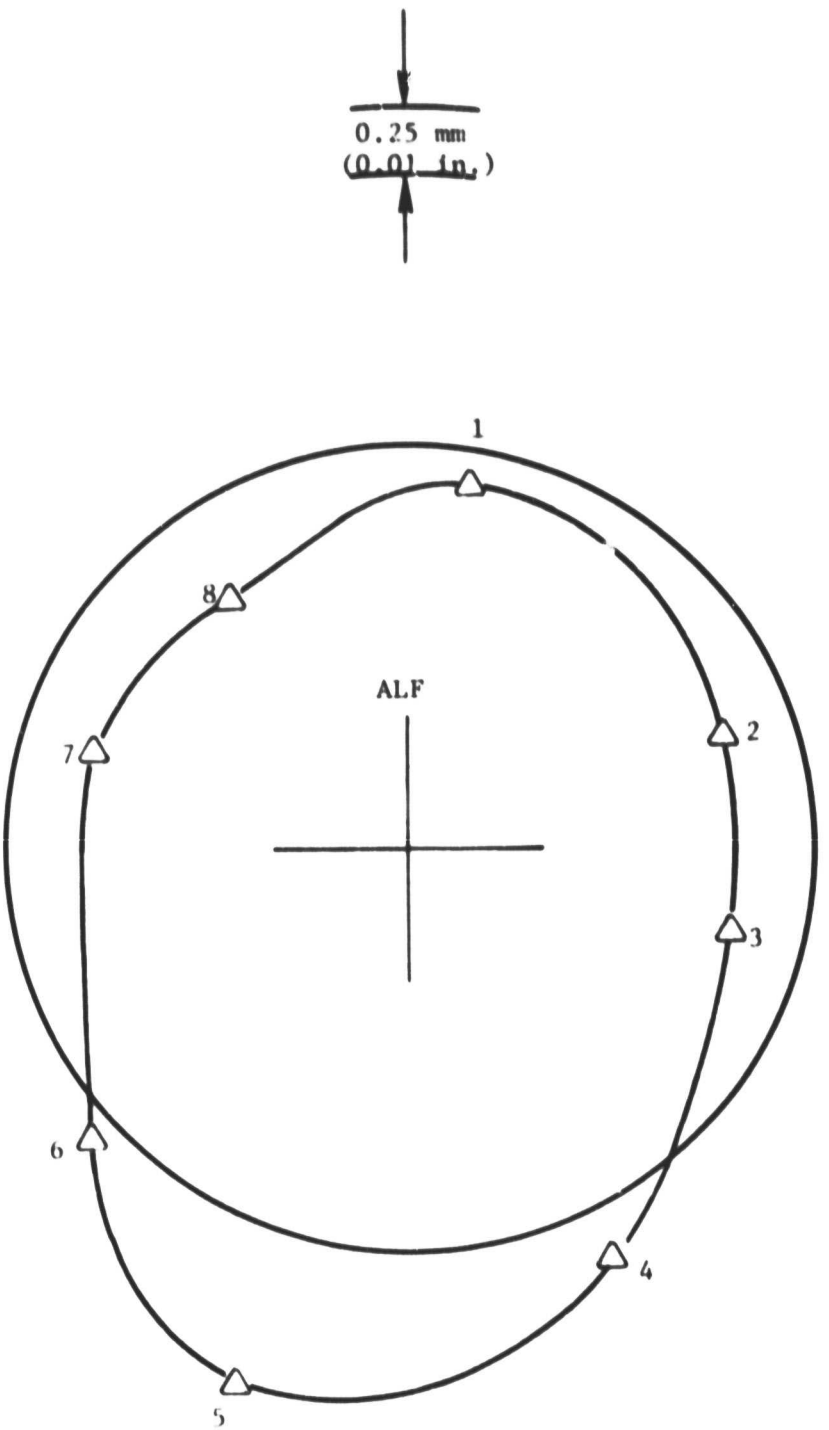

Figure 70. HP Turbine Stator Out-of-Roundness, 10 Seconds into Reburst.

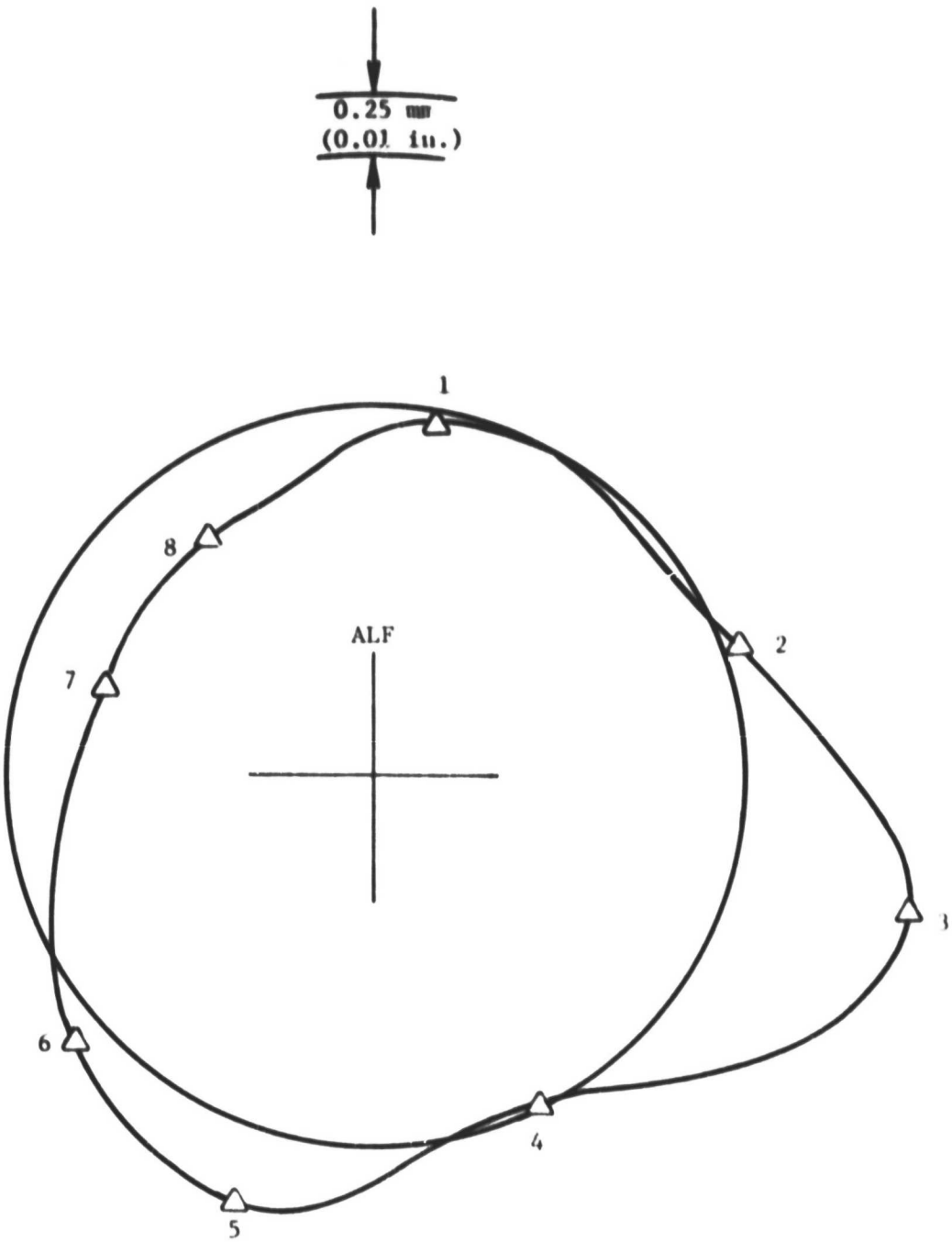

Figure 71. HP Turbine Stator Out-of-Roundness, 20 Seconds into Reburst.

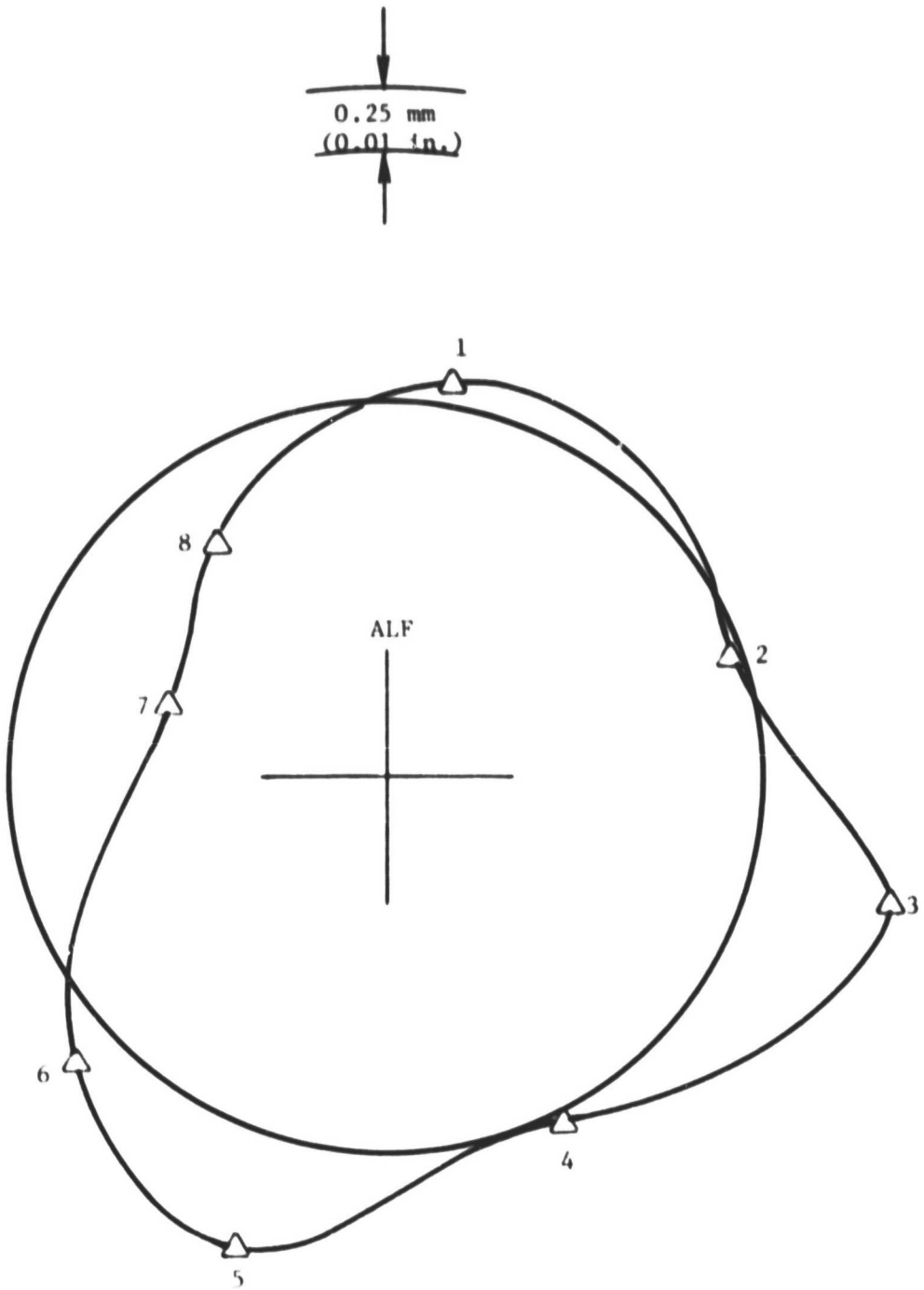

Figure 72. HP Turbine Stator Out-of-Roundness, 50 Seconds into Reburst.

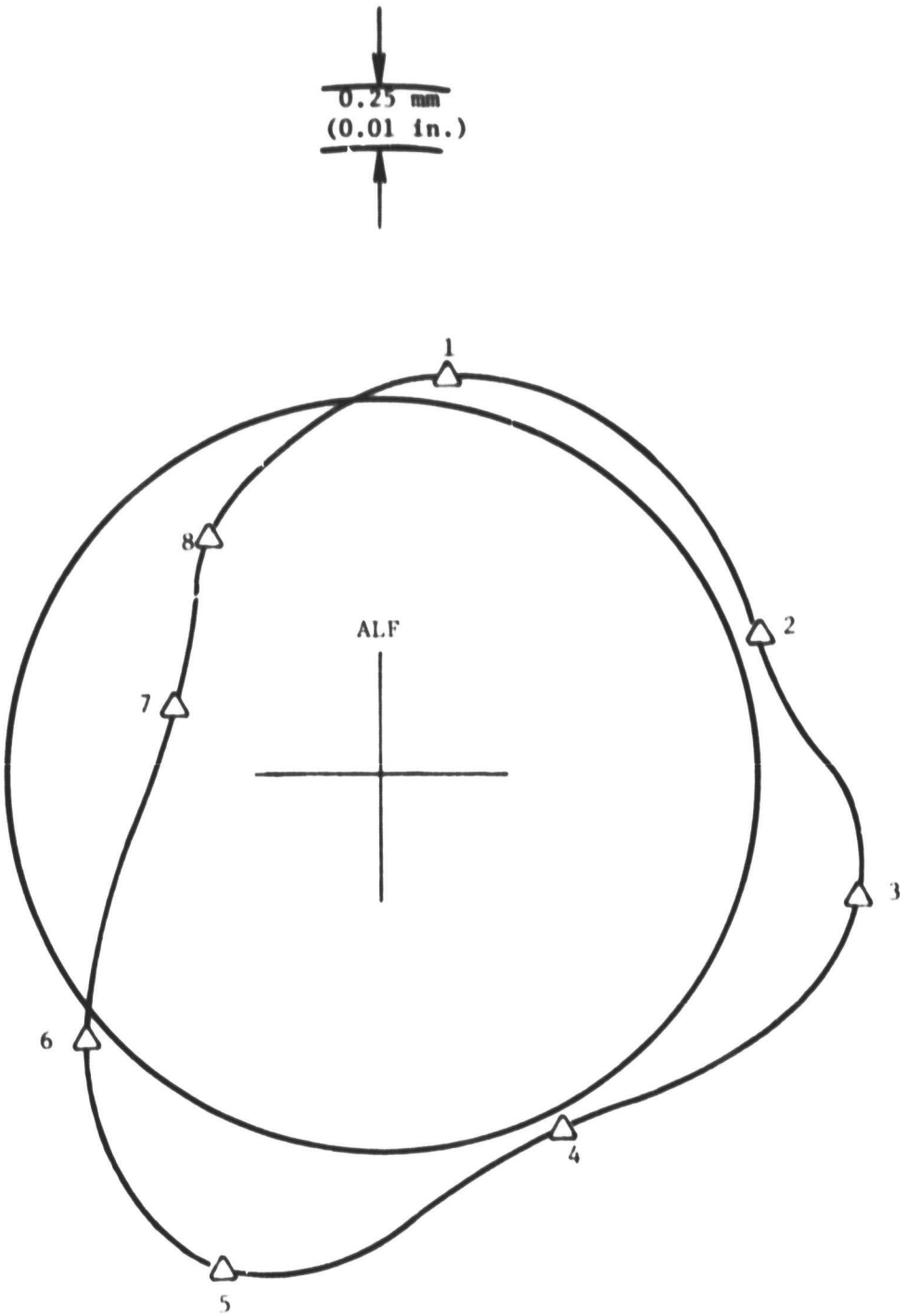

Figure 73. HP Turbine Stator Out-of-Roundness, 200 Seconds into Reburst.

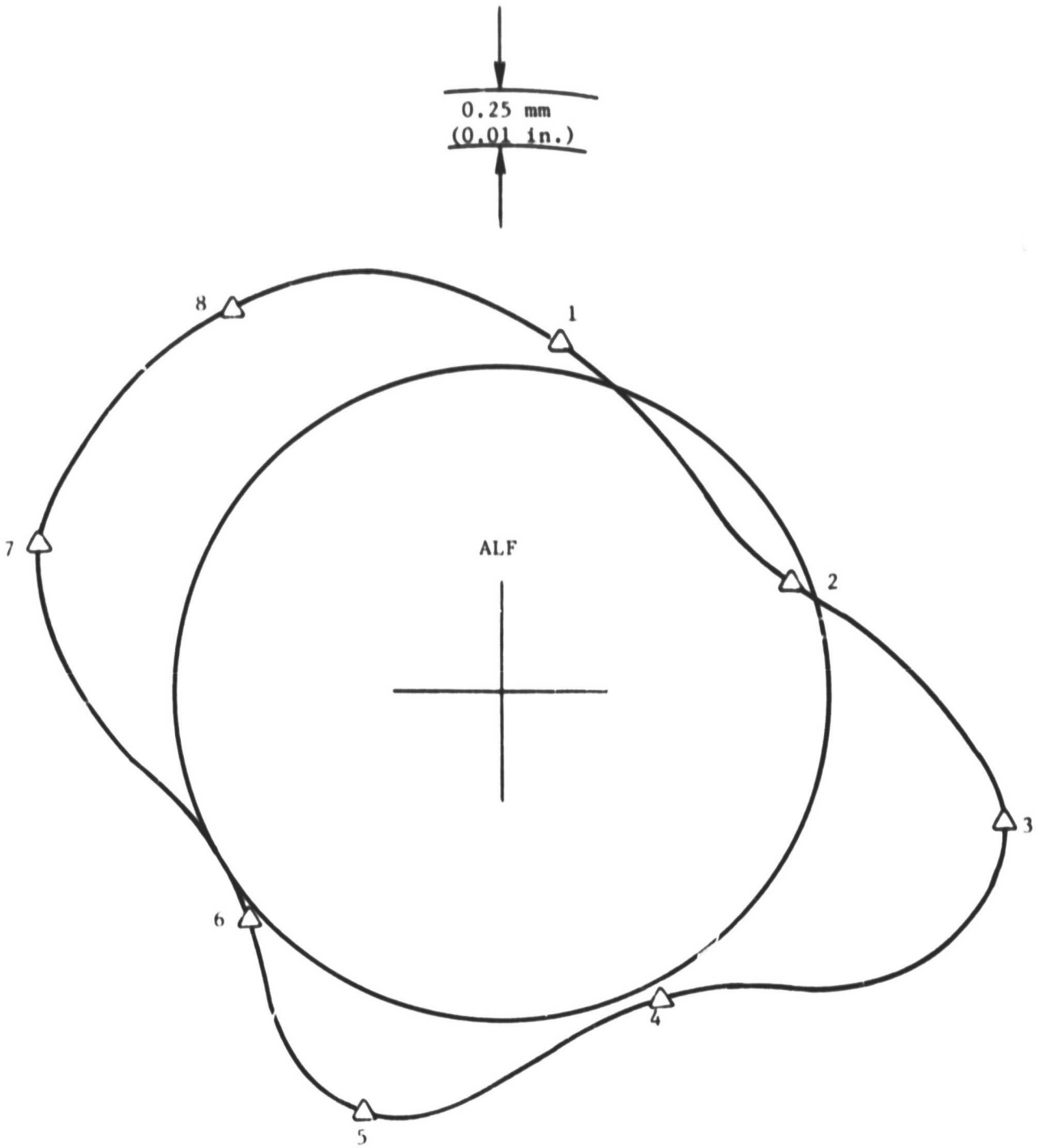

Figure 74. HP Turbine Stator Out-of-Roundness, 300 Seconds into Reburst.

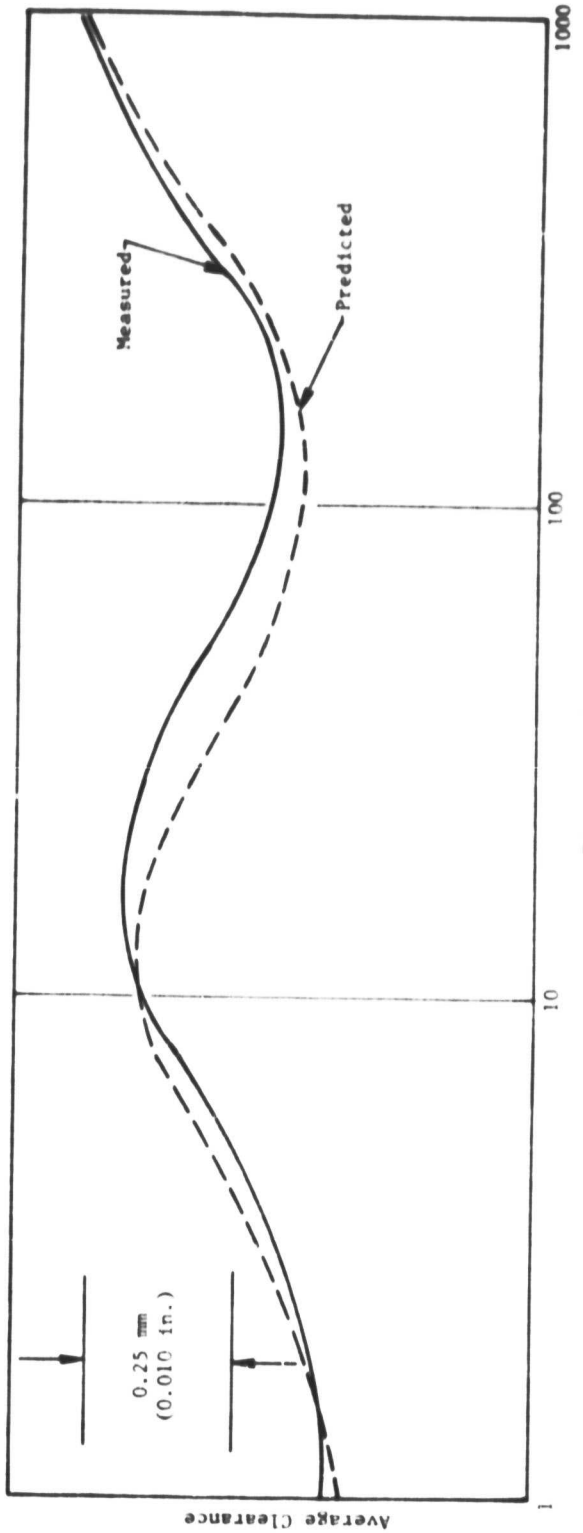

Figure 75. Clearance Versus Time During a Decel.

predicted curve is good. There is a slight mismatch which is probably due to heat transfer inaccuracies. The clearance during a decel from steady-state takeoff is characterized by three regions. The first region represents a clearance increase due to loss of speed and other mechanical effects. The second region is a clearance decrease because the stator is cooling and closing around a still warm rotor. Finally, the stator cooling stops but the rotor continues to cool causing clearance to increase.

Accel from Stabilized Ground Idle to Steady-State Takeoff

The measured and predicted clearance responses during an accel are shown in Figure 76. Again, the correlation between measured and predicted clearance is quite good. The predicted response suggests more closure early into the burst than was measured. This reflects differences between real-engine and assumed transient heat transfer rates. Other possible sources of mismatch, both for the accel and decel, are those modifications necessary to cause the data to reflect an engine which is always run to the same ambient conditions and which exhibits constant engine performance functions.

An accel also contains three specific regions. Clearance decreases as a result of increased rotor speed. The stator structure then warms, increasing clearance and finally, clearance decreases because the rotor slowly obtains the steady-state temperatures.

Reburst s

A reburst is a rapid accel from idle to high power after the engine had previously run at high power for a time sufficient to heat up the rotor components. The specified dwell time at ground idle prior to accel is used to identify the reburst, for example, a 4 min. reburst would have a 4 min. idle dwell time prior to reacceleration. The clearance characteristics of a reburst are a composite of those of a decel and accel. The minimum clearance during a decel occurs when the stator has cooled but the rotor is still quite warm. When an accel occurs from these conditions, the additional loss of clearance due to speed and other mechanical effects creates a minimum clearance condition. The clearance during the decel is the determining factor for the minimum clearance since the mechanical closure during an accel is essentially constant.

A family of reburst clearance response curves with idle dwell times of 8, 6, 4, 2, 1.5, 1, and 0.5 minutes is presented in Figure 77. Each curve starts with the clearance just before the final accel from the specified idle dwell time.

A two-minute reburst was analytically assessed as that which yields the minimum clearance or even a blade-on-shroud rub, dependent upon the cold clearance. However, for this particular test vehicle, 455-507/20, the minimum clearance condition was obtained during a 90-second reburst as shown on Figure 77. If the decel curve (Figure 75) is examined, it can be observed that the clearance is changing very little from approximately 80 seconds to 250 seconds. Since stator and rotor heat transfer are each contesting for domination in this region, the secondary effects, such as actual metal thicknesses and composition,

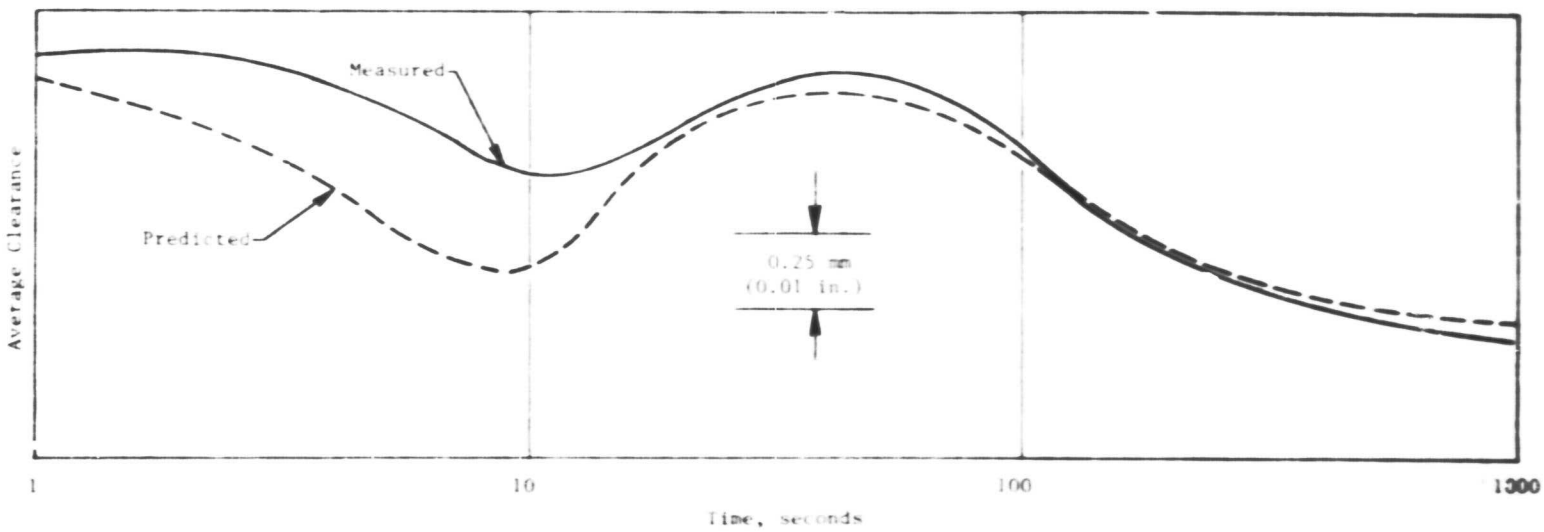

Figure 76. Clearance Versus Time During an Accel.

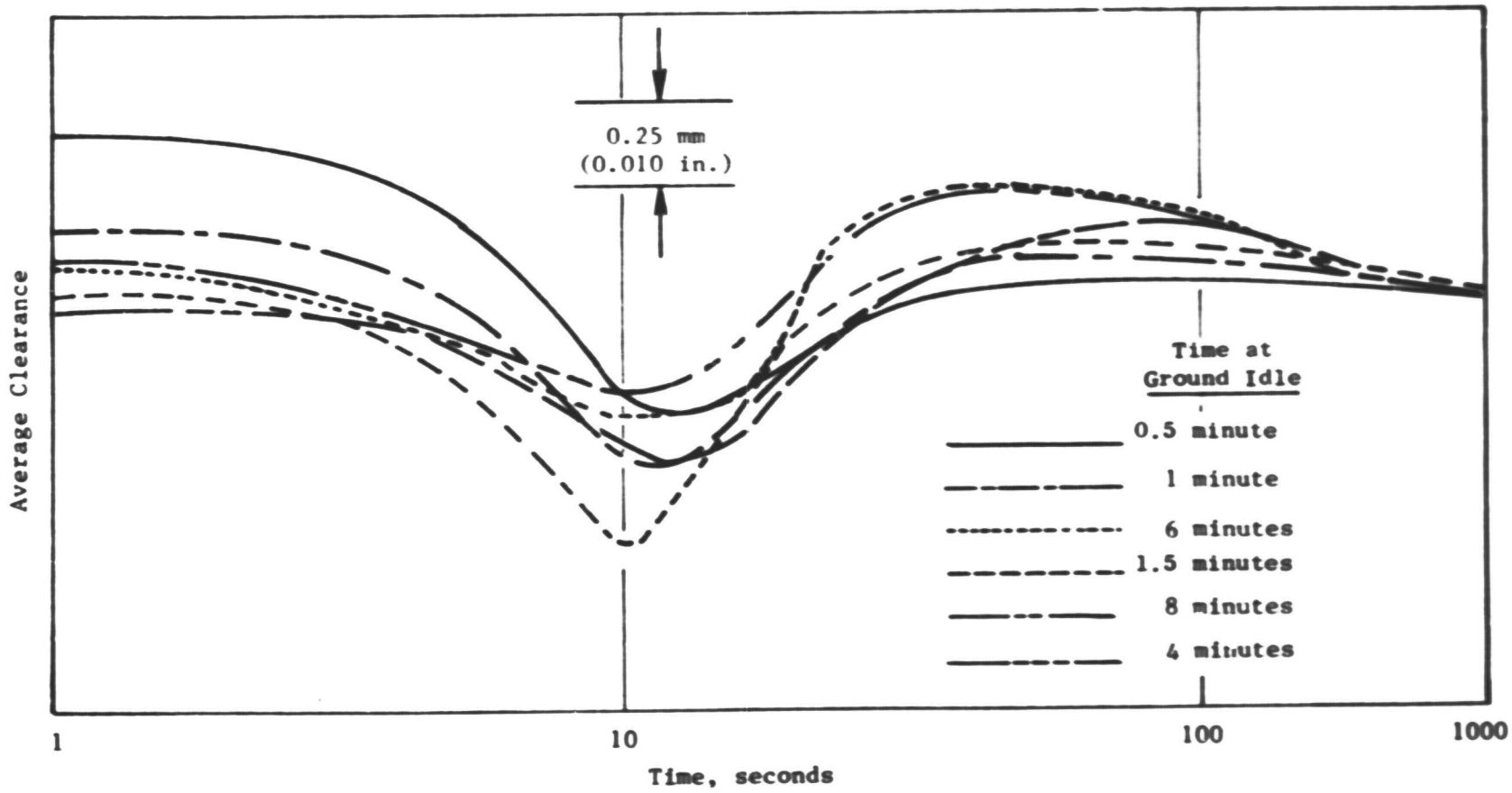

Figure 77. Measured Reburst Curves.

true rotor speed, etc., become very important. It is in this region that engine-to-engine differences will be observed.

One of the objectives of this task was to decrease the sensitivity to reburst, i.e., increased reburst margin, of the turbine. This will be demonstrated by comparison to the production turbine. A similar series of reburst clearances was obtained during the Diagnostics testing (Ref. 2). By examining the closure from the steady-state takeoff point to the minimum reburst clearance point, the Diagnostics testing reburst results may be compared to the reburst data obtained during this test. A graph of the closure from steady-state takeoff to minimum reburst clearance is shown in Figure 78. This graph exhibits the reburst margin improvement afforded by the redesigned components.

For the most severe reburst condition the improved stator components show an improvement in reburst margin of 0.381 mm (0.015 in). This means that if this were the only criterion which had to be evaluated to set clearances, the improved stator components would allow establishment of a reduced tip clearance of this magnitude. As the ground idle dwell time prior to reburst is increased, the improvement lessens. Since there is less closure and therefore less tendency for the longer dwell time (greater than 3 minutes) rebursts to cause a rub, the need to increase the margin during the longer swell time rebursts was not considered significant when compared to the closure problem of the shorter dwell time rebursts.

A 90-second reburst was not performed during the Diagnostic testing. The curve shown is based on a statistical curve fit of the Diagnostics reburst data (Ref. 2).

4.5.3 Performance

Engine performance was monitored throughout the testing to assure that the health of the complete engine was known. A complete computer study of the performance of the test vehicle was conducted including efficiency, exhaust gas temperature, and specific fuel consumption calculations. (See paragraph 3.3).

This test vehicle, 455-507 Build 20, was used to establish the effect of Stage 1 blade-to-shroud clearance upon performance for the Diagnostics testing (Ref 2). Since that testing established the baseline, only an analytical determination of those performance improvements, such as flow-path improvements, not associated with clearance reduction, could be made. The measurements taken, after analytical removal of the performance changes due to clearance changes, showed no other discernible effects on engine or high pressure turbine performance. This was expected because the non-clearance/roundness changes were small and, if incorporated by themselves, would not be expected to be measureable on the basis of a single engine test.

The effect of clearance change on performance was established in Diagnostics Program testing (Ref. 2). It was determined that an increase in Stage 1 clearance of 0.432 mm (0.017 in) resulted in a decrease of 1 percent in turbine efficiency. These values were used in the final evaluation of the roundness/clearance performance improvement concept.

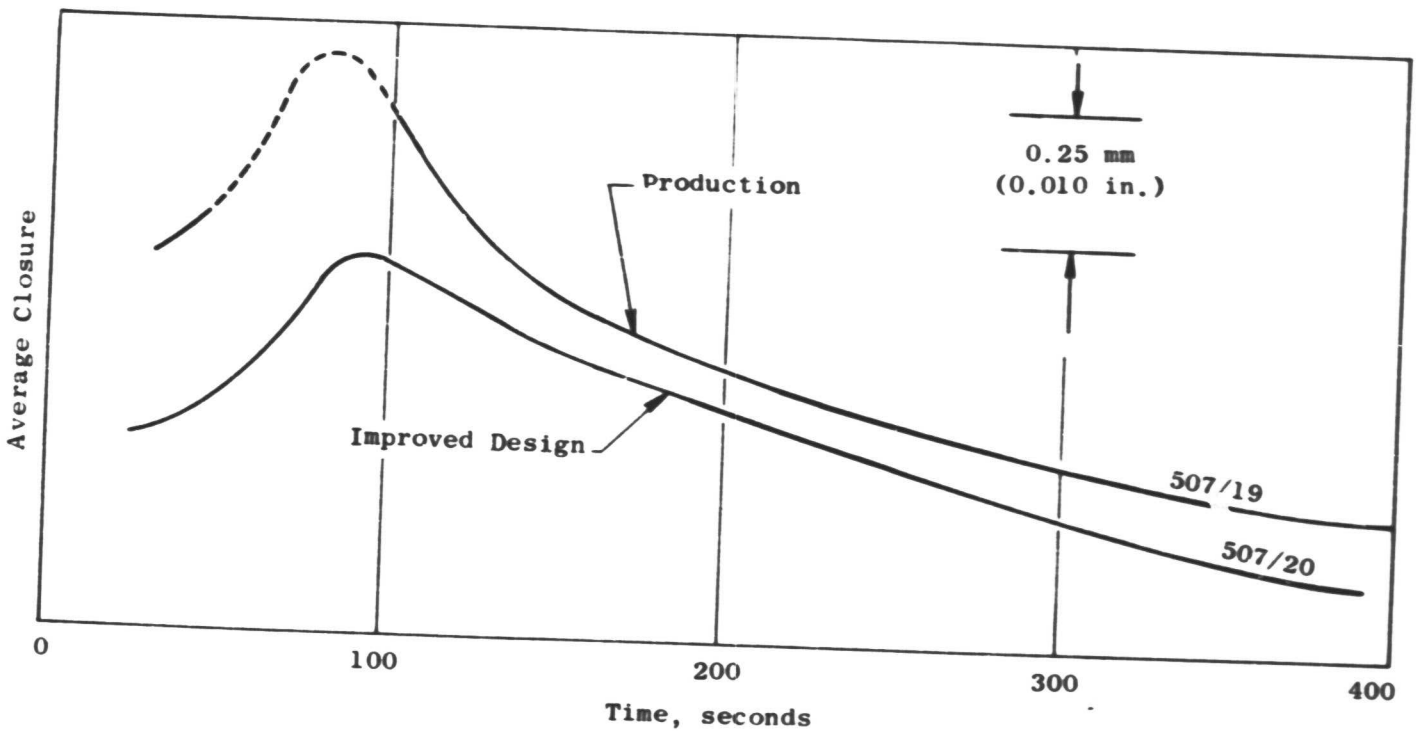

Figure 78. Closure from Takeoff to Min Clearance During Reburst as a Function of Ground Idle Dwell Time.

4.5.4 Application of Test Results

Turbine Midframe

Although the magnitude of the TMF caused HPT stator out-of-roundness was not appreciably reduced by the TMF redesign, the distorted shape was significantly changed. Figures 38 and 39 show that the TMF redesign over-compensated for the out-of-roundness caused by the present TMF design. By revising some of the elements incorporated in the redesign of the TMF the amount of compensation can be reduced resulting in less total HPT stator out-of-roundness. The elements of the TMF redesign, which would be revised to accomplish this, are the strut temperature control and CRF/TMF flange shielding. Based on the analysis of results from the testing accomplished under this program, it is estimated that the HPT stator out-of-roundness (max. inward distortion) could be reduced by 0.15 - 0.25 mm (0.006 - 0.010 in) by a revision to these areas. This results in a maximum of 0.13 mm (0.005 in) out-of-roundness at steady-state takeoff.

Clearance Response

Since the turbine studied during this test was modified to allow the use of clearanceometer probes and other instrumentation, a study was made of a configuration which would be representative of one which would be used in revenue service. The results of this test, such as temperature, pressures, heat transfer rates, etc., have been implemented into the heat transfer and aerodynamic models of the high pressure turbine area. The clearanceometer data have provided information allowing changes to the structural model. These concepts have been combined and a clearance response picture of a design suitable for revenue service is presented. The clearance during a decel from steady-state takeoff to stabilized ground idle is shown in Figure 79. The clearance during an accel from stabilized ground idle to stabilized takeoff is shown in Figure 80.

As a result of the roundness improvements to the turbine midframe a virtually round turbine can be obtained. The turbine operating clearances can now be determined by the round engine response of the shroud support structure and the response of the rotor. The clearance attainable by the HPT stator redesign are shown in the following table:

Round Engine Clearance Summary, mm (in)

Cruise	Steady-State Takeoff	Min Accel	Min Decel	Reburst	Cold Clearance
0.56(0.022)	0.28(0.011)	0.71(0.028)	0.69(0.027)	-0.18(-0.007)	2.03 (0.080

When these results are adjusted to allow a calculated 0.38 mm (0.015 in) rub (this is the same magnitude of rubs as experienced by the production engine) at the most limiting reburst case, the following results:

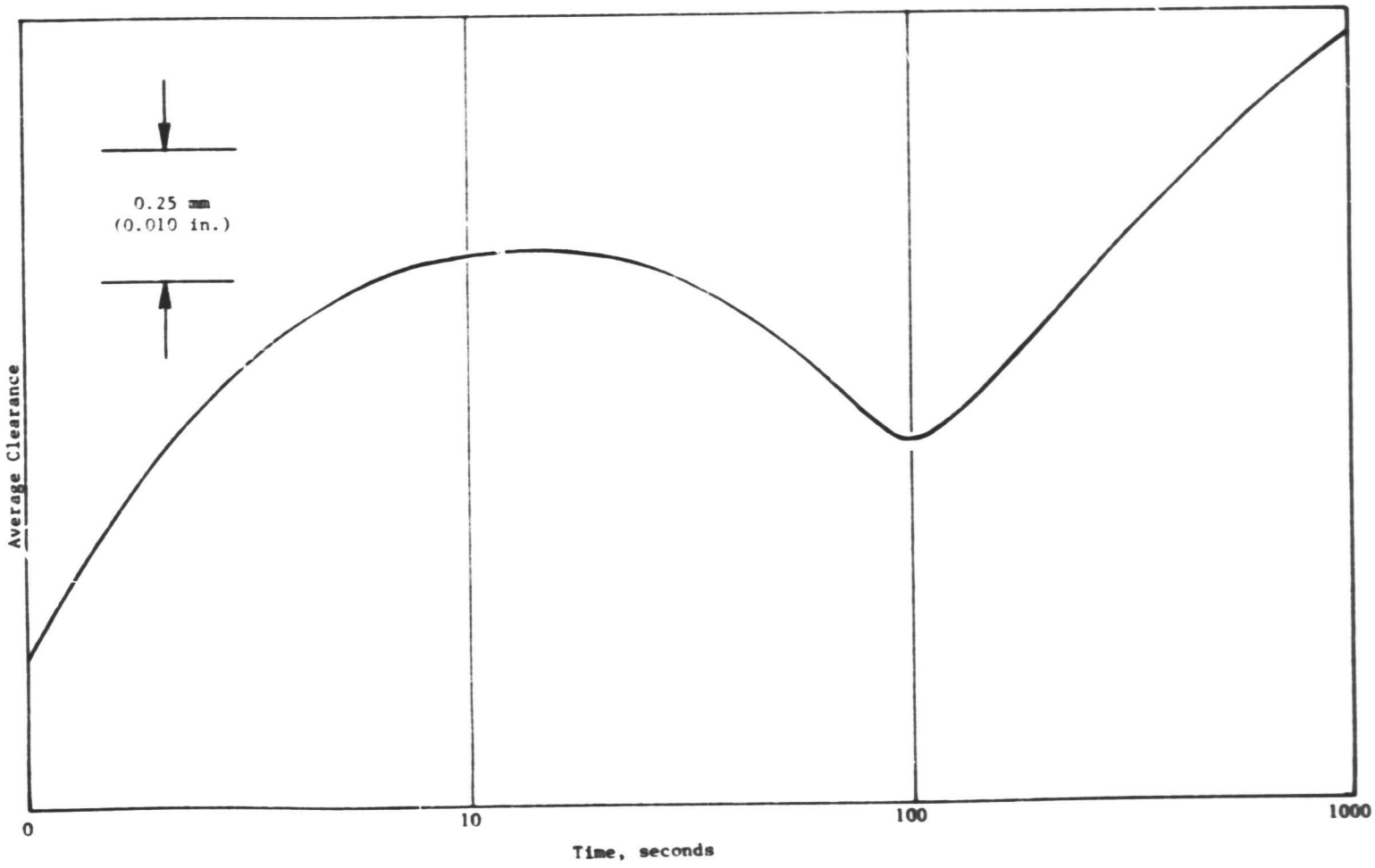

Figure 79. Analytical Model of Clearance Versus Time During a Decel (Takeoff to Ground Idle).

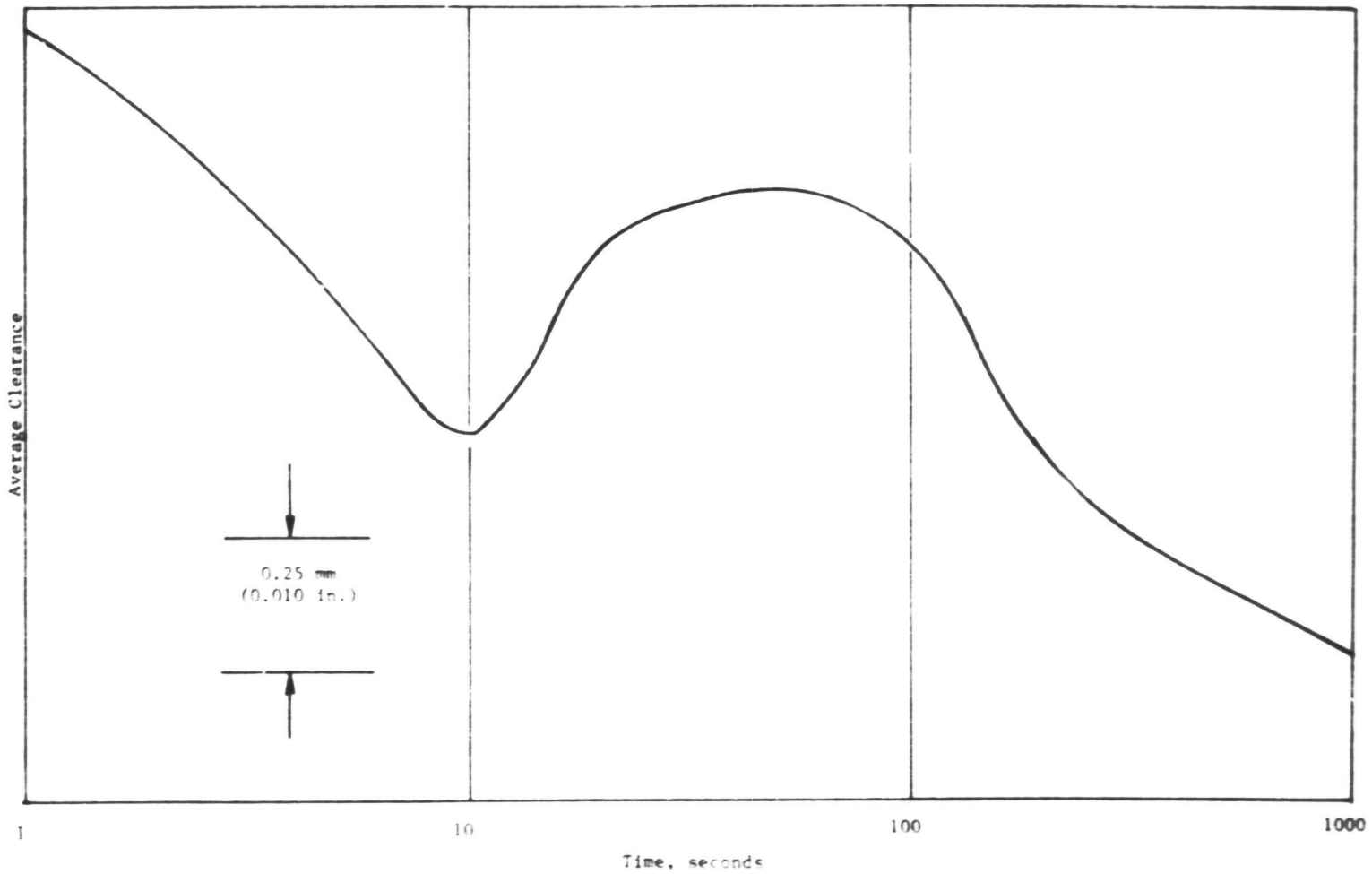

Figure 80. Analytical Model of Clearance Versus Time During an Accel (Ground Idle to Takeoff).

Adjusted Round Engine Clearance Summary, mm (in)

Cruise	Steady-State Takeoff	Min. Accel	Min Decel	Reburst	Cold Clearance
0.36(0.014)	0.08(0.003)	0.51(0.020)	0.48(0.019)	-0.38(-0.015)	1.83(0.072)

Composite Picture

The clearances given in the preceding table represent the minimum clearances which yield a 0.38 mm (0.015 in) round engine rub during a 90-120 second reburst. This clearance state does not represent the clearances required to eliminate rubs resulting from turbine midframe and assembly-caused out-of-roundness.

The effects of out-of-roundness are local rubs. By removing material from the shrouds only in the areas adversely affected by the repeatable out-of-roundness, rubs can be eliminated and the overall effect on clearance minimized. Such a shroud shape, obtained by a preferential grind, is currently used by the CF6-50C engine and will be required with the roundness/clearance improvement hardware (Figure 81).

The following tabulation shows the effects of turbine midframe-caused out-of-roundness, assembly-caused random out-of-roundness, and structural response upon the clearances of the current CF6-50C and those which result from the use of the hardware developed by this program.

Current CF6-50C Clearance, mm (in)

Round Engine Steady-State Takeoff	0.46	(0.018)
Preferential Grind Clearance Adder (based on current, empirically determined shroud grind)	0.13	(0.005)
Total Steady-State Takeoff Clearance	0.58	(0.023)
Measured Repeatable Out-of-Roundness from TMF (Ref. 2)	0.38	(0.015)
Assembly-Caused Random Out-of-Roundness	0.20	(0.008)

Improved Hardware Engine Clearance, mm (in)

Round Engine Steady-State Takeoff [0.08 (0.003) Round Engine Clearance plus 0.20 (0.008) Assembly-caused Out-of Roundness]	0.28	(0.011)
Preferential Grind Clearance Adder (based on TMF-caused Out-of-Roundness)	0.05	(0.002)
Effective Clearance at Steady-State Takeoff	0.33	(0.013)

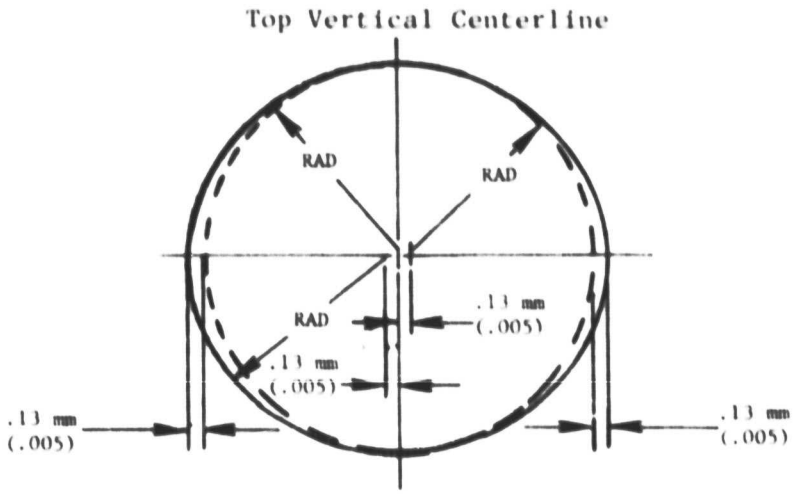

Figure 81. Shroud Grind to Eliminate Rubs Caused by Improved TMF Repeatable Out-of-Roundness.

At cruise, the CF6-50C engine has 0.86 mm (0.034 in) effective clearance and the redesigned hardware allows a 0.61 mm (0.024 in) cruise clearance. Therefore, a 0.25 mm (0.010 in) improvement in new engine cruise clearance is possible. Again, considering out-of-roundness effects and new engine clearances, the current CF6-50C would sustain a total 0.71 mm (0.028 in) rub during a 90-120 second reburst while the redesigned hardware would incur a total 0.38 mm (0.015 in) rub from the same rebursts. Consequently, a long-term engine which has been subjected to rebursts would realize a 0.33 mm (0.013 in) decrease in clearance in addition to the initial 0.25 mm (0.010 in) clearance decrease for a total of 0.58 mm (0.023 in) less clearance by utilizing the improved hardware.

This clearance reduction translates to an improvement of 0.58 percent in turbine efficiency and a 0.31 percent reduction in specific fuel consumption at takeoff power when using the derivatives determined from the Diagnostic testing (Ref. 2). The equivalent cruise SFC reduction is 0.22 percent.

The above improvement is for a new engine; for a long-term engine (3000 hrs) the roundness improvement amounts to an increase of 1.34 percent in turbine efficiency and a 0.71 percent reduction in specific fuel consumption at takeoff power. The equivalent cruise SFC reduction for a long-term engine is 0.50 percent.

5.0 ENGINE ENDURANCE TEST

The objectives of this test were to demonstrate the life capability and the performance deterioration characteristics of the improved clearance response HPT stator hardware and the improved roundness turbine midframe.

5.1 TEST SETUP

The test vehicle for this test was a model CF6-50 engine, Serial Number 455-509, Build No. 7. The engine was configured with the HP turbine stator roundness hardware and a modified turbine midframe. The test vehicle was instrumented with standard instrumentation to monitor the engine operation.

The test was conducted at Site V-B at General Electric's Peebles, Ohio Proving Ground. Figure 82 shows a photograph of the CF6-50 engine installed at this site.

5.2 TEST PROCEDURE

The endurance testing consisted of running 842 "C" cycles, as described in Figure 83. Initial testing was halted after Cycle 16 because of increased fan vibration. Borescope inspection showed heavy damage to the compressor airfoils. The engine was returned to the Evendale Plant for failure analysis and compressor airfoil replacement. Analysis indicated that the failure was caused by the impact of a foreign object.

The rebuilt engine was re-installed at Site V-B and testing continued. Testing was again halted when a borescope inspection of the HPT showed Stage 1 bucket cracking. A total of 842 "C" cycles had been completed by this data. The engine was returned to the Evendale plant for a teardown inspection.

5.3 TEST RESULTS

Results of the endurance test are highly encouraging. All hardware removed after 842 "C" cycles looked unusually good. It should be noted that factory endurance engines are tested to EGT limits 10° C higher than fully deteriorated field engines operating without derate. The condition of the hardware, as observed after test, is described by the following itemizations.

Stage 1 Nozzles

Inner platform burning and cracking is evident on the HPT Stage 1 nozzle vanes. This distress is attributed to the combustor temperature profile. The improved Stage 1 nozzles are in satisfactory condition except for the combustor-caused distress (see Figures 84 and 85).

Figure 82. CF6-50 Engine Installed at Site VB.

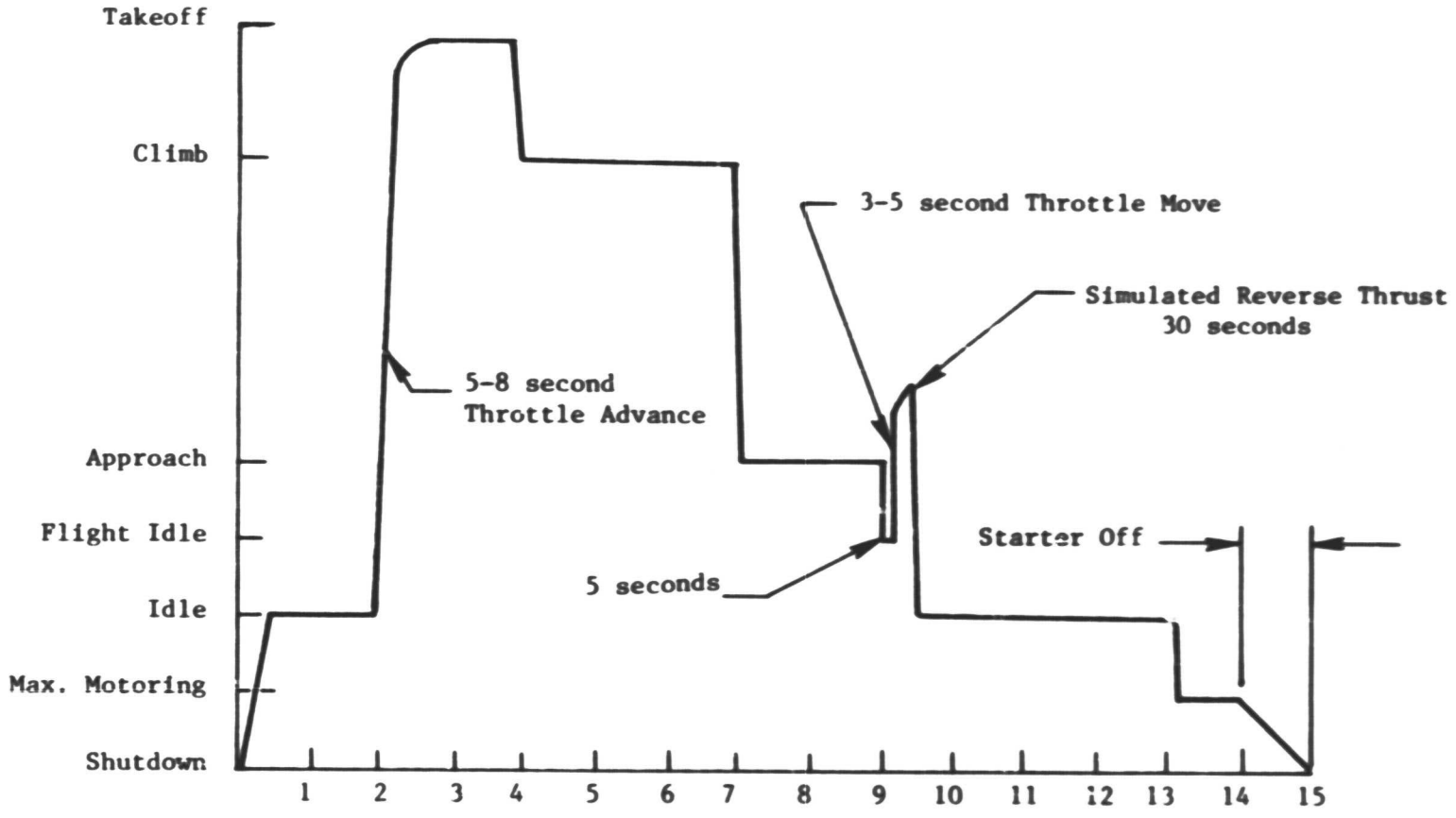

Figure 83. "C" Cycle Definition

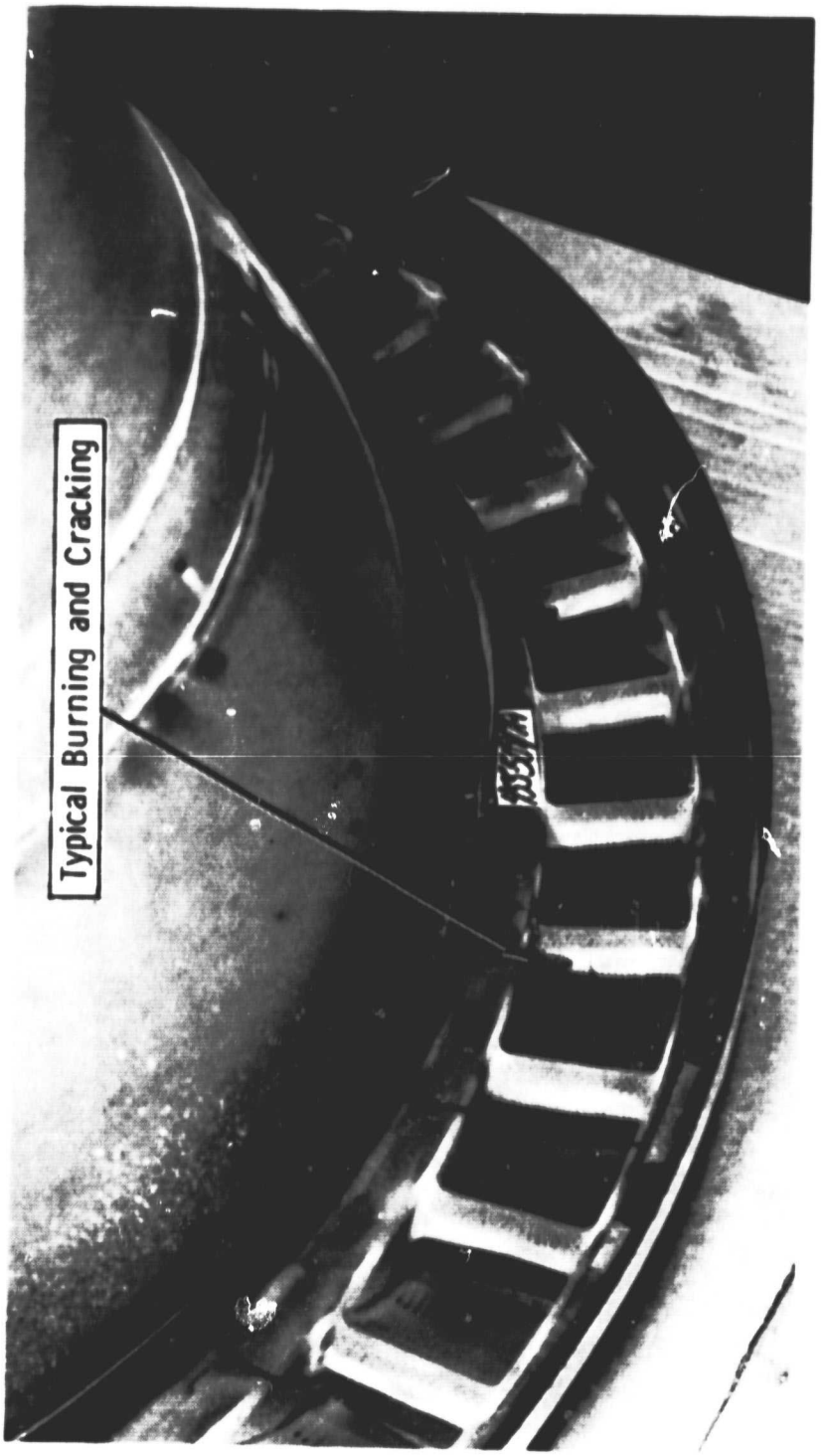

Figure 84. Front View of Stage 1 Nozzles Showing Inner Platform Burning and Cracking.

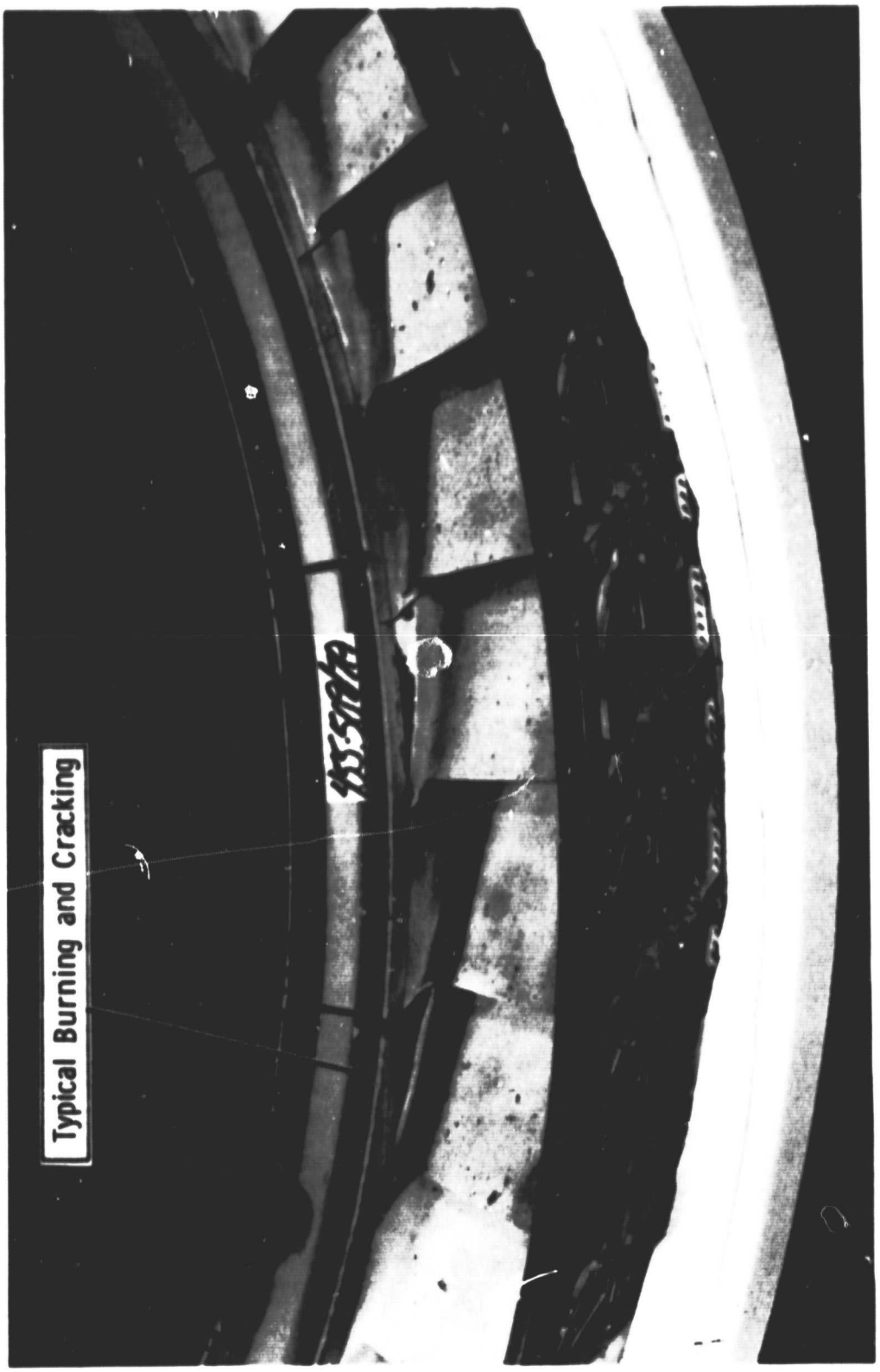

Figure 85. Aft View of Stage 1 Nozzles Showing Inner Platform Burning and Cracking.

Stage 2 Nozzles

The outer platforms of the Stage 2 nozzles exhibit cracking (see Figure 86). This cracking was caused by the "double-hook" feature which mounts the aft end of the Stage 1 shroud. The shroud retention feature of the stage 2 nozzles was removed to reflect a design similar to the current CF6-50 "C" clamp design. This change is shown in Figure 87. This is a necessary change since the "double-hook" feature was difficult to assemble and endurance testing of modified nozzles without the "double-hook" showed that the platform cracking was caused by this feature.

In the case of the stage 2 nozzles the gas recirculation fix proved to be more detrimental than the potential problem of recirculation (see Figure 13).

Stage 1 Shrouds

The improved solid shroud configuration was tested on Engine 455-509 builds 8 and 8a. The shrouds were tested for 1034 "C" cycles.

The improved shrouds performed very well. Minimum distress was noted. The design sustained rubs without appreciable deterioration. None of the film cooling holes were plugged or restricted.

Figure 88 is a photograph of solid shrouds on either side of a standard production shroud. It can be seen that the solid shroud on the left took a fairly wide rub and that the film cooling holes are all open. The surface is smooth and uncracked. The shroud on the right also took rubs without significant damage. This shroud shows some thermal distress on the right circumferential split line. These parts are typical of those tested. Overall the condition of the improved shrouds was excellent.

Stage 2 Shrouds

The Stage 2 shrouds are in excellent condition (see Figure 86). Compared to current production Stage 2 shrouds, these shrouds show less distress and should significantly reduce the loss of performance associated with shroud deterioration. The elimination of deterioration caused by operation, especially that wear and tear resulting from long exposure to the environment of a high pressure turbine, was the goal of the stage 2 shroud redesign.

Stage 2 Shroud Forward Hangers

The stage 2 shroud forward hangers have cracks originating at the shroud positioning hole at the hanger center. This cracking is probably due to the stiffer Stage 2 shroud.

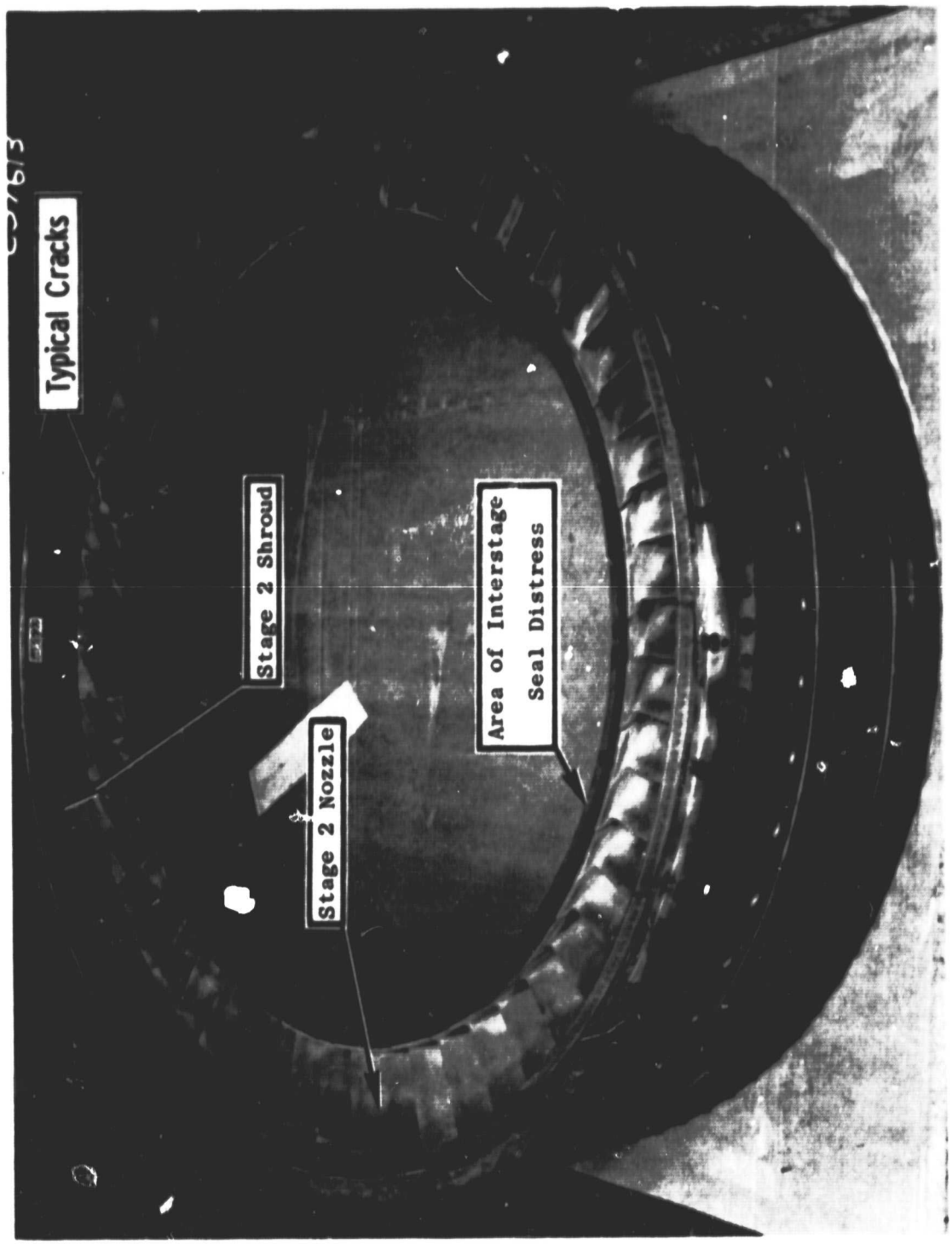

Figure 86. Aft View of Stage 2 Nozzle Assembly.

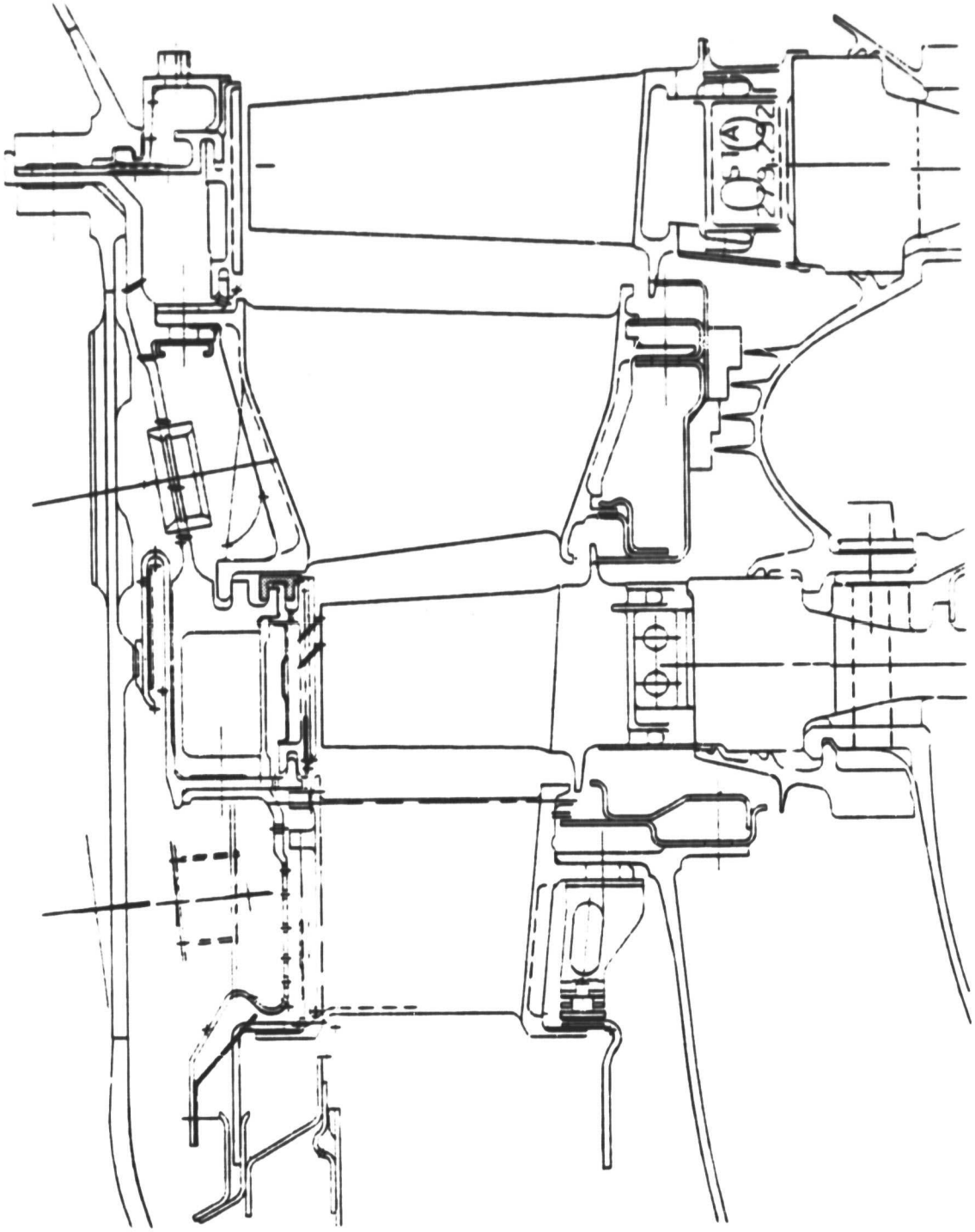

Figure 87. Redesigned HPT Stator.

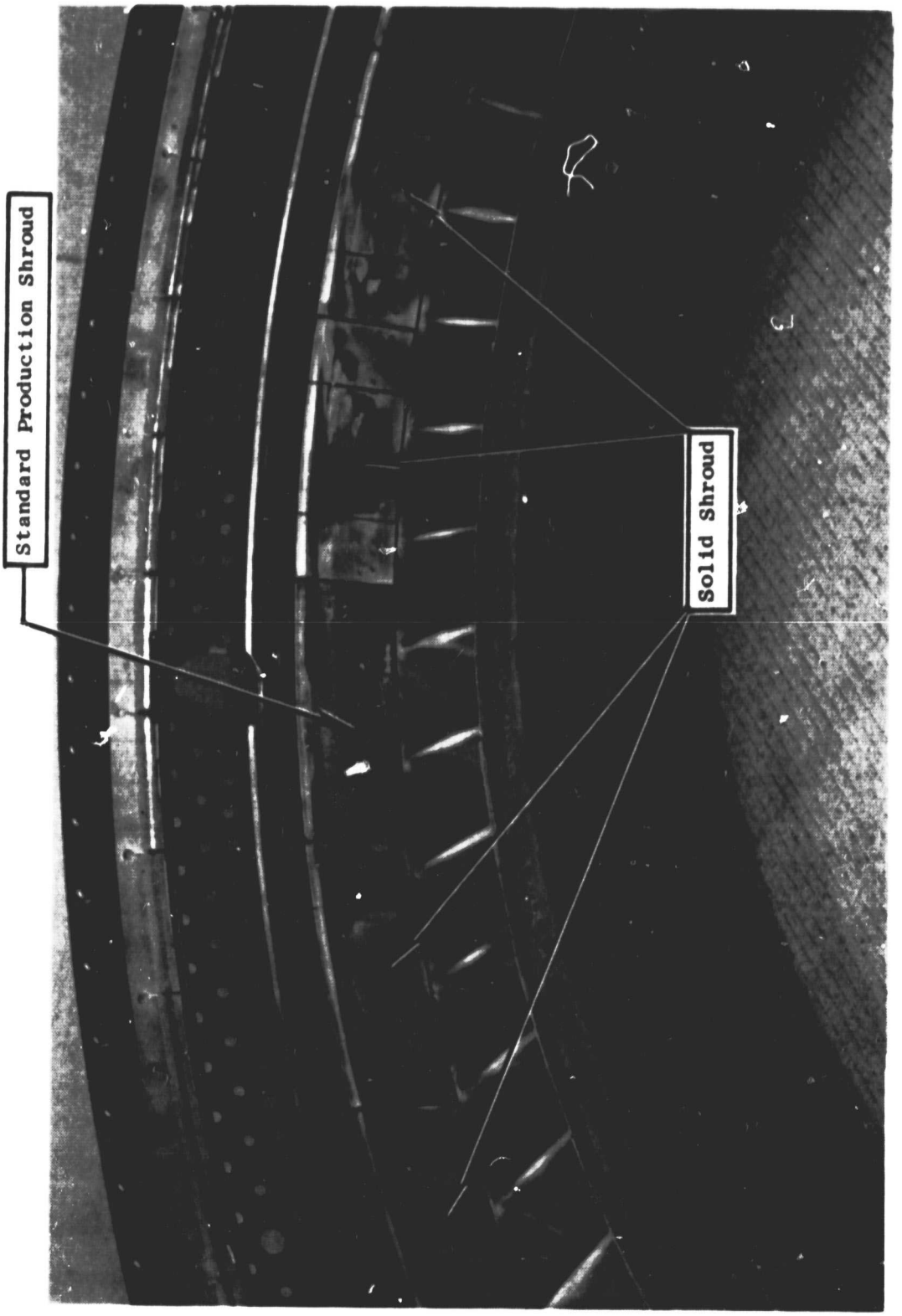

Figure 88. Stage 1 Shrouds.

Interstage Seals

Minor cracking originating from the bolt cutouts in the aft discouiager tip portion of the seals was observed (see Figure 86). Saw cuts and end holes have been incorporated into the design to eliminate this problem. Some wear on the forward tip where the stage 2 nozzle fits was also apparent. A coating which resists wear will be added to this area. Otherwise, the seals completed testing in satisfactory condition (Figure 89).

Remainder of Stator Hardware

The remaining hardware, i.e., Stage 2 nozzle support, impingement ring, Stage 1 shroud forward hanger, Stage 2 shroud aft hanger, and the seals associated with the improved shrouds and nozzles, completed the endurance test in very good condition. No distress or cracking is evident, and wear patterns appear to be in the correct position and depth (Figures 88 and 90).

Turbine Midframe

Posttest visual inspection revealed two areas of distress:

1. A 63 mm (2-1/2 inch) crack in the outer casing weld joint between the No. 2 strut end/mount casting and the aft sheet metal "hat section" stiffener. This crack was in the center of the weld bead indicating that it occurred due to a poor quality initial manufacturing weld rather than due to excessively high operating stresses. These types of cracks typically occur in the weld "heat-affected zone" immediately adjacent to the weld.

2. Seventeen liner cracks occurred in the liner fairing to shell fillet inserts at the fairing leading and trailing edges. The liner used in this frame was a used liner identical to that used in current field turbine midframe assemblies; the cracking is typical of that seen in field service, although more severe than would be expected from this amount of running. This was caused by the unusually hign operating temperatures encountered due to a combustor temperature profile problem associated with this engine build and not associated with the changes made for roundness.

Summary

The endurance testing of the hardware designed under this contract has been successfully completed on a CF6-50 engine at the Peebles Proving Ground Test Facility on Site V-B. The engine was run for a total of 842 simulated revenue-service cycles.

Overall, the endurance test results are very encouraging. The problems encountered are well understood and are being corrected by minor design modifications. The modifications will be incorporated in the next factory test engine utilizing the roundness performance improvement configuration hardware defined under this contract.

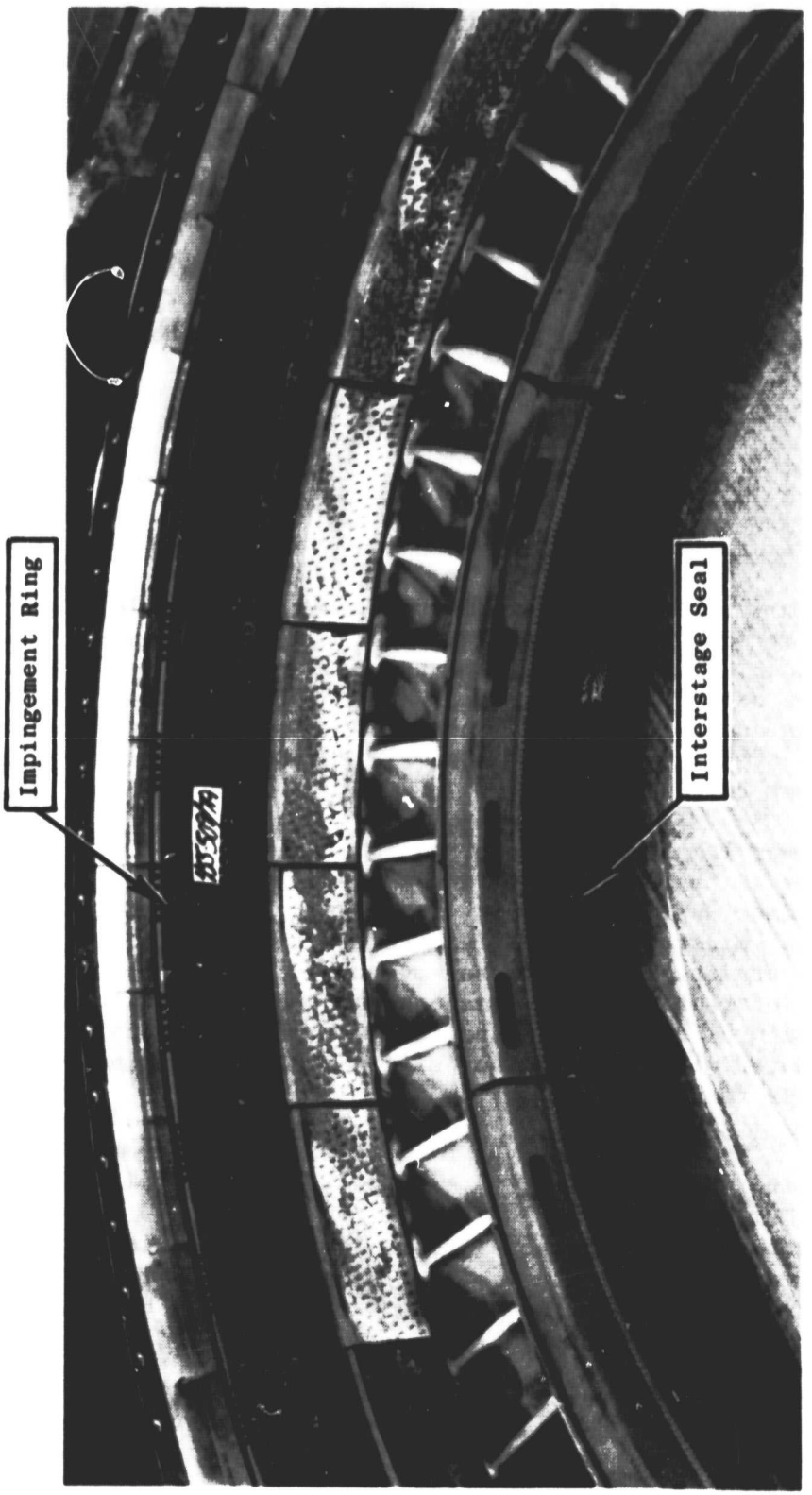

Figure 89. Forward-Looking-Aft View of Interstage Seals and Impingement Ring Depicting Hardware Condition.

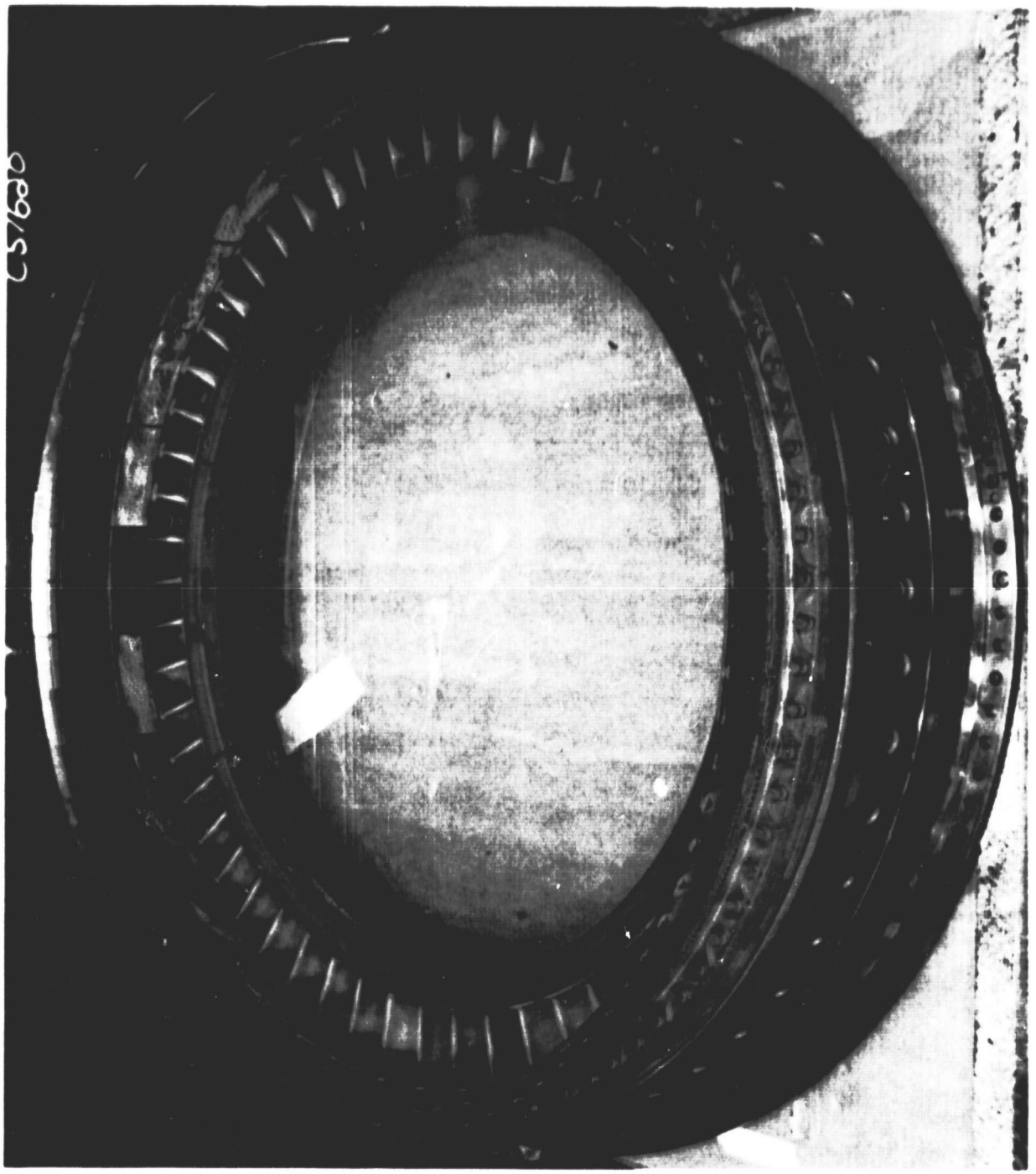

Figure 90. High Pressure Turbine Stator Stage 2 Module Assembly After 842 "C" Cycles.

6.0 ECONOMIC ASSESSMENT

The HP turbine roundness concept was evaluated by Boeing and Douglas under the feasibility study of the program (Reference 1). Since the concept would reduce sfc deterioration, the benefits would increase with engine age relative to current engines of comparative age. Therefore, this concept was analyzed to determine potential fuel savings for engines with 3000 hours since last high pressure turbine maintenance.

The estimated reduction in cruise sfc for engines with 3000 hours is 0.5 percent. Application of roundness concept will result in the following block fuel savings

HP TURBINE ROUNDNESS
BLOCK FUEL SAVINGS (3000 HRS)

(Minimum Fuel Analysis)

AIRCRAFT	RANGE km	FUEL kg	FUEL percent
DC-10-30	805	- 44	-0.47
	2735	-141	-0.55
	6725	-273	-0.61
B-747-200	770	- 25	-0.28
	3460	-116	-0.55
	6195	-236	-0.61

The estimated annual fuel savings per aircraft for the above block fuel savings are shown as follows:

ESTIMATED ANNUAL FUEL SAVINGS PER AIRCRAFT (3000 HRS)

(Minimum Fuel Analysis)

AIRCRAFT	RANGE km	FUEL Liters/AC/Year
DC-10-30	805	104,200
	2735	157,500
	6275	300,000
B-747-200	770	93,800
	3460	187,500
	6195	384,400

The medium fuel prices assumed for the study are dependent on the aircraft mission. Prices used were 14.5¢/l (55¢/gal) for the DC-10-30 (International) and 11.89¢/l (45¢/gal) for the B-747-200 (US Domestic). The economic assessment based on these prices is summarized in the following table:

ECONOMIC ASSESSMENT OF HP TURBINE ROUNDNESS CONCEPT (3000 HRS)

(Medium Range, Medium Fuel Price, Minimum Fuel Analysis)

AIRCRAFT	Payback (Years)	ROI percent
DC-10-30	1.0	100
B-747-200	1.25	80

Because of the increase in the cost of fuel by about 200 percent since the conduction of the feasibility analysis (Ref. 1) in 1978, the payback and the return on investment of this concept would be substantially more favorable now.

7.0 SUMMARY OF RESULTS

The high pressure turbine roundness improvement developed under this program has been evaluated in an instrumented engine test and an endurance test. The main results of these tests are summarized below:

Instrumented Engine Test

In the instrumented engine test real time Stage 1 blade-to-shroud clearance measurements were obtained for a CF6-50 engine for steady-state and transient operation. The improved high pressure turbine concept allows a reduction in HPT running clearances of 0.38 mm (0.015 in).

This clearance reduction translates in an improvement of 0.58 percent in turbine efficiency and a 0.31 percent reduction in specific fuel consumption at takeoff power. The equivalent cruise sfc reduction was 0.22 percent.

The above improvement is for a new engine; for a long-term engine (3000 hrs) the roundness improvement amounts to 0.50 percent in cruise sfc.

Endurance Test

The CF6-50 static endurance test demonstrated the life capability of the HP turbine roundness hardware in 842 flight cycles with indications of only minor distress.

APPENDIX A

QUALITY ASSURANCE

INTRODUCTION

The quality program applied to this contract is a documented system throughout the design, manufacture, repair, overhaul and modification cycle for gas turbine aircraft engines. The quality system has been constructed to comply with military specifications MIL-Q-9858A, MIL-I-45208, and MIL-STD-45662 and Federal Aviation Regulations FAR-145 and applicable portion of FAR-21.

The quality system and its implementation are defined by a complete set of procedures which has been coordinated with the DOD and FAA and has their concurrence. In addition, the quality system as described in the quality program for this contract has been coordinated with NASA-Lewis Research Center. The following is a brief synopsis of the system.

QUALITY SYSTEM

The quality system is documented by operating procedures which coordinate the quality-related activities in the functional areas of Engineering, Manufacturing, Materials, Purchasing, and Engine Programs. The quality system is a single-standard system wherein all product lines are controlled by the common quality system. The actions and activities associated with determination of quality are recorded, and documentation is available for review.

Inherent in the system is the assurance of conformance to the quality requirements. This includes the performance of required inspections and tests. In addition, the system provides change control requirements which assure that design changes are incorporated into manufacturing, procurement and quality documentation, and into the products.

Measuring devices used for product acceptance and instrumentation used to control, record, monitor, or indicate results of readings during inspection and test are initially inspected and calibrated and periodically are reverified or recalibrated at a prescribed frequency. Such calibration is performed by technicians against standards which are traceable to the National Bureau of Standards. The gages are identified as a control number and are on a recall schedule for reverification and calibration. The calibration function maintains a record of the location of each gage and the date it requires recalibration. Instructions implement the provisions of MIL-STD-45662 and the appropriate FAR requirements.

Work sent to outside vendors is subject to quality plans which provide for control and appraisal to assure conformance to the technical requirements. Purchase orders issued to vendors contain a technical description of the work to be performed and instructions relative to quality requirements.

Engine parts are inspected to documented quality plans which define the characteristics to be inspected, the gages and tools to be used, the conditions under which the inspection is to be performed, the sampling plan, laboratory and special process testing, and the identification and record requirements.

Work instructions are issued for compliance by operators, inspectors, testers, and mechanics. Component part manufacture provides for laboratory overview of all special and critical processes, including qualification and certification of personnel, equipment and processes.

When work is performed in accordance with work instructions, the operator/inspector records that the work has been performed. This is accomplished by the operator/inspector stamping or signing the operation sequence sheet to signify that the operation has been performed.

Various designs of stamps are used to indicate the inspection of status of work in process and finished items. Performance or acceptance of special processes is indicated by distinctive stamps assigned specifically to personnel performing the process or inspection. Administration of the stamp system and the issuance of stamps are functions of the Quality Operation. The stamps are applied to the paperwork identifying or denoting the items requiring control. When stamping of hardware occurs, only laboratory approved ink is used to assure against damage.

The type and location of other part marking are specified by the design engineer on the drawing to assure effects do not compromise design requirements and part quality.

Control of part handling, storage and delivery is maintained through the entire cycle. Engines and assemblies are stored in special dollies and transportation carts. Finished assembled parts are stored so as to preclude damage and contamination, openings are covered, lines capped and protective covers applied as required.

Nonconforming hardware is controlled by a system of material review at the component source. Both a Quality representative and an Engineering representative provide the accept (use-as-is or repair) decisions. Nonconformances are documented, including the disposition and corrective action if applicable to prevent recurrence.

The system provides for storage, retention for specified periods, and retrieval of nonconformance documentation. Documentation for components is filed in the area where the component is manufactured/inspected.

APPENDIX B - SYMBOLS

ALF	Aft Looking Forward
CDP	Compressor Discharge Pressure, N/cm^2 (lb/in^2)
CRF	Compressor Rear Frame
HPT	High Pressure Turbine
LPT	Low Pressure Turbine
N_1	Fan Speed, rpm
N_2	Core Speed, rpm
P_3	Compressor Exit Pressure, N/cm^2 (lb/in^2)
SFC	Specific Fuel Consumption, $\frac{kg}{hr\ da\ N}$ ($\frac{lb}{hr\ lb}$)
T_3	Compressor Exit Temperature, ^oC (^oF)
T/C	Thermocouple
TMF	Turbine Midframe
TRF	Turbine Rear Frame
W_{2c}	Core Inlet Flow, kg/sec (lb/sec)

APPENDIX C - REFERENCES

1. Fasching, W.A., "CF6 Jet Engine Performance Improvement Program," Task I Feasibility Analysis," NASA CF-159450 (GE R79AEG295), March 1979.

2. W.D. Howard, W.A. Fasching, "High Pressure Turbine Roundness/Clearance Evaluation," NASA CR- (Not Available), 1982

DISTRIBUTION LIST

AVCO LYCOMING DIVISION
550 SOUTH MAIN STREET
STRATFORD, CT 06497
ATTN: A. BRIGHT, ENG. PERFORM. (1)

AEROJET MANUFACTURING COMPANY
601 S. PLACENTIA
FULLERTON, CA 92634
ATTN: J. KORTENHOEVEN, VP ENG. (1)

AIR CALIFORNIA
OAKLAND INTL. AIRPORT
OAKLAND, CA 94614
ATTN: L. WUTH DIRECTOR ENGINEERING (1)

AIR RESEARCH MFG. CO. OF ARIZONA
DEPT. 93-200/503-3S
402 SOUTH 36TH STREET
PHOENIX, AZ 85010
ATTN: K. FLEDDERJOHN (1)

AIR RESEARCH MFG. CO. OF ARIZONA
DEPT. 93-010/503-4B
PO BOX 5217
PHOENIX, AZ 85010
ATTN: DR. M. C. STEELE (1)

AIR TRANSPORT ASSOCIATION
1709 NEW YORK AVE., NW
WASHINGTON, DC 20056
ATTN: E. THOMAS, ASST. VP. ENG. (1)

ALASKA AIRLINES, INC.
BOX 68900
SEATTLE, WA 98188
ATTN: J. S. BRACELEN ENG. & MAINT. ADMIN. (1)

AMERICAN AIRLINES, INC.
TULSA MAINT. & ENGINEERING CENTER
3800 N. MINGO ROAD
TULSA, OKLAHOMA 74151
ATTN: KEITH GRAYSON (1)

ARNOLD ENGINEERING & DEVELOPMENT CENTER
AEDC/XRFX
ARNOLD AFS, TN 37389
ATTN: DR. JAMES G. MITCHELL, DIRECTOR OF FACILITY PLANS AND PROGRAMS (1)

ARNOLD ENGINEERING & DEVELOPMENT CENTER
AEDC/XRFX
ARNOLD AFS, TN 37389
ATTN: R. ROEPKE (1)

BOEING COMPANY
PO BOX 3707
SEATTLE, WA 98124
ATTN: R. MARTIN MS: 73-07 (2)

BRANIFF INTERNATIONAL, BRANIFF TOWER
PO BOX 35001
EXCHANGE PARK, DALLAS, TX 75235
ATTN: HANK NELSON, DIRECTOR - POWER-PLANT ENGINEERING (1)

CIVIL AERONAUTICS BOARD
WASHINGTON, DC 20428
ATTN: J. E. CONSTANTZ, CHIEF, ECONOMIC ANALYSIS DIVISION, B-68 (1)

CONTINENTAL AIRLINES, INC.
LOS ANGELES INTERNATIONAL AIRPORT
LOS ANGELES, CA 90009
ATTN: FRANK FORSTER, DIRECTOR - POWER PLANT ENGINEERING (1)

COOPER AIRMOTIVE, INC.
4312 PUTMAN STREET
DALLAS, TX 75235
ATTN: TERRY HARRISON (1)

DELTA AIRLINES, INC.
HARTSFIELD-ATLANTA INTERNATIONAL AIRPORT
ATLANTA, GA 30320
ATTN: JIM GOODRUM (1)

DEPT. OF TRANSPORTATION
21000 SECOND ST., SW
WASHINGTON, DC 20591
ATTN: HAROLD TRUE (1)

DEPT. OF TRANSPORTATION, FAA
21000 SECOND ST., SW
WASHINGTON, DC 20591
ATTN: R. S. ZUCKERMAN, ARD 550, AIRCRAFT NOISE PROJECT MANAGER (1)

DETROIT DIESEL ALLISON DIV. GMC
PO BOX 894
INDIANAPOLIS, IN 46206
ATTN: R. A. SULKOSKE, DEPT. 8896 MS: V19 (1)

EASTERN AIR LINES, INC.
MIAMI INTERNATIONAL AIRPORT
MIAMI, FL 33148
ATTN: M. DOW, DIRECTOR PWRPLNT ENG. -MIAEW,
BLDG. 21 (1)

EASTERN AIR LINES, INC.
MIAMI INTERNATIONAL AIRPORT
MIAMI, FL 33148
ATTN: ARTHUR FISHBEIN, PWR. PLNT. ENG.-MIAEW,
BLDG. 21 (1)

EASTERN AIR LINES, INC.
MIAMI INTERNATIONAL AIRPORT
MIAMI, FL 33148
ATTN: P. M. JOHNSTONE VP ENGINEERING (1)

FEDERAL AVIATION ADMINISTRATION DOT/FAA/NAFEC
ANA-410, BLDG. 211
ATLANTIC CITY, NJ 08405
ATTN: GARY FRINGS, PROJECT ENGINEER (1)

FEDERAL EXPRESS CORP.
BOX 727
MEMPHIS, TN 38194
ATTN: J. R. RIEDMEYER, MAINT. AND ENGRG (1)

FLYING TIGER LINE, INC.
7401 WORLD WAY WEST, L. A. INTL. AIRPORT
LOS ANGELES, CA 90009
ATTN: J. DIMIN, POWERPLANT ENG. (1)

FLYING TIGER LINE, INC.
7401 WORLD WAY WEST, L. A. INTL. AIRPORT
LOS ANGELES, CA 90009
ATTN: B. LEWANDOWSKI (1)

FRONTIER AIRLINES, INC.
8250 SMITH ROAD
DENVER, CO 80207
ATTN: W. B. DURLIN ENGINEERING (1)

GENERAL ELECTRIC COMPANY, AIRCRAFT
ENGINE GROUP
1 NEUMANN WAY
EVENDALE, OH 45215
ATTN: MR. A. F. SCHEXNAYDER (10)

HAMILTON STANDARD DIV. UTC
WINDSOR LOCKS, CT 06096
ATTN: LOUIS A. URBAN - SENIOR
DESIGN PROJECT ENGINEER MS 3-2-36 (1)

HUGHES AIRWEST
SAN FRANCISCO INT'L AIRPORT
SAN FRANCISCO, CA 94128
ATTN: W. G. DRECHSLER, MAINTENANCE
AND ENGINEERING (1)

LOCKHEED-CALIFORNIA CO.
PO BOX 551
BURBANK, CA 91520
ATTN: T. F. LAUGHLIN JR, DIRECTOR
AIRCRAFT OPER. - TECH. (1)

MCDONNELL DOUGLAS
3855 LAKEWOOD BLVD.
LONG BEACH, CA 90846
ATTN: F. L. JUNKERMANN MC 36-41 (1)

MCDONNELL DOUGLAS
3855 LAKEWOOD BLVD.
LONG BEACH, CA 90846
ATTN: RONALD KAWAI MC 36-41 POWERPLANT
ENGINEERING (1)

MCDONNELL DOUGLAS
3855 LAKEWOOD BLVD.
LONG BEACH, CA 90846
ATTN: TECH. LIB. ADTL 246-75 (1)

NASA
WASHINGTON, DC 20546
ATTN: W. S. AIKEN/R (1)

NASA
WASHINGTON, DC 20546
ATTN: DR. R. S. COLLADAY/RT-6 (3)

NASA
WASHINGTON, DC 20546
ATTN: P. G. JOHNSON/RJT-2 (1)

NASA
WASHINGTON, DC 20546
ATTN: DR. J. L. KERREBROCK/R (1)

NASA
WASHINGTON, DC 20546
ATTN: C. R. NYSMITH/R (1)

NASA
WASHINGTON, DC 20546
ATTN: DR. W. B. OLSTAD/R (1)

NASA
WASHINGTON, DC 20546
ATTN: R. L. WINBLADE/RJT-2 (1)

NASA-HUGH L. DRYDEN FLIGHT RESEARCH CTR.
PO BOX 273, EDWARDS CA 93523
ATTN: DR. J. ALBERS MS E-PE (1)
ATTN: F. V. OLINGER/MS E-EAP (1)

NASA-HUGH L. DRYDEN FLIGHT RESEARCH CTR.
PO BOX 273, EDWARDS CA 93523
ATTN: HAROLD WASHINGTON, CHIEF - PROPULSION SYSTEMS BRANCH MS E-EA (1)

NASA-LANGLEY RESEARCH CENTER
HAMPTON, VA 23665
ATTN: DR. R. W. LEONARD/MS 158 (1)

NASA-LANGLEY RESEARCH CENTER
HAMPTON, VA 23665
ATTN: L. J. WILLIAMS/MS 249A (1)

NASA-AMES RESEARCH CENTER
MOFFETT FIELD, CA 94035
ATTN: J. ZUK/MS 237-11

NASA-LEWIS RESEARCH CENTER
21000 BROOKPARK ROAD
CLEVELAND, OH 44135
ATTN: DANIEL C. MIKKELSON/MS 86-7, HEAD SUBSONIC PROPULSION SECTION

NASA-LEWIS RESEARCH CENTER
21000 BROOKPARK ROAD
CLEVELAND, OH 44135
ATTN: MILTON A. BEHEIM/MS3-5, DIRECTOR OF AERONAUTICS (1)

NASA-LEWIS RESEARCH CENTER
21000 BROOKPARK ROAD
CELVELAND, OH 44135
ATTN: MILTON A. BEHEIM/MS 86-1, CHIEF, PROPULSION SYSTEMS DIV. (1)

NASA-LEWIS RESEARCH CENTER
21000 BROOKPARK ROAD
CLEVELAND, OH 44135
ATTN: CARL C. CIEPLUCH/MS 301-4, MGR. ENERGY EFFICIENT ENGINE PROGRAM (3)

NASA-LEWIS RESEARCH CENTER
21000 BROOKPARK ROAD
CLEVELAND, OH 44135
ATTN: MELVIN J. HARTMANN/MS 3-7, DIRECTOR OF SCIENCE & TECHNOLOGY (1)

NASA-LEWIS RESEARCH CENTER
21000 BROOKPARK ROAD
CLEVELAND, OH 44135
ATTN: LEWIS LIBRARY/MS 60-3 (2)

NASA-LEWIS RESEARCH CENTER
21000 BROOKPARK ROAD
CLEVELAND, OH 44135
ATTN: L. D. NICHOLS, CHIEF, FLUID MECHANICS & ACOUSTICS MAIL STOP: 5-3 (1)

NASA-LEWIS RESEARCH CENTER
21000 BROOKPARK ROAD
CLEVELAND, OH 44135
ATTN: NEAL T. SAUNDERS/MS49-1, CHIEF, MATERIALS DIVISION

NASA-LEWIS RESEARCH CENTER
21000 BROOKPARK ROAD
CLEVELAND, OH 44135
ATTN: TITO T. SERAFINI/MS 49-1, HEAD, POLYMER-MATRIX COMPOSITES SECTION

NASA-LEWIS RESEARCH CENTER
21000 BROOKPARK ROAD
CLEVELAND, OH 44135
ATTN: D. L. NORED/MS 301-2, CHIEF,
TRANSPORT PROPULSION OFFICE (1)

NASA-LEWIS RESEARCH CENTER
21000 BROOKPARK ROAD
CLEVELAND, OH 44135
ATTN: D. J. POFERL/MS 500-207 CHIEF,
ENGINE SYSTEMS DIV. (1)

NASA-LEWIS RESEARCH CENTER
21000 BROOKPARK ROAD
CLEVELAND, OH 44135
ATTN: ANTHONY LONG/MS 500-305,
CONTRACTING OFFICER (1)

NASA-LEWIS RESEARCH CENTER
21000 BROOKPARK ROAD
CLEVELAND, OH 44135
ATTN: REPORT CONTROL OFFICE/MS 5-5 (1)

NASA-LEWIS RESEARCH CENTER
21000 BROOKPARK ROAD
CLEVELAND, OH 44135
ATTN: R. J. ANTL/MS 301-4 (13)

NASA-LEWIS RESEARCH CENTER
21000 BROOKPARK ROAD
CLEVELAND, OH 44135
ATTN: J. A. ZIEMIANSKI/MS 49-6, CHIEF
STRUCTURES AND MECHANICAL TECHNOLOGIES
DIVISION (3)

NASA SCIENTIFIC AND TECHNICAL INFO.
FACILITY
PO BOX 8757
BALTIMORE/WASHINGTON INTL. AIRPORT,
MD 21240
ATTN: ACCESSIONING DEPT. (30)

NATIONAL AIRLINES, INC.
PO BOX 592055, AIRPORT MAIL FACILITY
MIAMI, FL 33159
ATTN: R. A. STARNER, DIRECTOR-ENGRG. (1)

NAVAL AIR PROPULSION CENTER
1440 PARKWAY AVENUE
TRENTON, NJ 08628
ATTN: W. L. PASELA - PE 63, PROJECT
ENGINEER-TEST & EVAL. (1)

NORTHWEST AIRLINES, INC.
MINNEAPOLIS-ST. PAUL INT'L. AIRPORT
ST. PAUL, MN 55111
ATTN: A. RADOSTA - MS 838, ASSISTANT DIRECTOR
POWER PLANT MAINT. (1)

OZARK AIR LINES INC.
BOX 10007
ST. LOUIS, MO 63145
ATTN: E. E. BOOCK, MAINT & ENGINEERING (1)

PACIFIC AIRMOTIVE CORP.
2940 N. HOLLYWOOD WAY
BURBANK, CA 91503
ATTN: ODDVAR BENDIKSON, DIRECTOR, PROJECT
ENGINEERING (1)

PACIFIC AIRMOTIVE CORP.
2940 N. HOLLYWOOD WAY
BURBANK, CA 91503
ATTN: J. R. GAST, SR. DIRECTOR ENGRG. (1)

PACIFIC SOUTHWEST AIRLINES
3225 HARBOR DR.
SAN DIEGO CA 92101
ATTN: L. NORWOOD, ENGINEERING (1)

PAN AMERICAN WORLD AIRWAYS, INC.
JOHN F. KENNEDY INTERNATIONAL AIRPORT
JAMAICA, NY 11430
ATTN: NIELS ANDERSEN, PROJECT ENGINEER (1)

PAN AMERICAN WORLD AIRWAYS, INC.
JOHN F. KENNEDY INTERNATIONAL AIRPORT
JAMAICA, NY 11430
ATTN: ANGUS MACLARTY, DIRECTOR - POWERPLANT
ENGINEERING (1)

PAN AMERICAN WORLD AIRWAYS, INC.
JOHN F. KENNEDY INTERNATIONAL AIRPORT
JAMAICA, NY 11430
ATTN: VP & CHIEF ENGINEER (1)

PAN AMERICAN WORLD AIRWAYS
JOHN F. KENNEDY INTERNATIONAL AIRPORT
JAMAICA, NY 11430
ATTN: ROBERT E. CLINTON, JR. (1)

PIEDMONT AIRLINES
SMITH REYNOLDS AIRPORT
WINSTON-SALEM, NC 27102
ATTN: H. M. CARTWRIGHT, V.P. MAINT. &
ENGINEERING (1)

PIEDMONT AIRLINES
SMITH REYNOLDS AIRPORT
WINSTON-SALEM, NC 27102
ATTN: PAUL M. REHDER, SUPERVISOR-POWER PLANT ENGINEERING (1)

PRATT & WHITNEY AIRCRAFT GROUP
400 MAIN STREET
EAST HARTFORD, CT 06108
ATTN: J. P. MURPHY, CHIEF QUALITY PERFORMANCE BRANCH, AFPRO-OL-AA, DET. 8 (1)

PRATT & WHITNEY AIRCRAFT GROUP
400 MAIN STREET
EAST HARTFORD, CT 06108
ATTN: W. O. GAFFIN (10)

REPUBLIC AIRLINES, INC.
3500 AIRLINE DR.
MINNEAPOLIS, MN 55450
ATTN: D. W. ATWOOD, MAINTENANCE & ENGINEERING (1)

SEABOARD WORLD AIRLINES, INC.
SEABOARD WORLD BUILDING, JFK INTL. AIRPORT
JAMAICA, NY 11430
ATTN: J. FARRAH, VP MAINTENANCE & ENGINEERING (1)

SEABOARD WORLD AIRLINES, INC.
SEABOARD WORLD BLDG., JFK INTL. AIRPORT
JAMAICA, NY 11430
ATTN: R. BARBA, MANAGER-POWERPLANT ENGINEERING (1)

SOUTHWEST AIRLINES, CO
BOX 37611
DALLAS, TX 75235
ATTN: J. A. VIDAL, MAINTENANCE & ENGINEERING (1)

TEXAS INTERNATIONAL AIRLINES, INC.
BOX 12788
HOUSTON, TX 77017
ATTN: R. STEPHENSON, ENGINEERING (1)

TRANS WORLD AIRLINES
PO BOX 20126, KANSAS CITY INTL. AIRPORT
KANSAS CITY, MO 64195
ATTN: KEN IZUMIKAWA 2-280 MCI (1)

TRANS WORLD AIRLINES
PO BOX 20126, KANSAS CITY INTL. AIRPORT
KANSAS CITY, MO 64195
ATTN: W. D. SHERWOOD (1)

USAIR
INTERNATIONAL AIRPORT
PITTSBURG, PA 15231
ATTN: W. G. PEPPLER, DEVELOPMENT ENGINEERING (1)

UNITED AIRLINES, INC.
SAN FRANCISCO INTERNATIONAL AIRPORT
SAN FRANCISCO, CA 94123
ATTN: JOHN CURRY (1)

UNITED AIRLINES, INC.
SAN FRANCISCO INTERNATIONAL AIRPORT
SAN FRANCISCO, CA 94128
ATTN: JAMES UHL (1)

WESTERN AIR LINES, INC.
6060 AVION DR. BOX 92005, WORLD WAY POSTAL CTR.
LOS ANGELES, CA 90009
ATTN: WALTER HOLTZ (1)

WIEN AIR ALASKA, INC.
4100 INT'L AIRPORT ROAD
ANCHORAGE, AK 99502
ATTN: J. E. COLBURN, OPERATIONS & MAINTENANCE (1)

WORLD AIRWAYS, INC.
BOX 2330
OAKLAND, CA 94614
ATTN: R. L. FUNK, MAINTENANCE & ENGINEERING (1)

WRIGHT-PATTERSON AFB
DAYTON, OH 45433
ATTN: E. BAILEY, AFWAL/NASA PO (1)

WRIGHT-PATTERSON AFB
DAYTON, OH 45433
ATTN: LT. COL. D. S. DICKSON, ASD/YZI (1)

WRIGHT-PATTERSON AFB
DAYTON, OH 45433
ATTN: C. M. HIGH, ASD/YZE (1)

WRIGHT-PATTERSON AFB
DAYTON, OH 45433
ATTN: MAJ. C. KLINGER, ASD/YZET (1)

WRIGHT-PATTERSON AFB
DAYTON, OH 45433
ATTN: E. C. SIMPSON, AFAPL/TB (1)